The Effects of Entrapped Gas Bubbles on Physical Flow and Dissolved Gas Transport – A Sand Tank Experiment

by

Lionel Andrew Sequeira

A thesis

presented to the University of Waterloo

in fulfillment of the

thesis requirement for the degree of

Master of Science

in

Earth Sciences

Waterloo, Ontario, Canada, 2014

Author’s Declaration

I hereby declare that I am the sole author of this thesis. This is a true copy of the thesis, including any required final revisions, as accepted by my examiners.

I understand that my thesis may be made electronically available to the public.

Abstract

Groundwater tables undergo natural fluctuations due to a variety of processes like snow melt, rain infiltration, aquifer recharge/discharge and river stage fluctuations. Water-table fluctuations result in the entrapment of air bubbles below the water table which will affect the physical properties of the soil and the geochemistry of the groundwater. Oxygen in the air bubbles will dissolve into the groundwater and can be a source of dissolved oxygen.

This thesis describes a series of experiments that were performed at a laboratory scale in a sand tank. The first phase of experiments involved measuring the change in water content and hydraulic conductivity of the sand under saturated and five water-table fluctuation scenarios. As the water-table fluctuation level increased, the amount of entrapped air increased, resulting in a decrease in water content and hydraulic conductivity of the zones with entrapped air. Bromide tracer tests were performed under fully saturated, 29 cm and 45 cm water-table fluctuations to identify physical properties like dispersivity and groundwater velocity. The tracer tests identified stratified velocity profiles across the sand tank such that the highest flow rate was deep at the inflow end while the lowest flow rate was at the shallow outflow end, resulting in preferential flow through the deep end of the sand tank.

The second phase of experiments involved measuring the dissolved argon and oxygen concentrations in the sand tank under saturated, 29 cm and 45 cm water-table fluctuation scenarios. Due to limitations associated with the sampling procedure, diffusion could not be quantified as a process that contributed dissolved oxygen and argon to the groundwater in the sand tank. The 45 cm fluctuation experiment was run for 149 days to measure the change in dissolved-gas concentrations. The experimental results were simulated with MIN3P to provide some insight into the control mechanisms that govern gas-bubble dissolution and dissolved-gas depletion. The quantity of entrapped bubbles and the equilibration between the gaseous and aqueous phase are the main factors that control the depletion of dissolved-gas concentrations across the sand tank.

Acknowledgements

I would like to thank my supervisor, Rich Amos for his trust, support and guidance through the highs and lows of my research, and my committee members, Dave Blowes, Carol Ptacek and Jim Barker, for their guidance and for the knowledge I gained from their courses and through my interaction with them. I would also like to thanks Laura Groza, Jeff Bain and everyone in our GGR research group for their assistance over the years.

Completing this degree was possible due to many friends who helped maintain my sanity and provided me with a lot of enjoyable moments. I want to thank all of them for their love and friendship. When I am older and Facebook is obsolete, I will read this section to remember the names of all the gems I met at Waterloo, so here goes:

Trouble: Jutta, Orin, Heather, Cassia, Pieter, Amanda, Eric, Natalie, Ulanna, Sean, MC, Takeda, Emily, Gonzalo, Jane, 93, Brent, Bobby, Neelmoy, Marcelo, Reza, Reynold, Maddy, Jana, Mariano, Cam, Will, Helen, Stacey, Brenda, Julia, Corina, all the Jenns (Parks, Hansen and Hood), Kim, A. Con, Ben, Adrienne, Rocky, Jess, Saad, Heather, Matt, Ashley, John, Steve, Pat....

More Trouble: Cam, Scottie, Miro, Derrick, Peter, Naomi, Denis, Tarek, Erika, Ivan, Krista, Cullen, all the Mathews (West, Cooper, Smith and Houlihan), Graham, Ned, Mal, Bonnie, Rose and Bill!

Dedication

To my parents, for all their love and support.

Table of Contents

List of Figures

List of Tables

1. Introduction

1.1 Background

A groundwater table can undergo positional fluctuations due to a variety of natural and anthropogenic processes. Seasonal variations induce changes in the groundwater table starting with higher levels following spring snow melt followed by a gradual lowering of the groundwater level over the course of the summer. The lowering of the water level can occur due to natural processes like uptake by vegetation, losses through evaporation, variability of precipitation thus reducing recharge into the aquifer and discharge to water bodies. Additionally, the water level can lower due to anthropogenic processes like groundwater extraction for municipal and industrial use along with soil and groundwater remediation procedures like pump and treat (Marinas et al., 2013), and can be raised due to irrigation and wastewater discharge. The water-table position can also be influenced by the proximity of an aquifer to a surface-water body like a river or lake. Williams and Oostrom (2000) monitored the river stage of the Columbia River and found that the natural fluctuation of the river surface resulted in a detectable fluctuation of the water table of the aquifer up to a distance of 100 metres inland. The amplitude of the fluctuation was highest closer to the river and dampened progressively inland. The annual and daily fluctuation of a river or lake surface will be influenced by natural processes; namely accumulation of snow and ice during the winter, precipitation, evaporation, uptake by vegetation and by anthropogenic processes; namely extraction of water for municipal and industrial use, water level control and discharge by hydroelectric dams (Boutt and Fleming, 2009). Additionally, groundwater- surface water interactions like recharge and discharge will influence the water level within aquifers.

Variably-saturated conditions exist above the capillary fringe in the vadose zone. When an aquifer undergoes water-table fluctuations, it results in the entrapment of air below the water table, and in quasi-saturated conditions below the water table. The term quasi-saturated (Faybishenko, 1995) will be used when referring to groundwater that has entrapped air below the water table

Air can be introduced below the water table by a variety of processes including water-table fluctuations, and remediation schemes like air sparging and pneumatic fracturing. It is important to also note that gas bubbles can form (exsolve) and be entrapped within an aquifer due to biogenic processes like methanogenesis (Fortuin and Willemsen, 2005; Amos et al., 2005) and denitrification (Ronen et al., 1989). For the purpose of this thesis, air that is entrapped due to water-table fluctuations and exists as an immobile-discontinuous phase below the water table will be strictly dealt with. The entrapment of air bubbles affects the physical properties of an aquifer and the geochemistry of the water.

Entrapped air reduces the hydraulic conductivity and permeability of the entrapped-air zone, which can reduce the surface infiltration rate (Christiansen, 1944) and the groundwater recharge rate (Faybishenko, 1995). The amount of entrapped air is directly proportional to the reduction in the quasi-saturated hydraulic conductivity (Fry et al., 1997). The decrease in the hydraulic conductivity has implications for the remediation of contaminated groundwater due to the presence of variable hydraulic conductivity zones within an aquifer thus potentially requiring longer remediation times. In addition, the presence of entrapped air will force contaminated water to flow deeper within an aquifer due to the higher hydraulic conductivity with depth. Dror et al. (2004) performed experiments involving the injection of air to create a lower conductivity barrier that would aid in reducing the effect of salt-water intrusion. They identified that the entrapped air can be a viable method to control the transport of salt water or contaminants.

Entrapped air can be a source of oxygen to a groundwater system (Williams and Oostrom, 2000). The oxygen within the entrapped-air bubbles will partition into the groundwater governed by Henry’s Law and will thus act as a source of dissolved oxygen for biological processes. This ingress of oxygen can aid the aerobic degradation of contaminants within an aquifer and may be highly useful for contaminated sites that utilize monitored natural attenuation as the remediation strategy, especially if the water-table fluctuations are frequent and significant (Amos et al., 2011). Conversely, the entrapment of air and the subsequent dissolution of oxygen will change the redox potential of the groundwater which could be detrimental in aquifers that are contaminated with organic solvents like perchloroethylene (PCE) and trichloroethylene (TCE), which are degraded under anaerobic conditions. Berkowitz et al. (2004) identified that the presence of entrapped air retards the transport of microbes within a groundwater system. Overall, the presence of entrapped air can either be highly beneficial or detrimental depending on the type of contaminant present in the groundwater and the remediation method being employed.

1.2 Literature Review

Christiansen (1944) was one of the first researchers who identified that the permeability of soil is reduced due to the entrapment of air. Three experimental soils; sand, sandy loam and clay loam underwent four wetting procedures namely wetting by capillarity from below, wetting from the bottom under pressure, wetting from the soil surface and wetting from the bottom under vacuum pressure. When soils are wetted by capillarity and from the water surface, the change in permeability follows three unique phases. Initially there is a minor decrease in the permeability; followed by a steady increase until the maximum permeability (up to 30 times the initial permeability) is achieved, followed by a slow steady decline in the permeability. When an air evacuated soil is wetted under vacuum pressure, the soil initially is at its maximum permeability, which steadily declines as the soil is wetted. Entrapped air reduces the permeability of soils. There is a linear relationship between the amount of entrapped air in a soil and the increase in soil permeability upon dissolution of the entrapped air, such that after all the air dissolves, the permeability of the soil reaches the saturated-soil permeability. Additionally, pressure and temperature also have an effect on the permeability of soil. As the temperature increases and pressure decreases, dissolved-gas solubility decreases resulting in the exsolution of gas bubbles which remain entrapped.

Experiments were performed by Orlob and Radhakrishna (1958) to identify the effect of entrapped air on the effective porosity, permeability and dispersion of seven sand samples. A linear relationship was identified between the increase in entrapped air volume and the decrease in permeability for all of the experimental soils. The entrapment of 10% of air in sand could reduce the effective porosity (pore space available for groundwater flow) by up to 15%, and result in a reduction of permeability by 25%. Higher amounts of entrapped air were also found to reduce the hydraulic dispersion (dispersivity, times the velocity) of the experimental media. Faybishenko (1995) performed experiments in which several infiltration methods were attempted on cores to quantify the amount of entrapped air. They measured air entrapment of 5 to 10% for ponded (downward) infiltration, less than 5% for upward imbibitions, and less than 0.2% for upward saturation under a vacuum and ponded (downward) infiltration following carbon dioxide flushing. These experiments provided a foundation for understanding how to achieve almost complete saturation of a soil core and identified the differences in air entrapment between upward imbibition versus downward infiltration. Faybishenko (1995) described a three-stage process in which the quasi-saturated hydraulic conductivity of soils evolves with time. Upon initial air entrapment, the conductivity decreases due to the entrapment of air. Due to capillarity, the air moves from the small pores into the largest pores and slowly dissolves into the water until the saturated hydraulic conductivity is achieved. Later, the conductivity decreases due to clogging of pores by microbiological activity.

Column tracer tests were performed by Fry et al. (1995) to evaluate the retardation factor between bromide and dissolved oxygen in the presence of entrapped air. The authors calculated a linear increase in the retardation of dissolved oxygen (from 1 to 6.6) relative to bromide with increasing amounts of air entrapment (0 to 4.4%). The retardation was due to the need for equilibrium to be obtained between the dissolved oxygen and the entrapped air. Fry et al. (1997) performed experiments under three distinct air emplacement methods to aid bioremediation, namely air sparging, injection of water supersaturated with air and the injection of hydrogen peroxide. It was identified that an increase in trapped gas volume from 14 to 55% results in a decrease in the relative hydraulic conductivity from 0.62 to 0.05. Sakaguchi et al. (2005) measured the change in the quasi-saturated hydraulic conductivity of a sandy loam and clay andisol as a function of air entrapment. The authors found that as the amount of entrapped air increased to 10%, it resulted in a decrease of the hydraulic conductivity by an order of magnitude for both soils. As the amount of entrapped air increases, soil with lower dry bulk densities are more likely to significantly decrease in the quasi-saturated hydraulic conductivity.

Marinas et al. (2013) performed a set of experiments on a variety of soil types to identify the change in the quasi-saturated hydraulic conductivity as a result of air entrapment. Entrapment of 8 to 15% air resulted in a decrease of the saturated hydraulic conductivity by two to six times. The authors performed water-table fluctuations of up to 250 cm and identified that as the water table was raised, it resulted in the compression of the underlying gas bubbles by 18 to 26% such that the quasi-saturated hydraulic conductivity increased by 1.16 to 1.57 times.

Bloomsburg (1964) performed experiments on multiple cores containing sandstone, Alundum (fused alumina) and glass beads to identify diffusion rates of entrapped air within the cores under non-flowing conditions. It took approximately 40 and 50 days for all the entrapped air to diffuse out of a 2 cm glass bead core and 6 cm Alundum core, respectively. Adam et al. (1969) identified that when water is allowed to imbibe a soil core, the amount of entrapped gas can vary from 5% in clay soils to 50% in sandstone. They determined that the rate of removal of entrapped gas by diffusion is highest for fine grained soil due to the effects of capillarity.

The presence of air bubbles due to air entrapment and biogenic gas production at field sites has also been documented. Ronen et al. (1989) measured specific discharge at various depths within the shallow groundwater surface at a field site, and identified the presence of a stagnant water layer that extended to a depth of 60 cm below the water table. Below the 60 cm depth, the specific discharged increased by an order of magnitude. This phenomenon was attributed to the presence of entrapped bubbles produced by denitrification rather than air infiltration during recharge. Due to the large bacteria colony, very high depletion of oxygen and high concentrations of N_2O were observed. Ryan et al. (2000) identified shallow stagnant water zones at three field sites by using surface applied tracer tests, multi point tracer tests and measuring nitrate concentrations. The fit between the field data and a numerical model was improved with the inclusion of a shallow stagnant water zone with lower hydraulic conductivity. The authors proposed a variety of plausible causes for the existence of the stagnant water zone including temperature variations resulting in exsolution of gas bubbles and geochemically produced gases like nitrogen and methane.

The use of argon and nitrogen as indicators to quantify the influence of physical processes including advective and diffusive gas fluxes, degassing of methane and gas transport near an oil spill plume was identified by Amos et al. (2005). The infiltration and transport of recharge water containing oxygen, nitrogen and argon results in enrichment of nitrogen and argon prior to contact with the plume. Methanogenesis and methane production within the plume results in the depletion of argon and nitrogen into the water due to bubble formation and subsequent degassing of methane.

Haberer et al. (2012) performed a series of experiments on a flow cell filled with glass beads in an attempt to evaluate the mass transfer of oxygen across a fluctuating water-table system. The authors performed three experiments, namely a single drainage and imbibition cycle over 15 minutes, along with rapid and slow fluctuations over 42 hours each. It was identified that up to six times more oxygen dissolves into anaerobic water during an imbibition cycle versus a drainage cycle. With rapid fluctuations, the entrapped gas is allowed a short period of time to equilibrate with the groundwater before undergoing another drainage-imbibition cycle. The drainage cycles transport oxygen deeper into the groundwater while the imbibition cycles entrap air and subsequently dissolve some of the oxygen, resulting in a thicker smear zone contributing more oxygen to the groundwater. With slow fluctuations, the entrapped air is not released at once during a drainage cycle, but is slowly released, thus allowing for a longer equilibration time with the water. The authors concluded that rapid fluctuations contribute a higher amount of oxygen rather than a system with slower fluctuations, especially under fast groundwater flow velocities, when more water contacts the entrapped air resulting in faster dissolution and transport. Conversely, slower groundwater systems can result in the accumulation of oxygen due to the slower equilibration between the aqueous and gaseous phase and slower transport rate out of the system.

Freitas (2009) studied the transport behavior of an ethanol-gasoline mixture (E10) following a controlled release at a field site that underwent natural water-table fluctuations. Initially, most of the ethanol stayed within the unsaturated zone (above the capillary fringe), while other hydrocarbons migrated to the saturated zone. After the water table rose above the zone of ethanol retention, higher concentrations of ethanol were detected at the source due to the eventual saturation of this zone of imbibition. The delayed transport of ethanol is correlated to the water content of the soil, resulting in slower mobility.

Williams and Oostrom (2000) quantified the dissolved oxygen concentrations within a flow cell under multiple water-table fluctuation scenarios. They effectively utilized a numerical model (STOMP) to simulate their experimental results. Amos et al. (2006) also simulated the data of Williams and Oostrom (2000) by using a reactive transport model (MIN3P). Both models use formulations on equilibrium gas partitioning and the hysteretic pressure head-water saturation relationships based on Kaluarachchi and Parker (1992).

1.3 Research Objectives

The objective of this research was to identify and measure the changes in physical properties and dissolved gas concentrations of a sand media under fully saturated and fluctuating water-table scenarios (flowing groundwater). These objectives were met by carrying out experiments in two phases; namely physical characterization and gas entrapment. In Phase 1 (physical characterization), the water saturation and hydraulic conductivity were measured under saturated conditions and five drainage-imbibition cycle scenarios, to identify the changes in water content and conductivity between each experimental scenario. Three bromide tracer tests were performed under fully saturated, 29 cm and 45 cm drainage-imbibition cycles. The break-through curves were monitored at multiple sampling points spread across the length and depth of the sand tank in order to quantify the changes in dispersivity and groundwater velocity over the duration of each tracer test. In Phase 2 (gas entrapment), the concentrations of dissolved argon and oxygen were measured across the sand tank under fully saturated, 29 cm and 45 cm drainage-imbibition cycles. Argon was monitored as a non-reactive tracer for dissolved oxygen. The 45 cm experiment was run for five months to capture the changes in dissolved gas concentrations over time. This experiment was modelled using a reactive transport model, MIN3P (Mayer et al., 2002), to help understand which physical mechanisms controlled the change in dissolved gas concentrations.

2. Methods

2.1 Sand Tank Design, Construction and Set-up

The sand tank (Figure 2.1) was constructed using ¾ inch Polyvinyl Chloride (PVC) sheets which were secured with stainless steel bolts and sealed with silicon caulking to make it air and water tight. Upon completion, the inner dimensions were 188 cm long, 60 cm high and 10 cm wide. A lid was constructed to fit across the top opening of the sand tank. A removable rubber lining was installed in between the lid and the top of the tank to help keep the sand tank air tight when required. Three windows were installed on the front face of the sand tank for visual observation of the sand and water level.

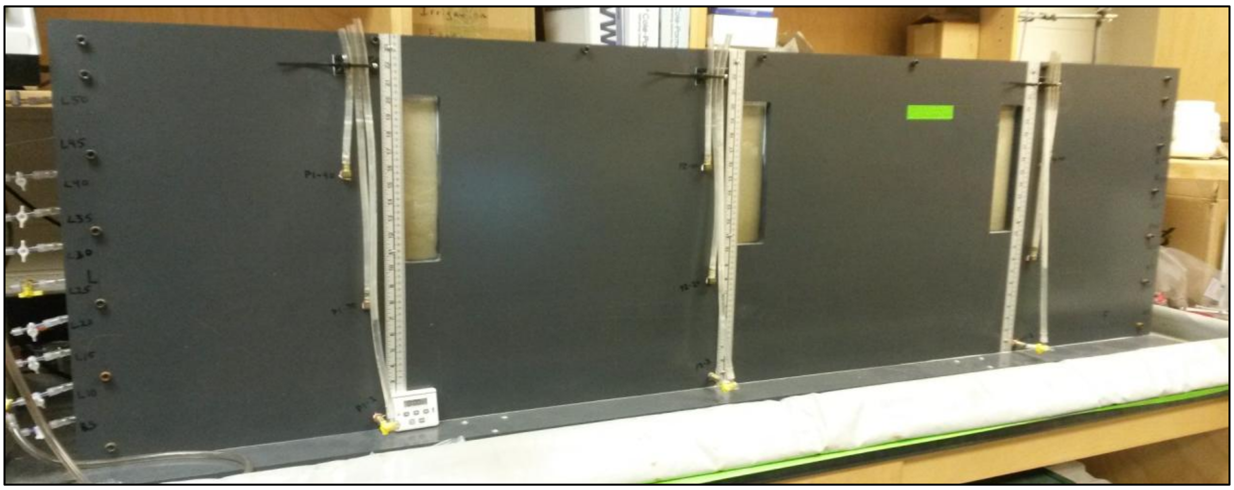

Figure 2.1 The front face of the sand tank, showing the locations of the three water level piezometer nests and the vertical positions of the inflow ports

Ten ¼” ports at 5 cm intervals were installed on each end of the sand tank from 5 cm to 50 cm above the base (Figure 2.2). Each port was then fitted with a 1/4” male NPT/ 1/8” barb brass fitting. The brass fittings were connected with Tygon tubing and two-way and three-way valves to form input and output manifolds. Three metal fittings were installed on the lid of the sand tank to serve as pressure bleed ports.

Three water-level piezometer nests were installed at 30 cm, 90 cm and 150 cm across the length of the front face of the sand tank (Figures 2.1 and 2.2). Each nest consisted of three piezometers that were installed at 2 cm, 20 cm and 40 cm above the base of the sand tank. The piezometers consisted of a brass fitting screwed into the side of the tank at the appropriate depth, attached to a length of ¼" Tygon tubing. All the fittings (side and front walls) were filled with glass wool to prevent the mobilization of sand or gravel.

A total of five multilevel piezometer nests were installed across the length of the sand tank at 30 cm, 60 cm, 90 cm, 120 cm and 150 cm from the left side and were named N1, N2, N3, N4 and N5, respectively. Each piezometer nest consists of 14 stainless steel piezometers with an outer diameter of 1/4".The 14 piezometer lengths are 2.5 cm, 5 cm, 7.5 cm, 10 cm, 12.5 cm, 15 cm, 17.5 cm, 20 cm, 25 cm, 30 cm, 35 cm, 40 cm, 45 cm and 50 cm. These piezometer lengths are denoted as depths from the top of the sand surface. The bottom 1 cm of each piezometer was fitted with glass wool to serve as a filter. Each piezometer nest was constructed by installing 14 piezometers into pre-drilled holes in a block of Plexiglas. The Plexiglas blocks with the attached piezometers were driven into the sand such that the Plexiglas blocks rested on the top of the sand surface while the base of each piezometer was located at the pre-determined depths. Each piezometer was fitted with a female luer fitting attached by Tygon tubing to aid the sample collection.

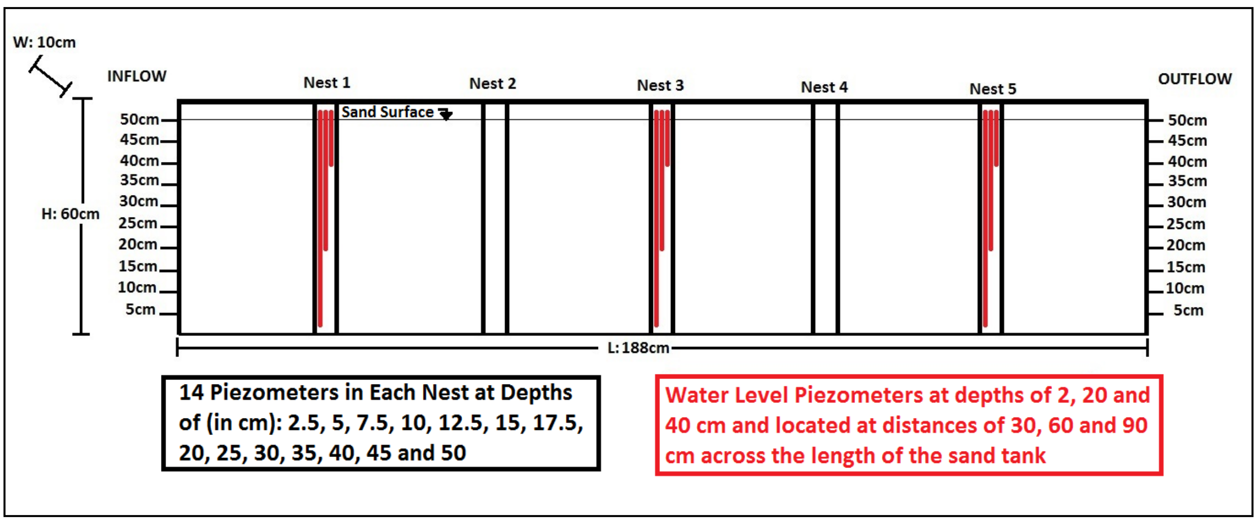

Figure 2.2 Graphical representation of the sand tank, showing inflow and outflow port locations, along with the locations of the water level piezometers and five multi-level piezometer nests

The tank was fitted with four iLoad Low Profile Digital USB Capacitive Load Cells (Loadstar Sensors) to continuously record the weight of the tank. Each load cell has a maximum capacity of 250 lb (113.4 Kg) for a total measurable weight of 1000 lbs (453.6 Kg). The reliability of the weight measurements were tested by measuring the reported weights of the load cells against gravimetric weights of water. The percent error was calculated for the weight measurements with increasing and decreasing weights and is listed in Table 2.1.

Increasing weight		
Gravimetric Weight (Kg)	Load Sensors (Kg)	% Error
19.40	19.40	0.00
20.40	20.44	0.17
21.40	21.43	0.14
22.40	22.41	0.05
23.40	23.48	0.34
24.40	24.47	0.26
25.40	25.43	0.10
26.40	26.45	0.18
27.40	27.44	0.12
29.41	29.46	0.18
	Average Error:	**0.15**
Decreasing weight		
Gravimetric Weight (Kg)	Load Sensors (Kg)	% Error
29.36	29.36	0.00
28.28	28.30	0.06
27.33	27.35	0.08
26.10	26.16	0.22
24.68	24.76	0.32
23.63	23.73	0.43
	Average Error:	**0.19**

Table 2.1 The reported weights from the load cells compared to gravimetrically weighed samples along with the percent error.

In an effort to promote homogeneous flow through the sand tank, two 10 cm wide vertical gravel bands were created at the inflow and outflow. The rest of the sand tank was filled with 30/40 mesh Ottawa sand. The packing of the sand tank was performed by creating a thin base layer and proceeding to fill up the sand tank in 2 cm layers to a height of 50.5 cm.

Carbon dioxide was used to flush the dry sand in the sand tank due to its high solubility in water relative to atmospheric gases. Once water was pumped into the tank, the carbon dioxide dissolved resulting in complete saturation. The lid of the sand tank was fastened and all the ports were sealed, with the exception of one port on the lid which served as a bleed line. Carbon dioxide was flushed at a slow flow rate to displace all the air in the tank. The carbon dioxide was input at various heights along the inflow and outflow sides of the sand tank to achieve maximum air displacement. Gas samples were collected from various ports and were analyzed with a Gas Chromatograph (GC) to confirm that all the air was removed (the peaks for argon, oxygen and nitrogen were all below the detection limit). De-Ionized water was pumped into the sand tank from the 5 cm input port using a Masterflex Console Drive, Model 7017-20 with Masterflex Silicone pump tubing. The water level in the sand tank was topped up until the dissolution of carbon dioxide stopped and a static water level at 47 cm was achieved. The measured weights of the sand tank, sand, gravel and water are presented in Table 2.2.

Components	Weight (Kg)	Total Weight (Kg)
Empty sand tank	86	86
Lid	10	96
Sand and Gravel	72	168
Water @ 47 cm	35	203

Table 2.2 Weights of the sand tank constituents

To maintain specific hydraulic heads at 1 cm intervals at the outflow end of the tank, a plastic reservoir was attached to two consecutive outflow ports with Tygon tubing. The reservoir was attached to a stable retort stand so that the elevation of the outflow port could be adjusted (Figure 2.3).

Figure 2.3 The outflow end of the sand tank showing the positions of each outflow port and the reservoir used to control the hydraulic head.

2.2 Hydraulic Conductivity Testing

The hydraulic conductivity was calculated by measuring the hydraulic gradient across the tank using three pump flow rates; 30 mL/min, 60 mL/min and 120 mL/min. Six hydraulic conductivity measurements were conducted under varying degrees of gas entrapment; fully saturated and five drainage-imbibition cycles (fluctuating water-table scenarios) to depths of 10 cm, 20 cm, 29 cm, 38 cm and 45 cm. In each of the fluctuating water-table scenarios, the water table was lowered to the specified depth by draining the tank (gravity drainage) from the outflow port that corresponds with the fluctuation level; the capillary fringe was allowed to stabilize by visually observing the distinction between the wet and dry sand using the three windows on the front face of the sand tank; and the water level was raised back up to the 47 cm level from the 5 cm inflow port using the Masterflex pump at a flow rate of 20 mL/min. The weight of the sand tank was constantly monitored during all the experiments to quantify the amount of water and entrapped air in the tank. For each experiment, the initial flow rate was set to 30 mL/min. Hydraulic head measurements were observed from all three piezometer nests and the values were recorded after the head stabilized across the sand tank. The measurements were repeated at flow rates of 60 mL/min and 120 mL/min. The flow rate was then decreased to 20 mL/min and water was pumped until the water level returned to the pre-experiment level.

2.3 Bromide Tracer Tests

Three tracer tests were conducted under a fully saturated condition, a 29 cm drainage- imbibition cycle and a 45 cm drainage- imbibition cycle. These three test conditions were selected so that a completely saturated test could be compared to an intermediate air entrapment and a 'full' air entrapment test. The pump flow rate was set to 2 mL/min to allow for a residence time of 14 days which would help monitor the break-through curve of the bromide over the course of the experiment.

Samples were collected from six specific piezometer depths (7.5 cm, 12.5 cm, 17.5 cm, 25 cm, 35 cm and 45 cm) across all five piezometer nests for a maximum of 30 samples per sampling event. To prevent significant drawdown, a sampling rate of 1 mL/min was used to collect 20 mL samples. The bromide concentrations were measured to capture the arrival of the peak bromide concentrations (break-through curve) at all of the selected piezometers. All the piezometers were sampled within an 18 hour period to capture a snapshot of the spatial distribution of the bromide concentrations across the sand tank. Samples were collected at an average frequency of every 36 hours.

Bromide measurements were performed using a Cole Parmer ISE double junction bromide probe connected to an Oakton Ion 6 Acorn Series pH/Ion/°C meter. The probe uses 10 % KNO_3 as the Reference Fill Solution. 1 ppm, 10 ppm and 100 ppm bromide concentration standards were prepared using a 1000 ppm Br standard (0.1 % NaBr, 99.9 % Water). The meter was calibrated by progressing from the 1 ppm to the 100 ppm standard. The readings were allowed to stabilize prior to the next standard being used. A stir bar was placed into the glass sample jar, which was placed on a stir plate. The stir plate was set to spin at a low speed, to allow for slow rather than turbulent mixing. The Br probe is highly sensitive to temperature variations; therefore a 2 cm thick Styrofoam block was placed between the stir plate and the glass sample jar. The Styrofoam block was replaced each time a new sample was collected to minimize any temperature variations.

2.4 Bubble Entrapment Experiments

The bubble entrapment experiments involved three experiments that were consistent with the Br tracer tests; namely fully-saturated conditions along with 29 cm and 45 cm fluctuating water-table conditions. For the fully-saturated experiment, argon and oxygen stripped (anaerobic) de-ionized water was allowed to flow through the sand tank, leaving the upper water surface exposed to the atmosphere. In each of the fluctuating water-table experiments, the water level was lowered by draining the output ports until the desired water level was attained. The lowering of the water level allowed air to enter the variably saturated soil. After the capillary fringe stabilized, the water level was raised back from the 5 cm input port using the same de-aerated water to allow air bubbles to be entrapped within the previously saturated shallow zone. Flow was then resumed so that the dissolved-gas concentrations could be monitored across the sand tank.

Anaerobic water was prepared by sparging de-ionized water in glass carbuoys with high purity nitrogen for 8 hours at a medium flow rate to strip the majority of the dissolved argon and oxygen. Upon completion, water samples were collected from these carbuoys, analyzed with the static headspace method (see section 2.4.1) and run on the GC, to ensure that the concentrations of argon and oxygen were low. The sparging method achieved 90 to 95 % removal of argon and oxygen. This air-stripped input water was pumped through the tank while maintaining a positive nitrogen pressure within the carbuoy, to prevent any air from diffusing in. In order to minimize the diffusion of air through the pump tubing, a sealed Plexiglas chamber was built to house an Ismatec compact analog pump. The chamber was constantly purged with nitrogen to maintain an oxygen and argon free environment. The pump in the chamber was fitted with Viton tubing which was connected to stainless steel tubing on either side of the pump. Stainless steel tubing in the glass carbuoy transported water to the pump. The Viton tubing made contact with the water within the anaerobic chamber and was pumped into the sand tank via stainless steel tubing. This setup ensured that the air stripped water never made contact with the atmosphere as it travelled from the glass carbuoy to the sand tank (Figure 2.4).

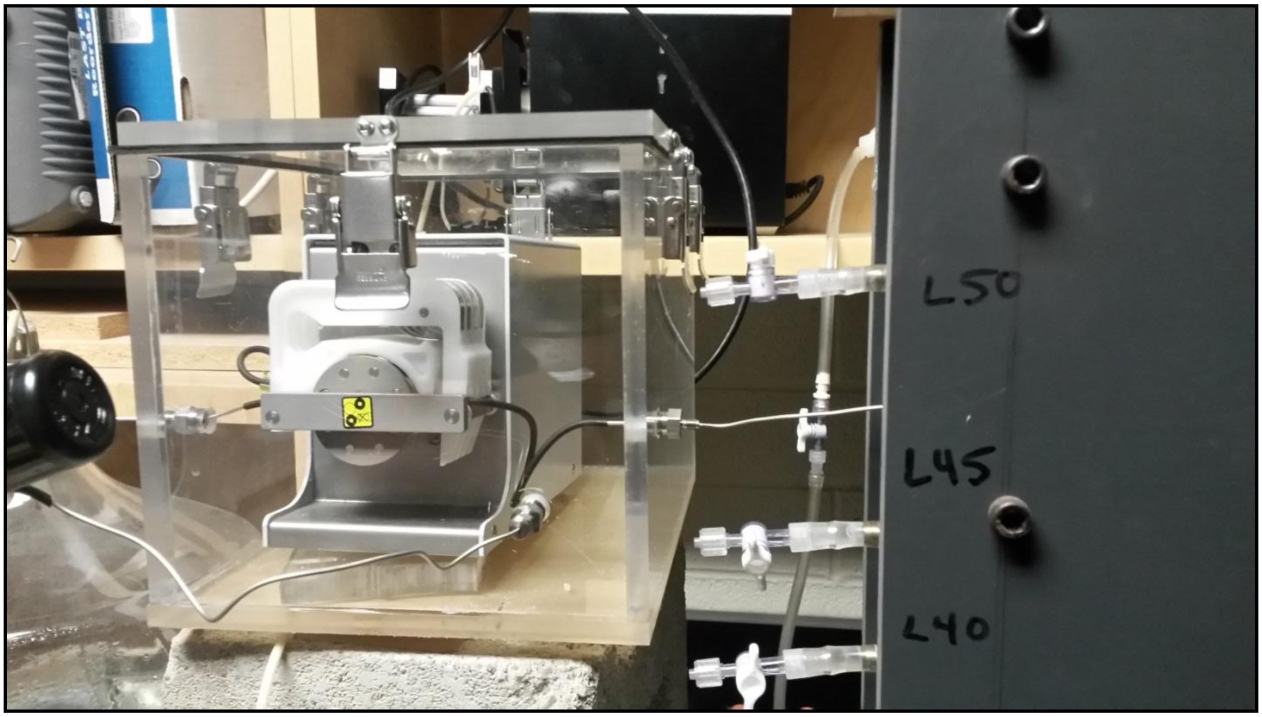

Figure 2.4 An Ismatec peristaltic pump housed within an anaerobic Plexiglas chamber

Prior to the commencement of the experiments, the sealed (except the bleed port on the lid) empty sand tank was flushed with carbon dioxide until the dry sand was stripped of air. Next, the sand tank was filled with anaerobic water up to the 47 cm level such that the sand was fully saturated. In each of the three experiments, the top face of the sand was left exposed to the atmosphere and flow was started from left (input) to right (output) at a rate of 2 mL/min. In the case of the 29 cm and 45 cm fluctuating water-table experiments, the water level was lowered by 29 cm and 45 cm, respectively by draining the adjacent outflow port until the level was achieved. The capillary fringe was allowed to stabilize for 12 hours after which the water level was raised up at a flow speed of 20 mL/min from the 5 cm inflow port. After the water level in the sand tank was raised back to the 47 cm, the flow rate was set to 2 mL/min and the experiment was started.

2.4.1 Sample collection

The sand tank contained 35 L when fully saturated and 22 L after the 45 cm drainage-imbibition cycle. These experiments required up to a maximum of 60 - 70 samples to be collected per sampling round, hence it was important to ensure that the volume of water withdrawn from the sand tank was minimized (less than 15 % removal of sand tank volume). For these experiments, US EPA 40 mL vials with caps fitted with 22 mm thick Teflon lined silicone septa were used.

The actual volume of these vials was approximately 43 mL and if 70 samples were collected, it would result in the extraction of 3.01 L of water from the sand tank during each sampling event. Since it took around 35 hours to collect 70 samples, the removal of 3.01 L over two days was less than 10 % of the total sand tank volume in both the saturated and the fluctuating water-table experiments.

A static headspace method was used to determine the dissolved-gas concentrations. A 60 mL plastic syringe was used to collect a 44 mL water sample from each piezometer. These samples were collected by instantly removing the set volume of water from a piezometer and inserting it quickly (to prevent exposure to air) and gently (to prevent mixing the water with air) into a pre-weighed dry vial. The vial was capped and weighed to determine the sample volume.

10 mL of helium was filled into a Hamilton H1010 Gastight syringe and was injected into the vial. Prior to the injection of helium, another needle was injected into the septa to allow water to escape while the 10 mL headspace was created. This vial was then placed on a shaker table and allowed to equilibrate for 10 minutes, after which the vial was weighed to determine the volume of the headspace. Another gastight syringe was used to collect a 5 mL gas sample from the headspace, and this sample was injected into the GC for analysis.

After the instantaneous sample was collected, the sand tank was left for at least 22 minutes (22 minutes x 2 mL/min = 44 mL) to allow the water level to recover. Hence, only two samples could be collected per hour which meant that 70 samples could only be collected over 35 hours. Each sampling round was intended to be a snap-shot of the concentrations in the sand tank at that moment. Due to the sample volume and time constraints involved, it meant that this snap-shot would essentially last up to 35 hours (provided that samples were constantly collected and that no other issues arose).

2.4.2 Sample analysis

All the samples collected during these experiments were analyzed using a SRI 8610A Gas Chromatograph with an attached SRI 110 detector chassis. The set up consisted of two columns; CTR I and CTR III manufactured by Alltech Associates, which used high-purity helium as the carrier gas.

CTR I and CTR III are both 6 feet long and consist of an inner and outer column. CTR I has an outer column that has an inner diameter of 0.25 inches which is packed with activated molecular sieve and an inner column that has an inner diameter of 0.125 inches which is packed with a porous polymer mixture. CTR III has an outer column that has an inner diameter of 0.25 inches which is packed with activated molecular sieve and an inner column that has an inner diameter of 0.125 inches which is packed with molecular sieve and oxy adsorbent. CTR I was used to detect oxygen and nitrogen while CTR III was used to detect argon and nitrogen. The nitrogen concentrations from both the columns were recorded for mass balance, but were not used for the analysis.

The GC was calibrated for argon and oxygen by analyzing de-ionized water that was in equilibrium with the atmosphere, using the static headspace method. A minimum of three samples were used to ensure precision and accuracy of the area/height ratio for the peaks. The GC was calibrated at the start of every sampling session. Re-calibration was performed after every 15 samples were run (after approximately seven hours) and especially if the concentration results were spurious.

The measured concentrations of oxygen and argon from each experimental scenario were contoured using Tecplot 360. The concentrations for each sampling session were input into the system and the krigging tool was used to contour dissolved-gas concentrations across the sand tank. The concentrations identified in each sampling event were graphically presented to help with the visualization

3. Physical Characterization

3.1 Introduction

The presence of air bubbles within a groundwater system will affect physical properties like permeability and hydraulic conductivity which results in a variable flow field. Gas bubbles are introduced into a groundwater system due to multiple processes including air entrapment, biogenic gas production and exsolution due to temperature and pressure variations. Thus, it is important to quantify and distinguish between the physical properties of a porous media under fully and variably-saturated flow conditions. The entrapment of air bubbles will reduce the overall water content of a soil unit which in turn will result in changes to the permeability (Christiansen, 1944) and hydraulic conductivity (Orlob and Radhakrishna, 1958; Fry et al., 1995; Faybishenko, 1995; Ryan et al., 2000; Sakaguchi et al., 2005; Marinas et al., 2013) of the groundwater. These changes have been determined from field measurements (Ronen et al., 1989; Ryan et al., 2000; Amos et al., 2005) and laboratory-scale experiments (Faybishenko, 1995; Fry et al., 1995; Sakaguchi et al., 2005; Marinas et al., 2013). The relationship between the amount of entrapped air and the resultant reduction in the relative hydraulic conductivity has been experimentally measured and fit (Faybishenko, 1995; Sakaguchi et al., 2005; Marinas et al., 2013) to analytical models by van Genuchten (1980) and Faybishenko (1995).

The experiments carried out in this chapter were intended to identify physical properties including hydraulic conductivity, porosity and water content (gravimetrically), flow velocity and dispersivity (tracer tests) under saturated flow conditions; and to distinguish these properties from variably-saturated conditions induced by water-table fluctuations and air-bubble entrapment.

3.2 Literature Derived Sand Parameters

The sand used to pack the sand tank was 30/40 mesh Ottawa sand. This sand was specifically chosen because it had been characterized by Williams and Oostrom (2000), which served as a foundation for the work conducted in this thesis.

To identify soil-water retention curve parameters, Williams and Oostrom (2000) used a saturation-capillary pressure cell method as described by Lenhard (1992). They fit the pressure head – water content data using the Brooks – Corey model and obtained values for the Brooks-

Corey air-entry pressure head (Ψa) and pore size distribution index (λ) as 13.0 cm H_2O and 5.0, respectively. Additionally, they identified the irreducible water saturation to be 0.01. The equation used was as follows (Brooks and Corey, 1964):

$$Se = \left\{\frac{\Psi a}{\Psi}\right\}^{\lambda}, \quad \Psi < \Psi_a \qquad (3.1)$$

where Se is the effective saturation, Ψa is the air-entry pressure head, Ψ is the pressure head and λ is the pore size distribution index. The Brooks-Corey parameters identified by Williams and Oostrom (2000) were used to prepare a soil-water retention curve which was then fit with the van Genuchten (1980) model (Figure 3.1). The equations used were as follows (van Genuchten, 1980):

$$\Theta = \left(\frac{1}{1+(\alpha h)^{n}}\right)^{m} \qquad (3.2)$$

$$\Theta = \left(\frac{\theta - \theta r}{\theta s - \theta r}\right) \qquad (3.3)$$

where Θ is the effective saturation, h is the pressure head, θ is the soil-water content, θr and θs represent the residual-water content and the saturated-water content, respectively. The parameters α, n and m are curve fitting parameters for the van Genuchten model where m = (1-(1/n)). The residual water content (θr) was not measured, hence it was identified by extrapolating the soil water retention graph in Figure 3.1 to higher pressure head values (van Genuchten, 1980), obtaining a value of 0.005. The value of θs was set to the porosity value of 0.363, which was measured gravimetrically. The values of α, n and m were identified as 0.065, 10.35 and 0.903, respectively, which was consistent with Amos and Mayer (2006).

These identified van Genuchten parameters were used to determine the relative hydraulic conductivity (Kr) versus pressure-head relationship (Figure 3.2). The equation used was as follows:

$$Kr(h) = \frac{\{1-(\alpha h)^{n-1}[1+(\alpha h)^n]^{-m}\}^2}{[1+(\alpha h)^n]^{m/2}} \qquad (3.4)$$

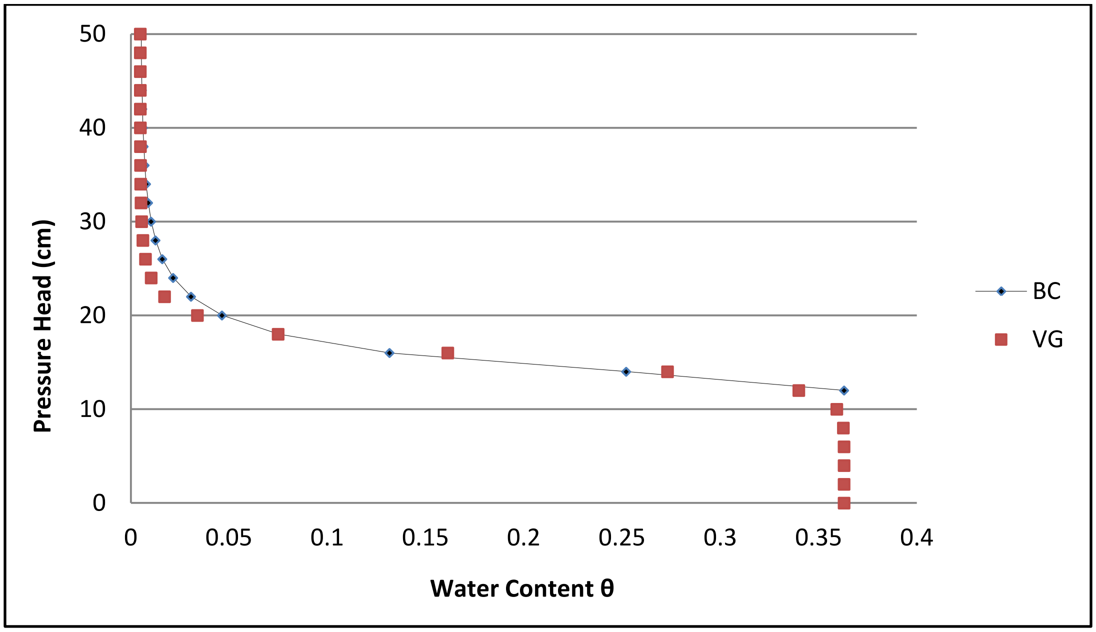

Figure 3.1 Water Content – Pressure Head relationship determined by fitting van Genuchten (VG) parameters to the Brooks-Corey (BC) parameters identified by Williams and Oostrom (2000). α = 0.065 cm, m = 0.903 and n = 10.35

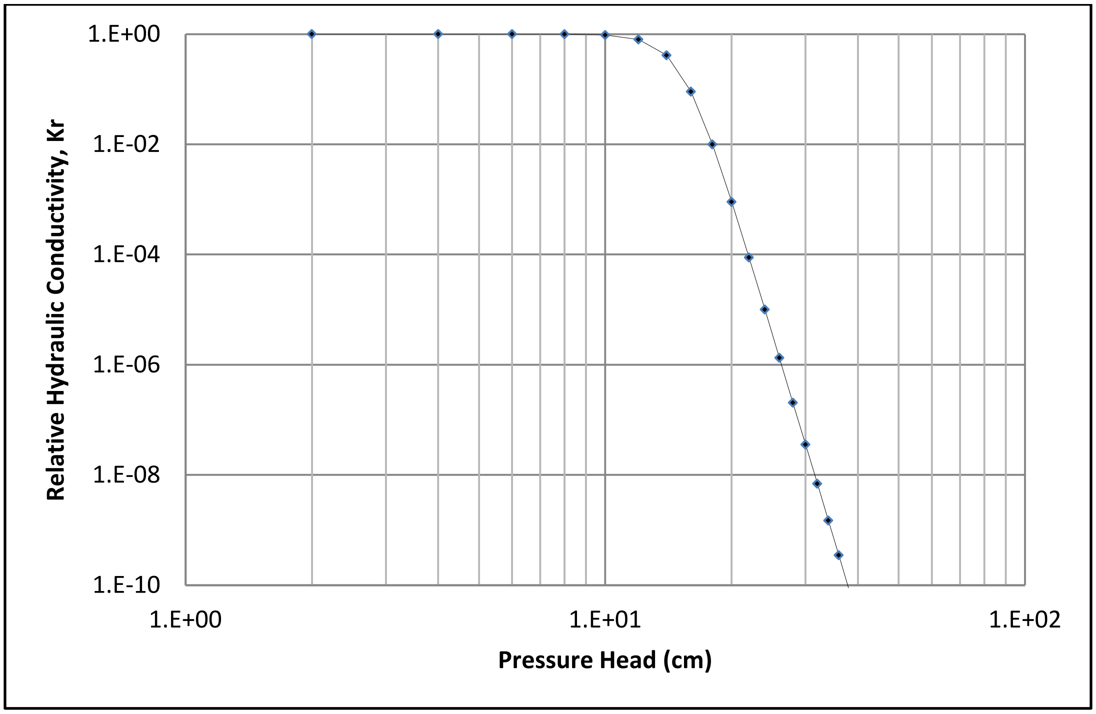

Figure 3.2 Relative Hydraulic Conductivity vs Pressure Head evaluated from van Genuchten parameters.

3.3 Hydraulic Conductivity

Hydraulic conductivity was measured at three flow rates through the sand tank, namely 30, 60 and 120 mL/min. The head was measured across the sand tank by measuring the water level at each water-level piezometer nest on the front face of the sand tank. The methodology was as follows:

Step 1: The volumetric flow rates (Q) of 30, 60 and 120 mL/min and the cross sectional area of the inflow (A) was used to calculate the respective values of the Darcy flux (q). The Darcy flux and the measured hydraulic heads (h) across the length of the sand tank (l) were used to calculate the saturated hydraulic conductivity (K_{Sat}) under all three flow rates. The average value of K_{Sat} from the three flow rates was 0.422 cm/s, with a standard deviation of 0.04 cm/s. This value of K_{sat} was used for all of the proceeding calculations. The equations used were as follows:

$$q = \frac{Q}{A} \qquad (3.5)$$

$$q = -K_{sat}\frac{dh}{dl} \qquad (3.6)$$

Step 2: The 10 cm fluctuating water-table experiment resulted in the creation of an entrapped air layer in the upper 10 cm, while the lower 37 cm remained fully saturated. This resulted in a reduction in the hydraulic conductivity of this 10 cm layer (K_{10}). The three flow rates would result in respective hydraulic gradients which were averaged to determine total hydraulic conductivity (K_{Tot10}), where total hydraulic conductivity refers to the hydraulic conductivity across the entire depth of the sand tank under the 10 cm fluctuating water-table scenario. The soil that undergoes water-table fluctuations that result in the entrapment of air bubbles below the water table will be defined as quasi-saturated soil (Faybishenko, 1995) or layers (experimental fluctuation thickness). The value of K_{10}, referring to the hydraulic conductivity of the 10 cm quasi-saturated layer, was calculated by inputting the calculated value of K_{Tot10} into the depth-weighted arithmetic mean equation. In this equation, b is the total depth below the water table (47 cm) and K_i and b_i are the hydraulic conductivity and thickness of the specific layers. A sample calculation is provided below:

$$K_{Tot10} = \frac{\sum K_i b_i}{\sum b} \qquad (3.7)$$

$$K_{Tot10} = \frac{(K_{Sat} * 37cm) + (K_{10} * 10cm)}{47cm}$$

$$(0.396\ cm\ s^{-1} * 47cm) = (0.422\ cm\ s^{-1} * 37cm) + (K_{10} * 10cm)$$

$$K_{10} = 0.298\ cm/s$$

Step 3: This process was repeated for all the experiments such that the 20 cm, 29 cm, 38 cm and 45 cm fluctuating water-table experiments had a total of 2, 3, 4 and 5 entrapped air layers respectively, along with a saturated layer. The depth-weighted arithmetic mean equation was used to calculate the hydraulic conductivities of each layer.

Figure 3.3 presents the results of the depth-weighted arithmetic mean of hydraulic conductivity for each of the 6 scenarios. In the 10, 20, 29, 38 and 45 cm fluctuating water-table scenarios, the values of hydraulic conductivity for each layer (K_{10}, K_{20}, K_{29}, K_{38} and K_{45}) are presented along with the thickness of each layer and the combined conductivity of the entire entrapped air zone.

For example, in the 20 cm fluctuating water-table experiment, the water level was initially at 47 cm. The level was dropped by 20 cm and raised back up. The hydraulic conductivity of each 10 cm layer contained within the 20 cm fluctuation zone were calculated to be 0.269 cm/s and 0.298 cm/s while the combined conductivity of the entire 20 cm zone was 0.284 cm/s. The combined conductivity value is presented to illustrate the hydraulic conductivity difference between the entrapped air zone and the saturated layer.

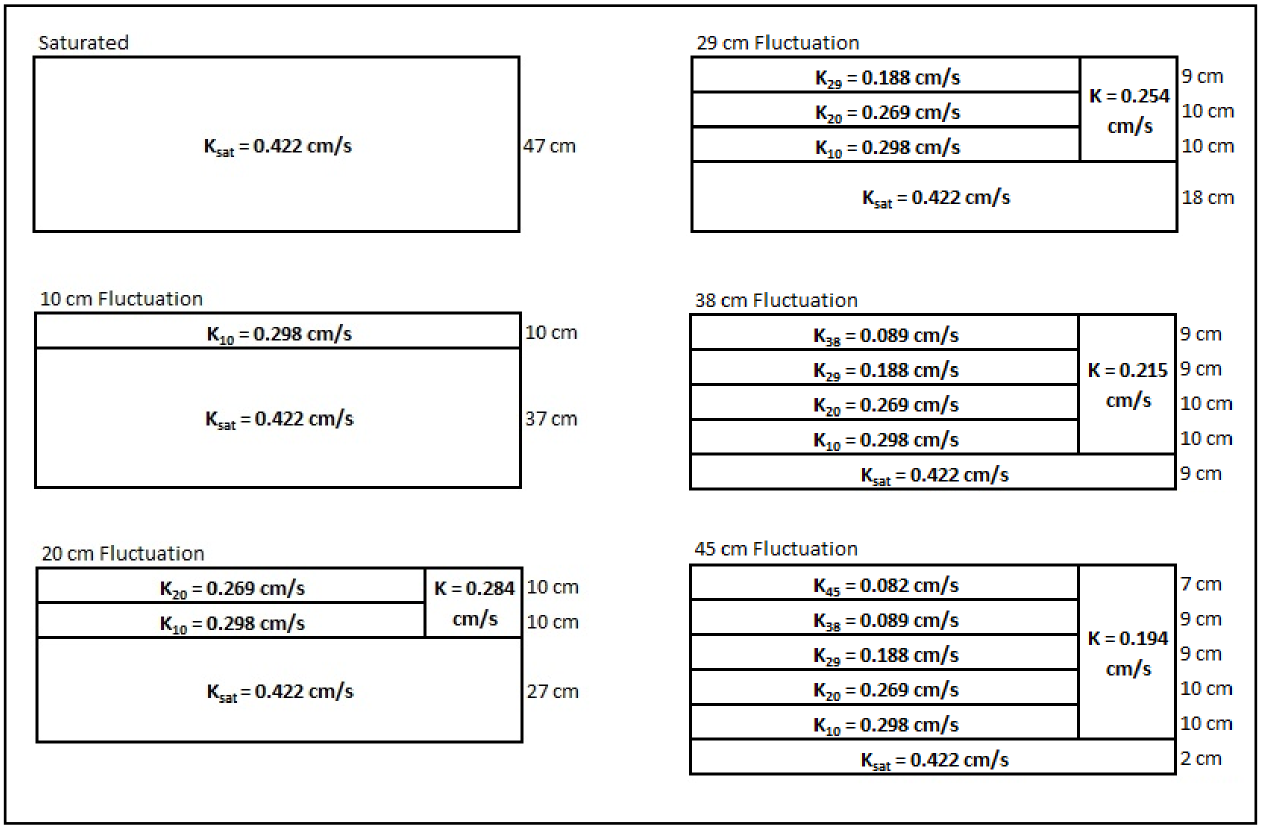

Figure 3.3 Schematic showing the hydraulic conductivities of the entrapped air layers as a result of each water-table fluctuation scenario.

The weight of the sand tank was monitored during each scenario and the weight was recorded as the water level was dropped and raised. The change in the weight during the water-table fluctuation accounts for the weight of entrapped air. The amount of entrapped air and the decrease in hydraulic conductivity in each fluctuating water-table scenario were plotted against the water-table fluctuation level and are presented in Figure 3.4. There is a direct relationship between the increase in entrapped air and the reduction in hydraulic conductivity. The 10 cm fluctuation resulted in 1.16 % entrapment of air. This low value is because the capillary fringe occupies the 12 cm above the water table and hence very little air enters. However, the 20, 29, 38 and 45 cm fluctuations allowed the air content to increase to 4.96, 8.26, 13.54 and 17.62 %, respectively. The increase in air content follows a linear trend after the first 10 cm fluctuation, such that each successive fluctuation results in the entrapment of approximately 4 % air. This linear increase in air entrapment and the resulting decrease in hydraulic conductivity could be extrapolated in the case of a deeper sand tank, which is particularly evident from the 29, 38 and 45 cm water-table fluctuation experimental data. However, the compression of the entrapped bubbles by overlying water pressure under greater water-level fluctuations will have to be considered (Ronen et al., 1989; Marinas et al., 2013), when evaluating the fate (dissolution) of these entrapped bubbles.

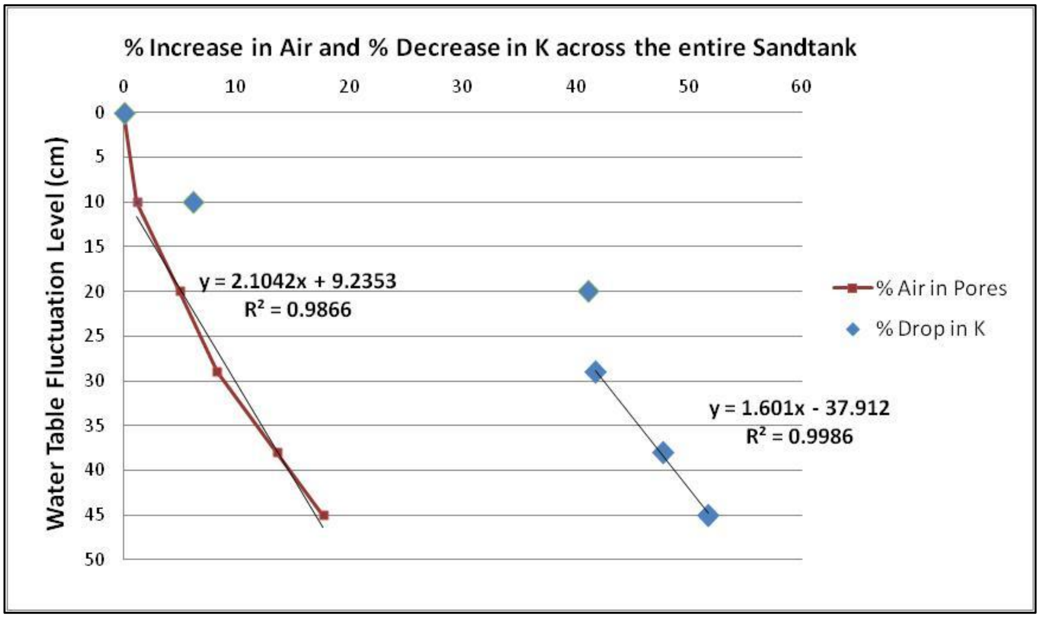

Figure 3.4 Relationship between the percent increase in entrapped air and percent decrease in hydraulic conductivity with each water-table fluctuation scenario

3.3.1 Hydraulic conductivity models

The sand tank was flushed with carbon dioxide prior to filling; therefore complete saturation of the porous media was achieved. Hence, the terms fully saturated and saturated hydraulic conductivity apply to the soil layers that have not undergone any water-table fluctuations. Air in soils is found in two general states, namely mobile air that forms a continuous-entrapped phase and immobile-discontinuous entrapped air. The water table was lowered and then raised, therefore the entrapped air exists primarily as immobile-entrapped air, which can leave the system through dissolution only (Faybishenko, 1995).

Figures 3.3 and 3.4 both show a trend between the increase in air entrapment and the subsequent decrease in the hydraulic conductivity across the entire sand tank. As the depth of the water-table fluctuation increases, the amount of entrapped air increases and this results in the creation of multiple quasi-saturated layers. For example, the scenario with a 45 cm water-table fluctuation resulted in the formation of six distinct quasi-saturated layers, based on the 10 cm sampling resolution. To evaluate this relationship, the experimental relative hydraulic conductivity (measured conductivity across the sand tank divided by the saturated hydraulic conductivity) was plotted (Figure 3.5) against the percent entrapped air. These results were fit with two analytical models formulated by van Genuchten (1980) and Faybishenko (1995).

The van Genuchten (1980) equation is defined by:

$$\mathrm{Kr}(\Theta) = \Theta^{\frac{1}{2}}\left[1 - \left(1 - \Theta^{\frac{1}{m}}\right)^{m}\right]^{2} \qquad (3.8)$$

$$\Theta = \left(\frac{\theta - \theta r}{\theta s - \theta r}\right) \qquad (3.9)$$

where $\mathrm{Kr}(\Theta)$ is the relative hydraulic conductivity, Θ is the effective saturation, m is a curve fitting parameter where ($0 < m < 1$), θ, θr and θs are water content, residual water content and saturated water content, respectively.

The Faybishenko (1995) equation is defined by:

$$\mathrm{K}(\omega) = \mathrm{K}_0 + (\mathrm{K}_s - \mathrm{K}_0)\left(1 - \frac{\omega}{\omega_{max}}\right)^{n} \qquad (3.10)$$

where ω is the volumetric fraction of entrapped air, $\mathrm{K}(\omega)$ is the relative hydraulic conductivity, K_0 is the minimum quasi-saturated hydraulic conductivity, K_s is the saturated hydraulic conductivity, ω_{max} is the maximum entrapped-air content and n is a curve-fitting power factor.

Both the models calculate the relative hydraulic conductivity as a function of the entrapped-air content. The data used in the models is presented in Table 3.1 and the plots are presented in Figure 3.5.

The van Genuchten (1980) model was used by Fry et al. (1997) and Marinas et al. (2013) and the Faybishenko (1995) equation was used by Faybishenko (1995), Sakaguchi et al. (2005) and Marinas et al. (2013) to evaluate the relationship between the relative hydraulic conductivity and entrapped air.

Scenario	K_{Tot} (cm/s)	Experiment K_{Tot}/K_{Sat}	Air Content (%)	Water Content θ	Θ = (θ-θr) /(θs-θr)	Van G Kr(Θ)	ω = Air Content/ 100	Faybishenko $K_{(\omega)}$	Faybishenko $K_{(\omega)}/K_{sat}$
Saturated	0.422	**1.000**	0.000	0.363	1.000	1.000	0.0000	0.422	**1.000**
10 cm	0.396	**0.937**	1.160	0.359	0.989	0.911	0.0116	0.392	**0.928**
20 cm	0.249	**0.589**	4.960	0.345	0.949	0.733	0.0496	0.308	**0.730**
30 cm	0.246	**0.582**	8.260	0.333	0.915	0.623	0.0826	0.255	**0.603**
40 cm	0.221	**0.523**	13.540	0.314	0.861	0.485	0.1354	0.205	**0.485**
50 cm	0.204	**0.483**	17.620	0.299	0.819	0.398	0.1762	0.194	**0.460**

Table 3.1 Data used to evaluate the van Genuchten (1980) and Fabishenko (1995) models for relative hydraulic conductivity versus entrapped air content. The van Genuchten model was fit with a value of 0.783 for m and the Fabishenko model was fit with a value of 2.12 for n.

The van Genuchten soil parameters (m = 0.903 and n = 10.35) from Figure 3.1 were used to fit the van Genuchten (1980) model to the experimental data. However, a good statistical (least squares analysis) fit was only obtained by lowering the value of the van Genuchten soil parameters m and n from 0.903 to 0.783 and 10.35 to 4.60, respectively.

Fry et al. (1997) used the van Genuchten model and obtained a good fit to their experimental data. Sakaguchi et al. (2005) (using clay andisol and sandy loam) found a good fit using the Faybishenko model. Marinas et al. (2013) (using several sand columns) used the van Genuchten and Faybishenko models and observed that the fit of the Faybishenko model was better at capturing the steepness of the graph compared to the van Genuchten model which runs through the middle of data in a relatively linear manner. The experimental results are consistent with the observations of Marinas et al. (2013) showing a better fit to the Faybishenko model (Figure 3.5) since the curvature of the experimental data was captured well. A value of n = 2.12 provided the best statistical fit between the Faybishenko model and the experimental data.

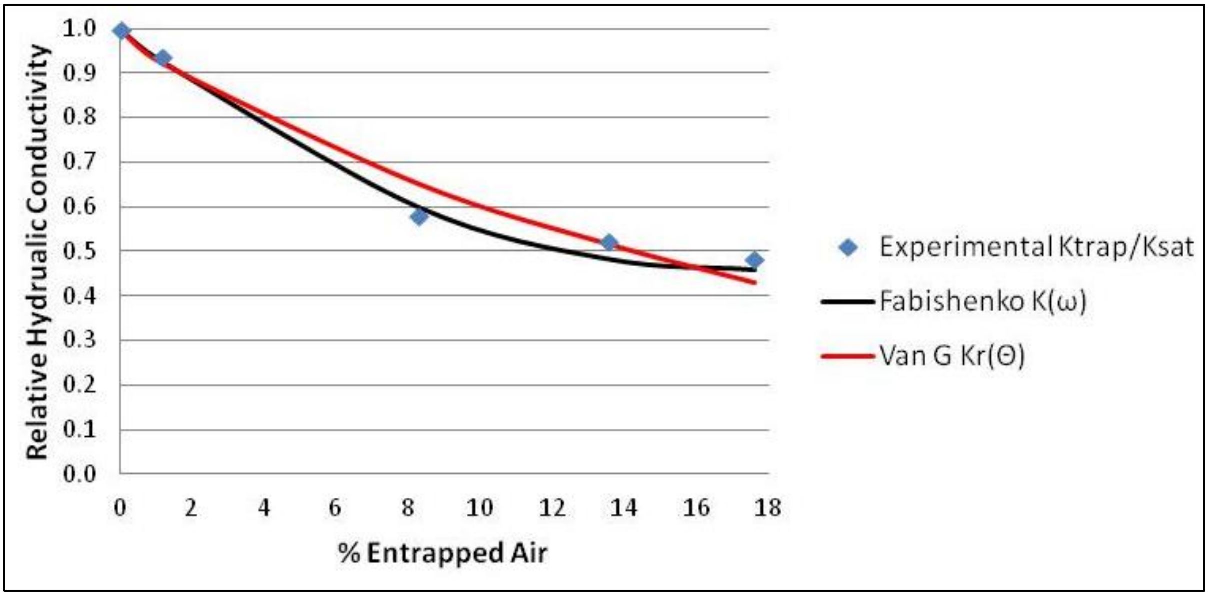

Figure 3.5 Relative hydraulic conductivity as a function of entrapped-air content for the experimental results along with the model results by van Genuchten (1980) and Fabishenko (1995).

3.4 Bromide Tracer Tests

Bromide was used as a conservative tracer under three flow conditions, namely fully saturated, 29 cm and 45 cm water-table fluctuations. In each of these experiments, samples were collected from six piezometers at depths of 7.5 cm, 12.5 cm, 17.5 cm, 25 cm, 35 cm and 45 cm in each of the five piezometer nests. The sampling would ensure that the breakthrough curve was captured and would allow the change in concentration in each piezometer to be monitored. The concentrations in the sand tank were monitored for 26, 15 and 18 days for the saturated, 30 cm entrapment and 47 cm entrapment experiments, respectively. The data for all three experiments is provided in Appendix A.

The break-through curve data for each sampling point was modelled using a Microsoft Excel adaptation of CXTFIT (Tang et al., 2010). Our experimental results of normalized tracer concentration and time were input into an inverse model to identify values of velocity and longitudinal hydrodynamic dispersion. The experimental breakthrough curve was fit to a theoretical breakthrough curve based on specific input parameters, namely; inlet distance, dimensionless time, a pulse flow condition, and the tracer concentrations. The fit of the two curves was optimized by using the Excel solver to obtain the maximum coefficient of determination (R^2) by adjusting values of velocity and dispersion. The plots for each sampling location are provided in Appendix A.

Saturated		α (cm)						Statistics by depth		
Well	Depth (cm)	Nest 1	Nest 2	Nest 3	Nest 4	Nest 5		Mean	Median	St. Dev.
3	7.5	3.9	1.0	7.1	10.6	2.2	→	5.0	3.9	3.9
5	12.5	5.2	0.7	6.9	2.3	1.1	→	3.2	2.3	2.7
7	17.5	-	1.4	1.0	0.2	0.8	→	0.8	0.9	0.5
9	25	-	8.7	3.3	3.3	1.5	→	4.2	3.3	3.1
11	35	-	12.1	1.4	1.1	8.0	→	5.6	4.7	5.3
13	45	-	-	5.9	2.2	5.9	→	4.7	5.9	2.1
		↓	↓	↓	↓	↓	Average	**3.9**	**3.5**	**2.9**
Statistics by distance	Mean α (cm)	4.5	4.8	4.3	3.3	3.3	**4.0**			
	Median α (cm)	4.5	1.4	4.6	2.2	1.9	**2.9**			
	St. Dev α (cm)	0.9	5.3	2.7	3.7	3.0	**3.1**			

29 cm Fluctuation		α (cm)						Statistics by depth		
Well	Depth (cm)	Nest 1	Nest 2	Nest 3	Nest 4	Nest 5		Mean	Median	St. Dev.
3	7.5	-	-	0.5	9.5	7.7	→	5.9	7.7	4.8
5	12.5	-	-	0.2	0.3	0.2	→	0.2	0.2	0.1
7	17.5	-	-	0.2	0.6	1.1	→	0.6	0.6	0.4
9	25	-	-	0.6	0.7	1.9	→	1.1	0.7	0.7
11	35	-	-	4.0	1.3	3.9	→	3.1	3.9	1.5
13	45	-	-	0.2	0.2	0.9	→	0.4	0.2	0.4
		↓	↓	↓	↓	↓	Average	**1.9**	**2.2**	**1.3**
Statistics by distance	Mean α (cm)	-	-	1.0	2.1	2.6	**1.9**			
	Median α (cm)	-	-	0.4	0.6	1.5	**0.8**			
	St. Dev α (cm)	-	-	1.5	3.6	2.8	**2.6**			

45 cm Fluctuation		α (cm)						Statistics by depth		
Well	Depth (cm)	Nest 1	Nest 2	Nest 3	Nest 4	Nest 5		Mean	Median	St. Dev.
5	12.5	0.8	0.3	0.2	3.1	0.2	→	0.9	0.3	1.2
7	17.5	0.1	0.3	0.4	1.1	0.4	→	0.4	0.4	0.4
9	25	0.1	0.9	0.8	0.3	1.1	→	0.7	0.8	0.4
11	35	0.8	3.4	1.9	0.4	0.5	→	1.4	0.8	1.3
13	45	0.2	0.3	1.4	2.2	2.3	→	1.3	1.4	1.0
		↓	↓	↓	↓	↓	Average	**0.9**	**0.7**	**0.8**
Statistics by distance	Mean α (cm)	0.4	1.1	1.0	1.4	0.9	**0.9**			
	Median α (cm)	0.2	0.3	0.8	1.1	0.5	**0.6**			
	St. Dev α (cm)	0.4	1.3	0.7	1.2	0.8	**0.9**			

Table 3.2 Dispersivity values evaluated by CXTFIT and the mean, median and standard deviation along the length and depth of the sand tank.

The concept of using higher dispersivity values with increasing travel distance was first introduced by Sudicky et al. (1983) and is more appropriate at larger scales. Since this sand tank is 188 cm long, the amount of tortuosity along the flow path should not be significant enough such that higher dispersivity values need to be used as the travel length increases from 0 to 188 cm, especially under fully-saturated conditions. However, with the 29 cm and 45 cm entrapment experiments, the overall permeability of the sand would decrease when there is entrapped air present and hence the tortuosity and variability of the flow field may increase. The dispersivity values that were identified by CXTFIT are presented in Table 3.2 along with the mean, median and standard deviation of the data along the length and depth of the sand tank, while the velocity values identified are presented in Table 3.3. The dispersivity and velocity values are only presented for sampling locations where the measured concentration on the first sampling event was less than a normalized concentration (C/C_0) of 1, so that a proper break-through curve was used for the fit. Additionally, the number of sampling points on each break-through curve was dependent on the maximum bromide concentration that was captured as the leading edge of the tracer front travelled through the sand tank.

Groundwater flow through a porous medium occurs by advection and dispersion, which govern the flow velocity and the spreading of the advancing front. Due to the variability in pore sizes, path length and pore scale friction, the groundwater mixes, resulting in dilution of the advancing front in the direction of primary flow (longitudinal dispersion). The coefficient of longitudinal dispersion is equal to the dispersivity (α) times the average linear groundwater velocity (v). When air is entrapped within a sand media, it occupies the largest pores (faster flow), forcing flow through the smaller, slower-flow pores. As a result, the tortuosity (due to entrapped air) increases (Haberer et al., 2011), resulting in fewer and longer flow paths, which could increase the dispersivity of the flow field.

The average dispersivity across the sand tank under the saturated, 29 cm and 45 cm fluctuation experiments was 4 cm, 2 cm and 1 cm, respectively. It was expected that the zones with entrapped air would have a higher value of dispersivity relative to the saturated zones. However, in all three experiments, the dispersivity values for the saturated zones were higher than the entrapped air zones which were consistent with the results of Orlob and Radhakrishna (1958).

The flow rate for the fluctuating water-table experiments was 2.0 mL/min (Darcy flux q = 5.7 cm/day) which corresponds to a groundwater velocity of 15.7 cm/day, while the flow rate for the saturated experiment was set to 1.4 mL/min (Darcy flux q = 4.0 cm/day) which corresponds to a groundwater velocity of 11.0 cm/day. CXTFIT adequately identified the average groundwater velocities (Table 3.3) for the saturated, 29 cm and the 45 cm fluctuation experiments as 10 cm/day (relative to the calculated 11 cm/day), 17.37 cm/day and 15.13 cm/day (relative to the calculated 15.7 cm/day), respectively. The average groundwater velocities identified by CXTFIT were close to the calculated average groundwater velocities but a main trend can be seen in all of the experiments (Figure 3.6), such that the flow velocities are highest at the bottom left corner and lowest at the top right corner, resulting in preferential flow through the bottom. The higher velocity at the deep inflow end is possibly due to a shift in the pea gravel position further into the sand tank at the inflow end.

Saturated		Velocity (cm/day)						Statistics by depth		
Well	Depth (cm)	Nest 1	Nest 2	Nest 3	Nest 4	Nest 5		Mean	Median	St. Dev.
3	7.5	8.3	7.6	6.1	4.9	5.8	→	6.5	6.1	1.4
5	12.5	10.0	9.3	7.6	7.1	6.8	→	8.1	7.6	1.4
7	17.5	-	10.7	9.4	7.4	7.2	→	8.7	8.4	1.7
9	25	-	15.5	10.7	9.2	8.1	→	10.9	10.0	3.3
11	35	-	20.7	14.6	11.8	10.3	→	14.3	13.2	4.6
13	45	-	-	18.1	13.6	11.3	→	14.3	13.6	3.5
		↓	↓	↓	↓	↓	Average	**10.5**	**9.8**	**2.6**
Statistics	Mean (cm/d)	9.1	12.8	11.1	9.0	8.2	**10.0**			
by	Median (cm/d)	9.1	10.7	10.1	8.3	7.6	**9.2**			
distance	St. Dev (cm/d)	1.2	5.3	4.5	3.2	2.1	**3.3**			

29 cm Fluctuation		Velocity (cm/day)						Statistics by depth		
Well	Depth (cm)	Nest 1	Nest 2	Nest 3	Nest 4	Nest 5		Mean	Median	St. Dev.
3	7.5	-	-	14.6	11.5	11.4	→	12.5	11.5	1.8
5	12.5	-	-	16.2	16.0	14.0	→	15.4	16.0	1.2
7	17.5	-	-	17.2	17.3	15.1	→	16.5	17.2	1.2
9	25	-	-	19.6	19.0	15.7	→	18.1	19.0	2.1
11	35	-	-	21.9	20.3	17.3	→	19.8	20.3	2.3
13	45	-	-	24.0	21.1	20.6	→	21.9	21.1	1.8
		↓	↓	↓	↓	↓	Average	**17.4**	**17.5**	**1.8**
Statistics	Mean (cm/d)	-	-	18.9	17.5	15.7	**17.4**			
by	Median (cm/d)	-	-	18.4	18.2	15.4	**17.3**			
distance	St. Dev (cm/d)	-	-	3.6	3.5	3.1	**3.4**			

45 cm Fluctuation		Velocity (cm/day)						Statistics by depth		
Well	Depth (cm)	Nest 1	Nest 2	Nest 3	Nest 4	Nest 5		Mean	Median	St. Dev.
5	12.5	16.0	13.8	11.8	10.3	11.0	→	12.6	11.8	2.3
7	17.5	15.6	14.6	12.5	12.3	11.3	→	13.3	12.5	1.8
9	25	15.5	16.6	14.5	14.1	12.1	→	14.6	14.5	1.7
11	35	16.0	19.4	16.7	15.3	13.9	→	16.3	16.0	2.0
13	45	17.0	22.9	20.7	17.2	17.3	→	19.0	17.3	2.7
		↓	↓	↓	↓	↓	Average	**15.1**	**14.4**	**2.1**
Statistics	Mean (cm/d)	16.0	17.4	15.2	13.8	13.1	**15.1**			
by	Median (cm/d)	16.0	16.6	14.5	14.1	12.1	**14.7**			
distance	St. Dev (cm/d)	0.6	3.7	3.6	2.6	2.6	**2.6**			

Table 3.3 Velocity values evaluated by CXTFIT and the mean, median and standard deviation along the length and depth of the sand tank.

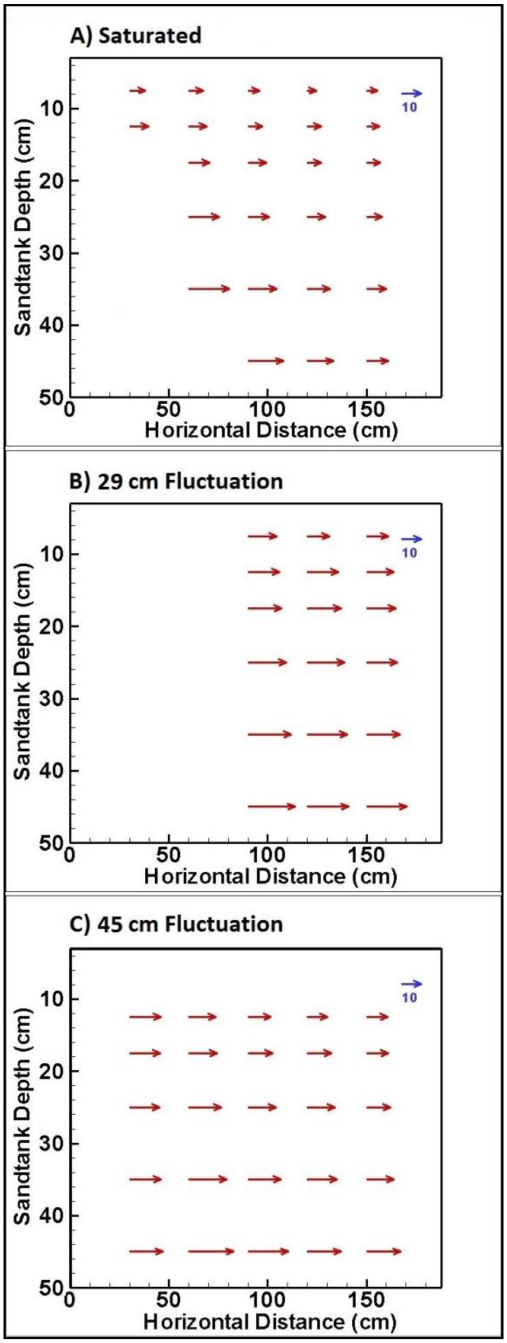

Figure 3.6 Spatial profile showing the magnitude of the horizontal velocities identified by CXTFIT under A) saturated, B) 29 cm flucutation and C) 45 cm flucutation experiments

3.5 Bubble Entrapment under Each Fluctuating Water Table Scenario

Figure 3.7 shows the change in the water content of each layer during the fluctuating water-table scenarios. The water content of each layer was calculated by using a depth-weighted arithmetic mean (equation 3.7). It is important to note that while the overall water content of the entrapped air zone (left side of Figure 3.7) decreased from 0.333 (29 cm fluctuation) to 0.299 (45 cm fluctuation), the individual-entrapped gas layers (right side of Figure 3.7) show a greater decrease in water content from the fluctuation level (minimum water table level) to the top of the water table.

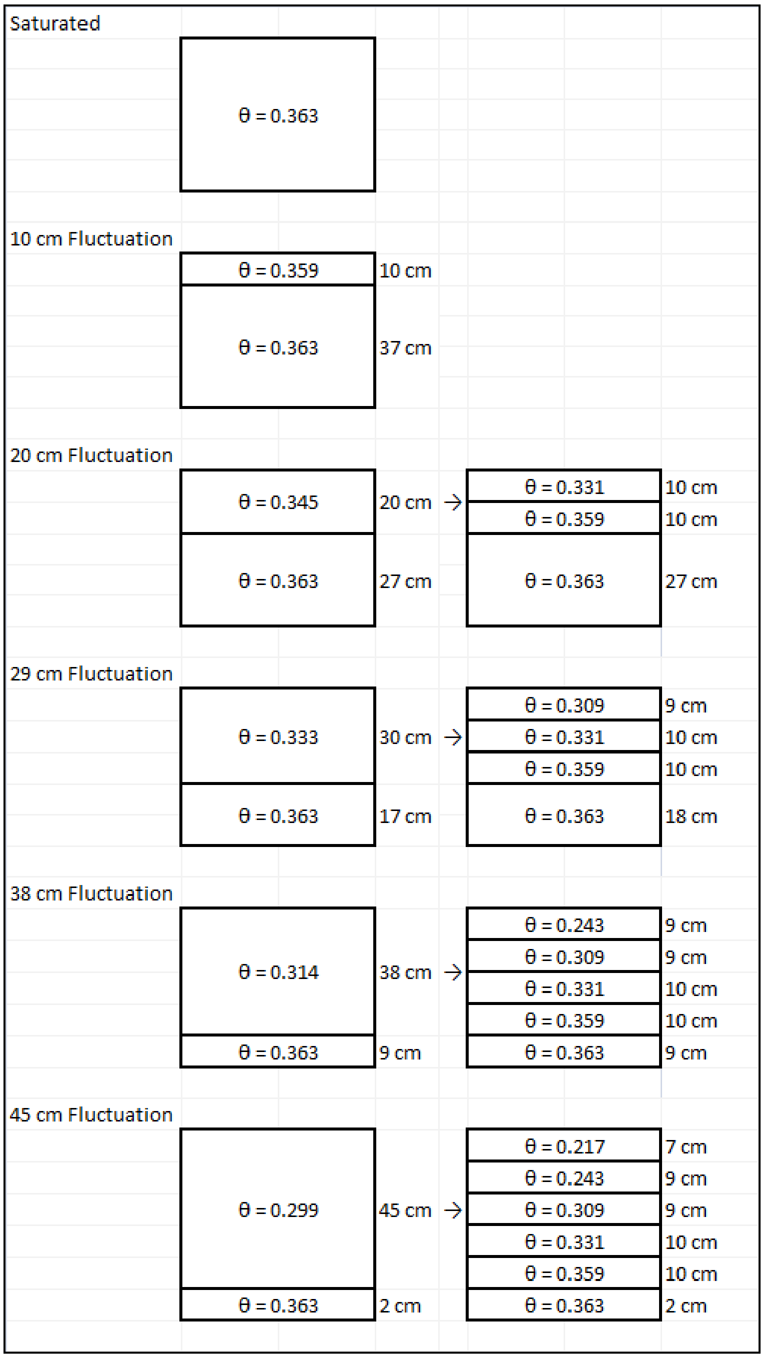

Figure 3.7 : Water-table fluctuations and water content of each layer. Figures on the left show the water content of the entrapped air and saturated zones, while figures on the right show the water content of each entrapped air and saturated layers.

The measured and calculated water content data were input into a mathematical model by Kaluarachchi and Parker (1992), which was used to calculate the effective entrapped-gas saturation, S_{egt} (difference between the main drainage curve and a scanning-imbibition curve) of each entrapped-air layer in the 30 cm and 47 cm fluctuation experiments. The terminology used for the equations will be kept consistent with the work of Amos and Mayer (2006).

$$S_{egt} = \left\{\frac{1-S_{ea}^{min}}{1+R_L(1-S_{ea}^{min})} - \frac{1-S_{aa}}{1+R_L(1-S_{aa})}\right\} \qquad (3.11)$$

S_{ea}^{min} is the minimum effective-aqueous saturation (saturation at the depth of the entrapped-air layer, read off the main-drainage curve), S_{aa} is the apparent-aqueous saturation (saturation at the each pressure-head value, read off the main-drainage curve) and R_L is the Land's parameter;

$$R_L = \frac{1}{S_{egt}^{max}} - 1 \qquad (3.12)$$

where S_{egt}^{max} is the maximum effective trapped-gas saturation, which is the difference between 100% saturation and the maximum saturation of each scanning-imbibition curve. The scanning-imbibition curves are derived using the relation;

$$S_{ea} = S_{aa} - S_{egt} \qquad (3.13)$$

where S_{ea} is the effective aqueous-phase saturation. Actual saturation values are corrected to effective saturation values based on the relationship of Parker and Lenhard (1987), given by:

$$S_{ea} = \frac{S_a - S_{ra}}{1 - S_{ra}} \qquad (3.14)$$

where S_a is the actual saturation and S_{ra} is the residual saturation.

Figure 3.8 shows the main-drainage curve and representative imbibition curves for each experimental fluctuation level for the 29 cm and 45 cm experiments using values of α and n identified by Williams and Oostrom (2000). Equations 3.11 to 3.14 were used to create imbibition curves which corresponded to the layer thicknesses in Figure 3.7, such that the maximum water saturation attainable from each fluctuation level was identified by the model equations.

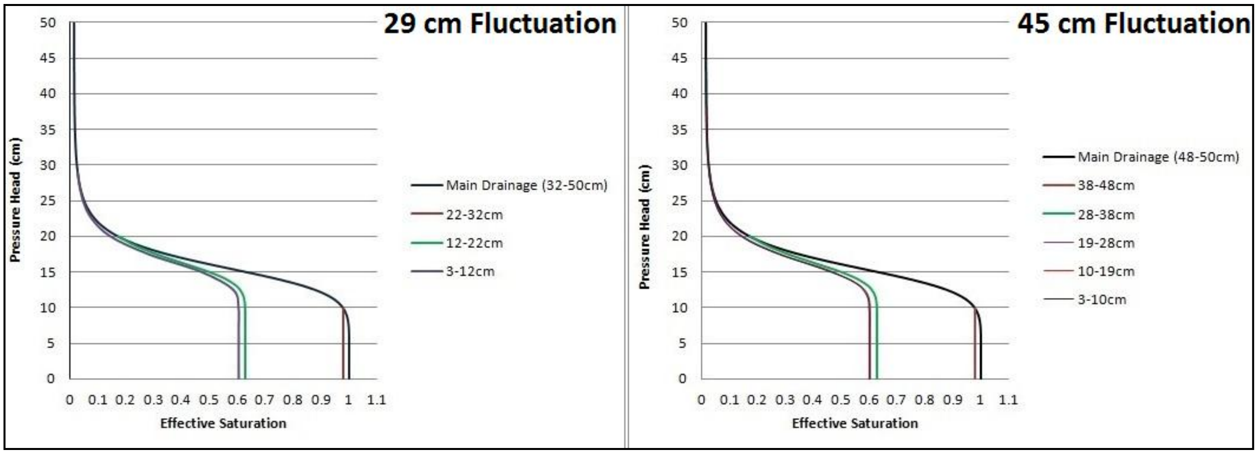

Figure 3.8 Schematic of the main drainage and scanning imbibition curves for each entrapped-air layer within the fluctuation levels using the values of 0.065 and 10.35 for α and n, respectively, identified by Williams and Oostrom (2000)

Using values of α and n identified by Williams and Oostrom (2000), the trapped-gas saturation versus depth in the sand tank (Figure 3.9) showed that the model results match the measured values reasonably well in the 10 cm above the saturated zone in both the 29 cm and 45 cm fluctuation experiments. Above this depth, the fit between the model and the experimental results was poor.

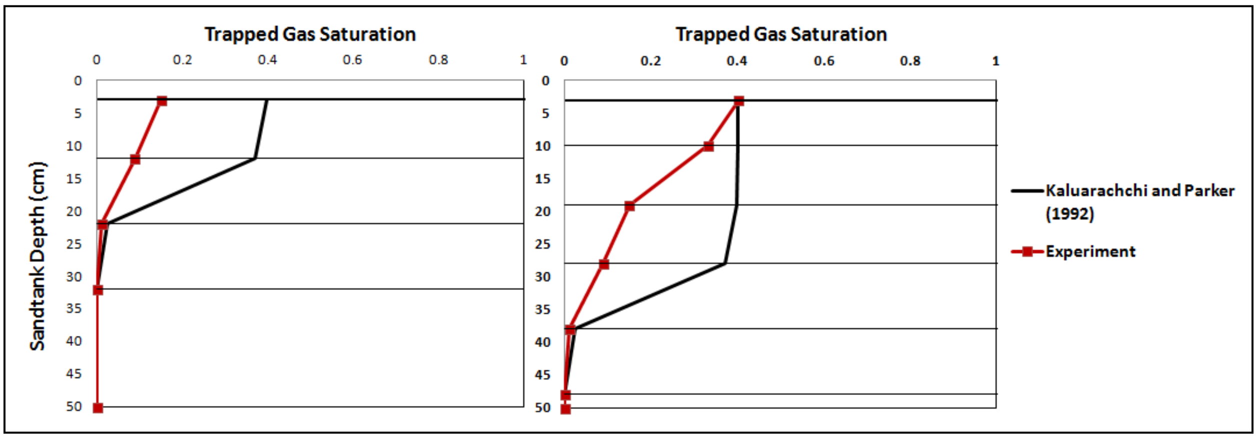

Figure 3.9 Schematic showing the change in trapped-gas saturation with depth in the sand tank for the 29 cm and 45 cm fluctuation experiment, using values of 0.065 and 10.35 for α and n, respectively, identified by Williams and Oostrom (2000).

To improve the fit between the model and the experimental data, the van Genuchten soil parameters were adjusted. A statistical best fit (using least squares analysis) between the model and experimental data was achieved with values of 0.030 and 4.60 for α and n, respectively. This is consistent with Figure 3.5, where the van Genuchten (1980) model fit the experimental relative hydraulic conductivity data better with the van Genuchten parameter n equal to 4.60. The need to lower n to a value of 4.60 to fit both models suggests that the properties of the experimental sand used here may be different from the sand used by Williams and Oostrom (2000).

Figure 3.9 shows the shape of the main drainage and scanning-imbibition curves using values of 0.065 and 10.35 for the van Genuchten parameters α and n, respectively. Figure 3.10 shows the shape of the adjusted main drainage and scanning-imbibition curves using the van Genuchten parameters (α = 0.030 and n = 4.60), that improved the fit of the trapped-gas saturation curves (Figure 3.11).

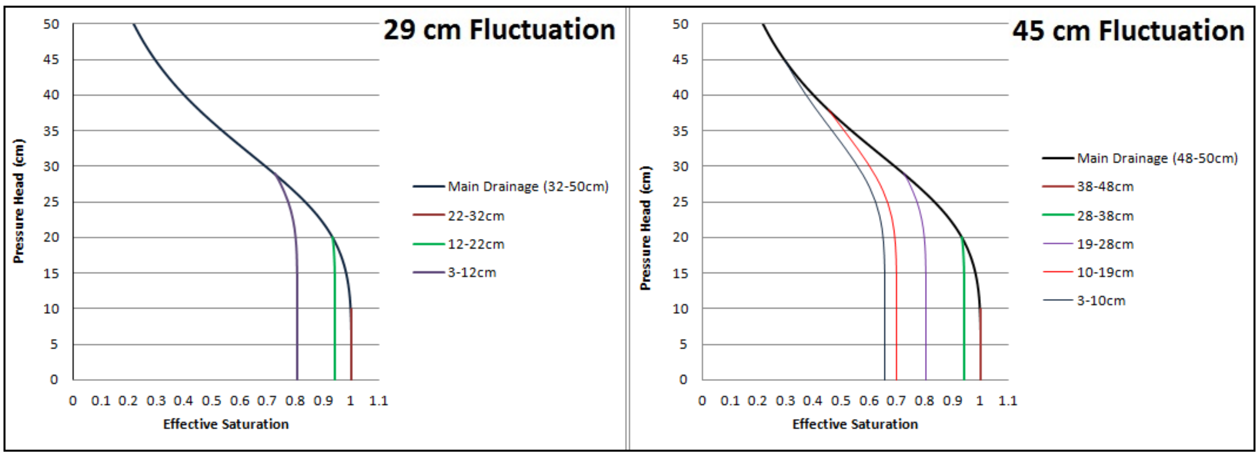

Figure 3.10 Schematic of the main drainage and scanning imbibtion curves for each entrapped-air layer within the fluctuation levels using the adjusted the van Genuchten soil parameters (α = 0.030 and n = 4.60) to fit the experimental data.

After adjusting the van Genuchten soil parameters, the curves went from resembling well-sorted sand to poorly-sorted sand, which was interesting considering that the sand used was pre-sieved and well sorted. The adjusted soil parameters increased the spacing of each drainage-imbibition curve and this matched the experimental data of water-content reduction with each fluctuation cycle.

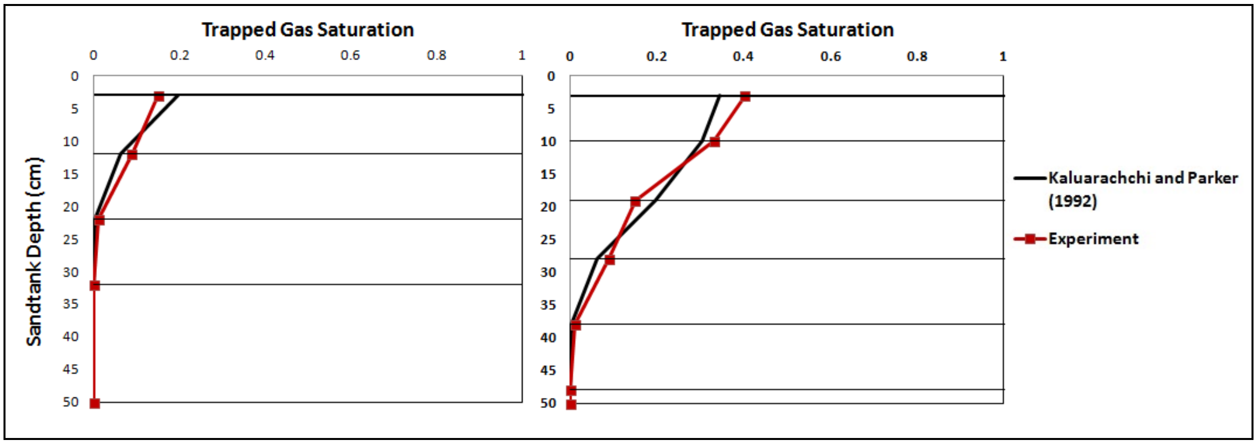

Figure 3.11 Schematic showing the change in trapped-gas saturation with depth in the sand tank for the 29 cm and 45 cm fluctuation experiments using the adjusted van Genuchten parameters (α = 0.030 and n = 4.60)

By adjusting the soil parameters using least squares analysis, the fit between the Kaluarachchi and Parker (1992) model and the experimentally derived values for trapped-gas saturation improved (Figure 3.11). Although the fit of the two curves improved, the model either over-predicted or under-predicted the trapped gas saturation for each entrapped air zone. The model also under-predicted the maximum trapped-gas saturation at the top of the water surface. The overall fit of the model to the experimental results was important because the results from Chapter 3 would be modelled using a reactive transport model (MIN3P) which uses equations 3.11 to 3.14 (Kaluarachchi and Parker, 1992) as the main governing equations regarding air-bubble entrapment.

3.6 Conclusion

A series of experiments were performed to quantify the changes in hydraulic conductivity and water content due to fluctuating water-table scenarios. Each fluctuation scenario resulted in entrapped air which reduced the water content and conductivity of the entrapment zone. Two analytical models, namely van Genuchten (1980) and Faybishenko (1995) were fit to the experimental relative hydraulic conductivity data. The Faybishenko (1995) model provided a better fit because it captured the curvature of the experimental data points. The van Genuchten (1980) model fit the data only after the van Genuchten soil parameters (from the water content-pressure head relationship) were lowered. The good fit obtained from both models along with the consistency of these results with Sakaguchi et al. (2005) and Marinas et al. (2013) suggests that the system behaviour is quite normal.

Three bromide tracer tests were performed under saturated, 29 cm and 45 cm fluctuation scenarios. The break-through curve from each sampling location was modelled using CXTFIT to identify the dispersivity and horizontal velocity profile in the sand tank. The average dispersivity decreased from 4 cm in the fully saturated experiment to 1 cm in the 45 cm fluctuation experiment possibly suggesting that increased air entrapment reduces the number of flow paths resulting in less variability of the flow field. The velocity values obtained from CXTFIT identified vertical stratification of the groundwater velocities coupled with high flow rates at the lower inflow end and low flow rates at the upper outflow end, which caused preferential flow through the bottom of the sand tank. The change in the water content with increasing air-entrapment was fit to an analytical model by Kaluarachchi and Parker (1992). The model did not fit the data well; therefore the van Genuchten soil parameters were lowered until a good fit was obtained. As a result, the updated soil moisture curves for the experimental sand resembled poorly sorted sand, rather than a well sorted one. The van Genuchten soil parameter n was lowered to a value of 4.6 in order to fit both, the van Genuchten (1980) and the Kaluarachchi and Parker (1992) models. This consistency between the models provided insight into the differences in the physical properties of this experimental sand compared to the sand used by Williams and Oostrom (2000), despite the fact that they are both 30/40 mesh Ottawa sand. This highlights the importance of measuring the physical properties of any experimental soil media irrespective of whether soil measurements are available in the literature.

4. Air Bubble Entrapment Experiments

4.1 Introduction

Gas bubbles can be introduced into a groundwater system due to natural processes including daily and seasonal water table fluctuations (Williams and Oostrom, 2000), biogenic gas production (Ronen et al., 1989; Ryan et al., 2000; Amos et al., 2005) by exolution due to temperature and pressure variations (Ronen et al., 1989); and by anthropogenic processes including groundwater extraction, flow regulation by dams and remediation strategies including pump and treat, pneumatic fracturing and air sparging. Air sparging is specifically designed to try to increase the amount of air in the groundwater when coupled with enhanced bioremediation, but is flawed due to the creation of preferential gas flow paths which lead to the ground surface. Water-table fluctuations however, occur over a larger area and do not necessarily create any preferential flow paths for air.

Water-table fluctuations result in the entrapment of air within a porous media, which affects the overall permeability (Christiansen, 1944; Orlob and Radhakrishna, 1958) and hydraulic conductivity of the soil (Faybishenko, 1995; Fry et al., 1997; Sakaguchi et al., 2005; Marinas et al., 2013), as seen in Chapter 3. Although the entrapped air alters the flow system, it can also act as a source of oxygen for a groundwater system. Oxygen can enter a groundwater system naturally, by the infiltration of oxygen rich water across the soil surface, diffusion through the vadose zone and into the capillary fringe, and through water-table fluctuations that result in air entrapment (Williams and Oostrom, 2000). The oxygen in the air bubbles will dissolve into the flowing groundwater and can increase the dissolved-oxygen concentration of the groundwater.

Dissolved argon and nitrogen can be used as tracers for geochemical processes like denitrification (Blicher-Mathiesen et al., 1998) and methanogenesis (Amos et al., 2005), and for physical transport processes (Amos et al., 2005). Water-table fluctuations and the subsequent entrapment of air can be a viable source of oxygen (Williams and Oostrom, 2000) for Monitored Natural Attenuation (MNA) remediation strategies especially when the water-table fluctuations are substantial and/or frequent (Amos et al., 2011). We hypothesize that the entrapped air will dissolve into the groundwater based on the biogeochemical system that exists, and that the pre-existing dissolved-gas concentration gradient along with the biological and chemical oxygen demand will determine the dissolution rate of the entrapped air. Groundwater systems with contaminants like petroleum based hydrocarbons have a higher demand for oxygen due to aerobic degradation relative to anaerobically degraded contaminants including PCE and TCE.

The physical processes that contribute to the depletion of entrapped air provide insight into the influence and importance of physical transport processes, namely advection, dispersion and diffusion. The physical removal of entrapped air by diffusion within a stagnant groundwater system is a slow process (Bloomsburg and Corey, 1964) and is dependent on the grain size of the soil (Adam, 1967; Adam et al., 1969). Under flowing groundwater conditions, the effects of reduced permeability and hydraulic conductivity due to entrapped air can be more prominent.

The experiments carried out in this chapter were designed to understand the physical interactions between entrapped-air bubbles and anaerobic water under fully saturated, 29 cm and 45 cm water-table fluctuations. With each scenario, the mechanisms of gas transport, upon dissolution, within the groundwater system were quantified.

4.2 Results and Discussion

The saturated experiment was run for two weeks to assess the change in dissolved-gas concentrations across the entire sand tank, especially across the water surface. The sand tank was fully saturated with anaerobic water (the input water was also anaerobic), therefore the only exposure to air was across the top of the water table which would result in the diffusion of air into the water.

The 30 cm entrapment experiment was run for two weeks, capturing the early stages of entrapped-bubble dissolution, but it did not capture the evolution of the dissolved-gas concentrations. The 45 cm entrapment experiment was run for 149 days to monitor the change in dissolved-gas concentrations. Each sampling session lasted for 2 days which resulted in the collection of four sets of samples for the saturated and 29 cm entrapment experiments. In the case of the 45 cm entrapment experiment, the sand tank was sampled with the same frequency during the first 2 weeks, but the average sampling frequency was lowered to an average frequency of 10 to 12 days for the remainder of the experiment due to the relatively slow change in concentrations. The data for all the experiments are presented in Appendix B.

It is important to restate that complete removal of oxygen and argon from the input solution was not achieved. The maximum removal of these two gases was between 90 to 95%. The minimum levels of the two gases in the input solution were relatively consistent with the levels measured within the sand tank initially. The baseline minimum concentrations for oxygen and argon were at least 2% and 0.093%, which are approximately 10% of their atmospheric compositions of 20.95% and 0.93%, respectively.

Figure 4.1 is a graphical representation of the sand tank and the piezometer locations. The piezometer nests are located between 30 cm and 150 cm across the length of the sand tank and the water table for all the experiments was 3 cm below the sand surface. Hence, the figures are constrained to between 30 cm and 150 cm along the length, and between 3 cm and 50 cm over the depth of the sand tank.

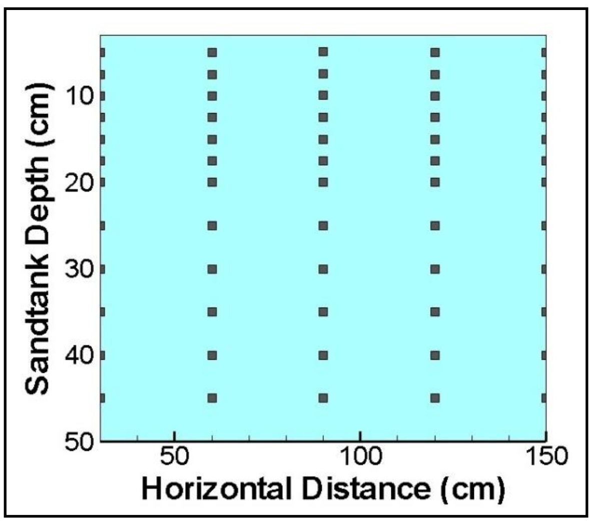

Figure 4.1 Schematic representation of the sand tank and the sampling locations.

4.2.1 Saturated experiment

Prior to the commencement of the saturated experiment, five pore volumes of nitrogen purged water had been flushed through the sand tank. However, during the first sampling event, it was identified that complete flushing was not achieved, as seen in Figures 4.2a and 4.3a for argon and oxygen, respectively. The middle and outflow end of the sand tank still had concentrations above 0.2 % for argon and 5 % for oxygen. Subsequent flushing of the tank reduced the dissolved argon and oxygen concentrations to levels consistent with the input solution (Figures 4.2c, 4.2d, 4.3c and 4.3d).

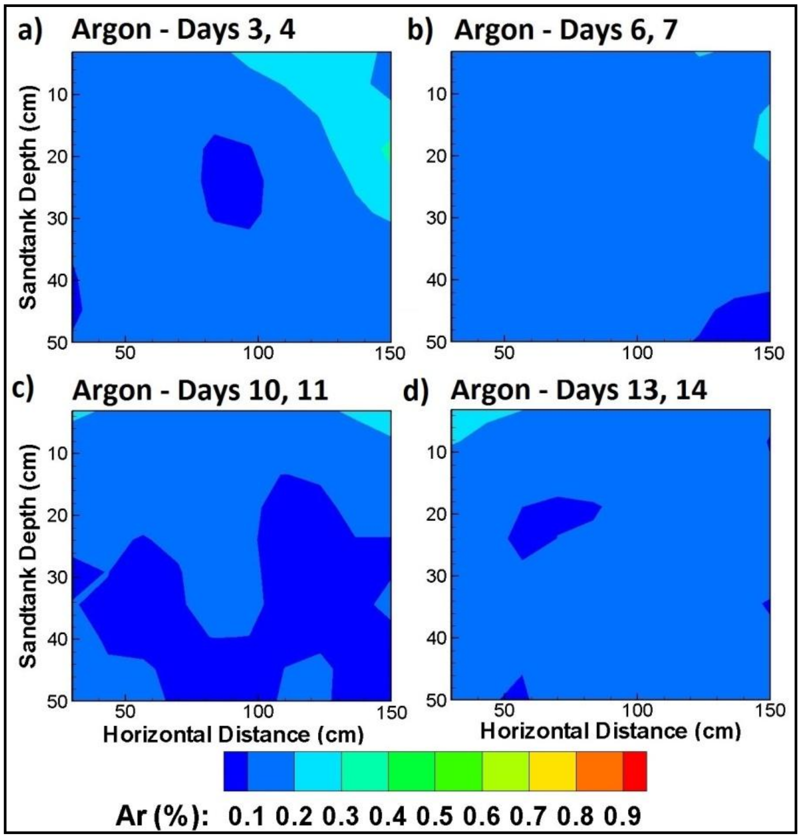

Figure 4.2 Argon concentrations in the sand tank during the saturated experiment

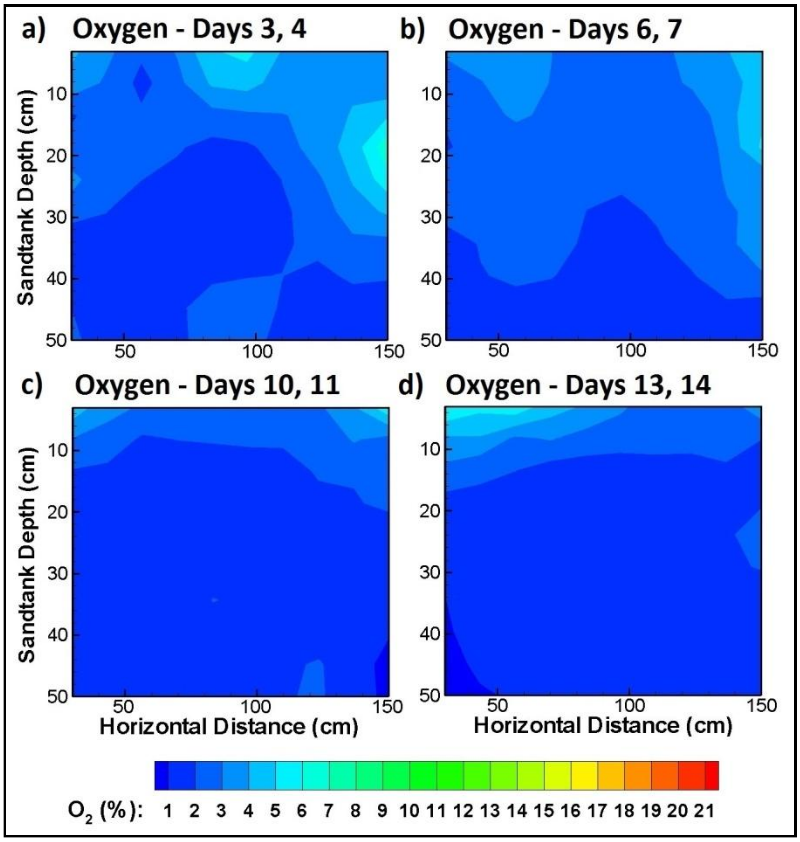

Figure 4.3 Oxygen concentrations in the sand tank during the saturated experiment

By the final sampling event, a zone of higher concentrations (6 % oxygen) extended to a depth of 16 cm (Figure 4.3d). This increase in dissolved oxygen concentrations is possibly due to the sampling method.

The main compromise with collecting an instantaneous sample using a syringe was that the capillary fringe at the piezometer nest location was locally depressed. The capillary fringe and overall water level was allowed to re-stabilize prior to the collection of another sample. During each sampling event, a minimum of 40 samples were collected across the sand tank which caused multiple dips in the local water level across the entire sand tank. As a result, some air was likely entrapped which contributed to the higher dissolved air concentrations below the water table. The groundwater samples were not allowed to make contact with the atmosphere since it was collected quickly; hence diffusion of air through the syringe was negligible.

The saturated experiment was conducted to evaluate the effect the diffusion of air across the water surface. Since the sampling method resulted in the entrapment of air, the dissolved air concentrations were probably higher than they would be with just diffusion of air across the water surface. Hence, concentration increases due to diffusion could not be accurately quantified by these experiments. This experiment confirmed that a de-aired (anaerobic) groundwater system can be achieved, which served as the baseline for the subsequent experiments.

4.2.2 29 cm and 45 cm air entrapment experiments

For the 29 cm air entrapment experiment, the water level was lowered by 29 cm (capillary fringe was at 22 cm). After the capillary-fringe level stabilized, the water level was subsequently raised back up to the initial position and flow was resumed. The entrapment of air above a depth of 22 cm was evident by the elevated concentrations of argon and oxygen (Figures 4.4a and 4.5a).

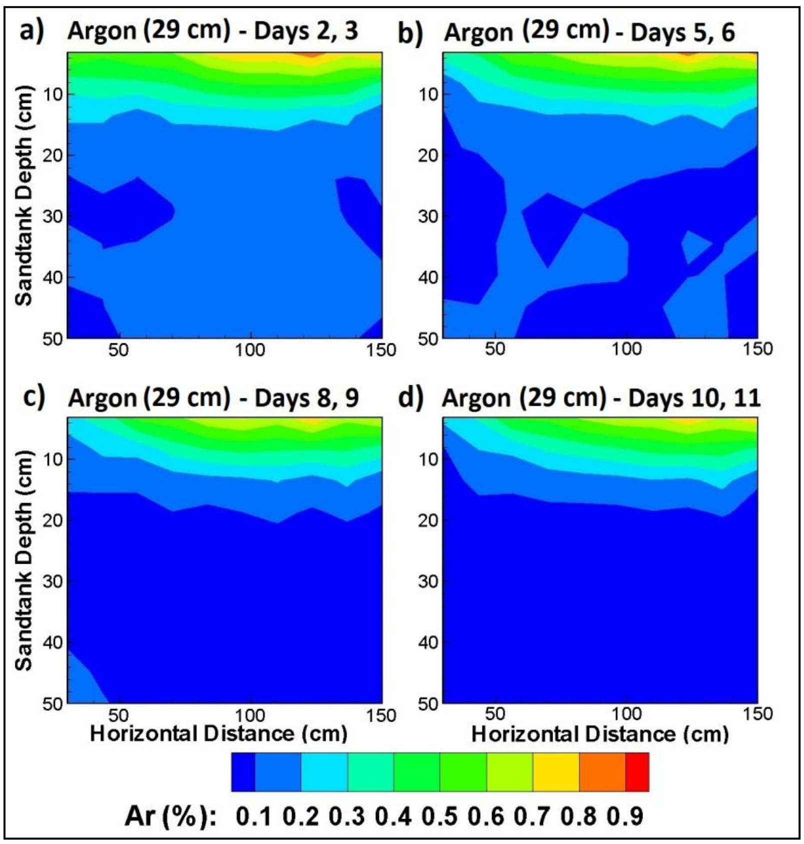

Figure 4.4 Argon concentrations in the sand tank during the 29 cm air-entrapment experiment

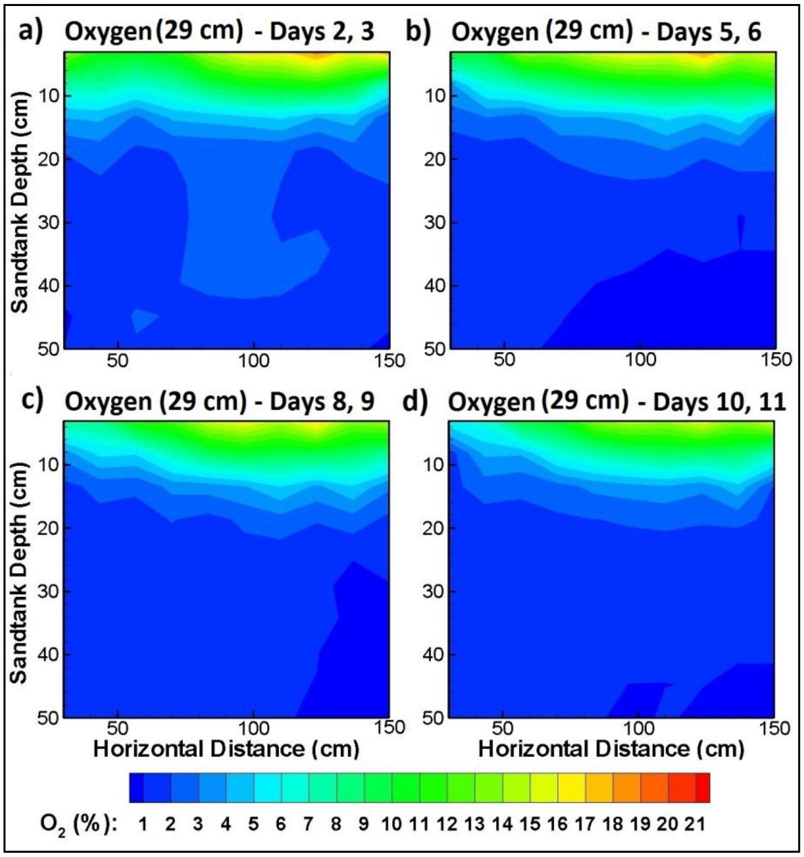

Figure 4.5 Oxygen concentrations in the sand tank during the 29 air-entrapment experiment

Upon initial entrapment, a zone of higher concentrations developed such that the highest concentrations (0.7 % argon and 17 % oxygen) were at the top of the groundwater surface and decreased linearly down to 0.2 % argon and 3 % for oxygen to a depth of 22 cm. Initially, this horizontal zone was fairly uniform across the entire length of the sand tank. As the experiment progressed, two main trends were apparent, namely; the argon and oxygen concentrations were preferentially depleted at the inflow end; and the overall thickness of the entrapped air zone decreased. Initially, this zone extended to 22 cm, but by the final sampling day the zone extended to a depth of 15 cm at the inflow end.

The uniform gradient of dissolved-gas concentration toward the water table reflects the increase in the entrapment of air from the top of the capillary fringe to the water table. In Chapter 3, we identified the changes in water content due to entrapment of air. In the case of the 29 cm fluctuating water-table experiment, the groundwater below a depth of 29 cm was fully saturated (water content = porosity = 0.363), while the water content decreased to 0.359 in the preimbibition capillary fringe, followed by a decrease to 0.309 at the top of the sand surface. The change in water content relates to an increase in the entrapped air volume. Very little air was entrapped within the capillary fringe and the entrapment progressively increased towards the top of the sand surface. The highest dissolved argon and oxygen concentrations were 0.7 % and 17 %, indicating that not enough air was entrapped to allow atmospheric levels of these gases to be detected.

Although this experiment was only run for two weeks, the changes in dissolved-gas concentrations with time were apparent. Over the course of the experiment, the zone of entrapped air got shallower as the entrapped air was depleted through dissolution and the peak concentrations at the water table decreased as well. Initially, the concentration gradient followed a vertical stratification. After two weeks, the dissolution of the air bubbles at the shallow and intermediate depths near the inflow side of the sand tank resulted in an angled stratification across the tank, due to depletion of air bubbles near the inflow end.

For the 45 cm air-entrapment experiment, the water level was lowered by 45 cm (capillary fringe was at 33cm) and subsequently raised back up to the initial position. In this experiment, argon and oxygen concentrations were near atmospheric levels at the water surface and decreased linearly until the deep saturated zone (deeper than 40 cm) where concentrations were equal to the input solution (0.1 % argon and 2 % oxygen; Figure 4.6a and 4.7a). The subplots for Figures 4.6 and 4.7 represent the concentrations of argon and oxygen, respectively during each sampling session.

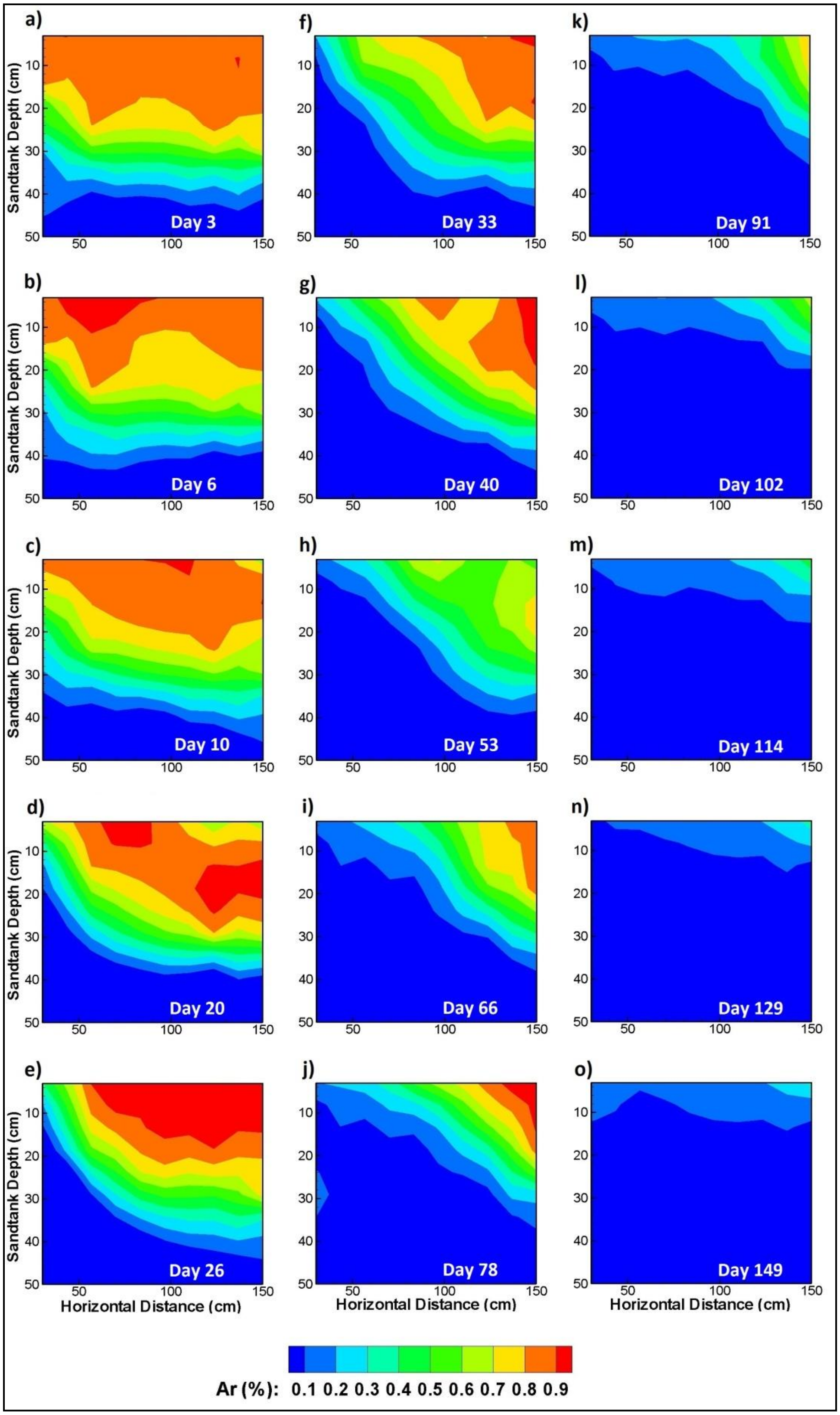

Figure 4.6 Argon concentrations in the sand tank during the 45 cm air-entrapment experiment

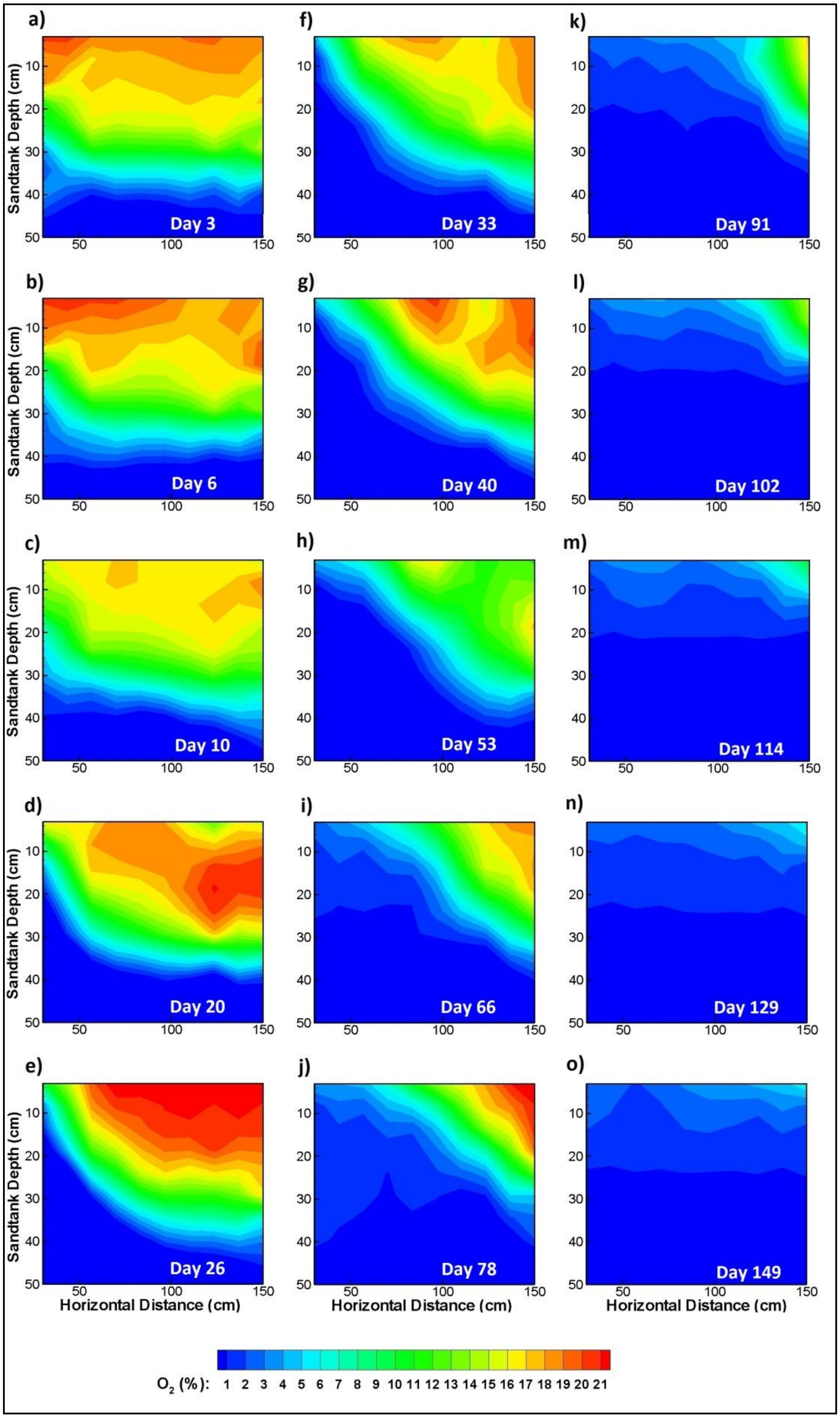

Figure 4.7 Oxygen concentrations in the sand tank during the 45 cm air-entrapment experiment

Elevated concentrations of argon and oxygen were expected at the top of the capillary fringe (at 33 cm). However, the concentrations above background, below a depth of 33 cm suggest some drainage of the capillary fringe and air entrapment below the 33 cm depth. The water contents identified in Figure 3.7 suggest that the deepest 2 cm was fully saturated (water content = porosity = 0.363) while the capillary fringe had a water content of 0.359. Above this, the water content decreased from 0.359 to 0.217 at the water surface, such that the water content at the top of the sand tank was only 60 % of the saturated water content. The water-content reduction toward the water surface was an indication of increased air entrapment and the atmospheric argon and oxygen concentrations observed near the water table initially. The horizontal stratification (vertical gradient) of the dissolved argon and oxygen concentrations was due to the increasing air entrapment and gas saturation, from the capillary fringe to the water surface. As the experiment progressed, the gas concentrations at the bottom of the sand tank were depleted due to the lower degree of gas content with depth, while the decrease at the inflow end was because the anaerobic input water encountered the gas concentrations first.

Oxygen concentrations were monitored due to its importance as a potential source of dissolved oxygen into a groundwater system, while argon was monitored as a non-reactive tracer to the oxygen concentrations. Argon can be used as a conservative tracer to understand physical processes, while oxygen will be affected by both physical and biogeochemical processes. For the experiments, nitrogen was used to de-aerate the inflow water. If an alternate gas was used, nitrogen (assuming no biogenic nitrogen production or consumption) in conjunction with argon, could also have been used as a tracer for oxygen (Amos et al., 2005).

4.3 Reactive Transport Model – MIN3P

A reactive transport geochemical model (MIN3P) was used to simulate the 45 cm entrapment experiment. MIN3P (Mayer et al., 2002) was modified to describe air-bubble entrapment by Amos and Mayer (2006) as governed by the equations presented in Kaluarachchi and Parker (1992) (Equations 3.11 to 3.14). Furthermore, Amos and Mayer (2006) included a formulation to describe the partitioning of gases between entrapped-gas bubbles and the aqueous phase as governed by Henry’s law. The model input parameters were derived from experimental measurements along with literature derived parameters from Williams and Oostrom (2000) and are presented in Table 4.2. The model dimensions were kept consistent with the sand in the sand tank and the simulation was run for 149 days.

Model Parameters	**Value**	**Dimensions**
Atmospheric Pressure	0.93	Atmospheres
Porosity	0.363	
Temperature	20	° Celcius
Hydraulic Conductivity	4.20E-03	metres/day
Residual Saturation	0.01*	
van Genuchten alpha	3.5	
van Genuchten n	4	metres
van Genuchten m	0.75	metres
Max. Bubble Entrapment	0.155*	
Longitudinal Dispersivity	0.02	metres
Transverse Dispersivity	0.002	metres

Table 4.1 Model input parameters; * indicates parameters obtained from Williams and Oostrom (2000), all other parameters were derived from experimental results.

The model was set up by starting with a fully drained soil in a simulated sand tank with the water level at 2 cm. The water level was raised back to 47 cm from the bottom in four simulation hours (consistent with the experimental filling time) allowing for air-bubble entrapment. Next, flow was started from the inflow end at a rate of 2 mL/min and the experiment was run for 149 simulation days. After the imbibition cycle, the top and bottom were assigned no flow boundary conditions, while the inflow and outflow were assigned fixed-flow boundary conditions. The output times for the model results were kept consistent with the experimental sampling dates to allow for a direct comparison of both data sets. The model results captured the observed evolution of argon and oxygen concentrations over the duration of the experiment (Figures 4.8 and 4.9).

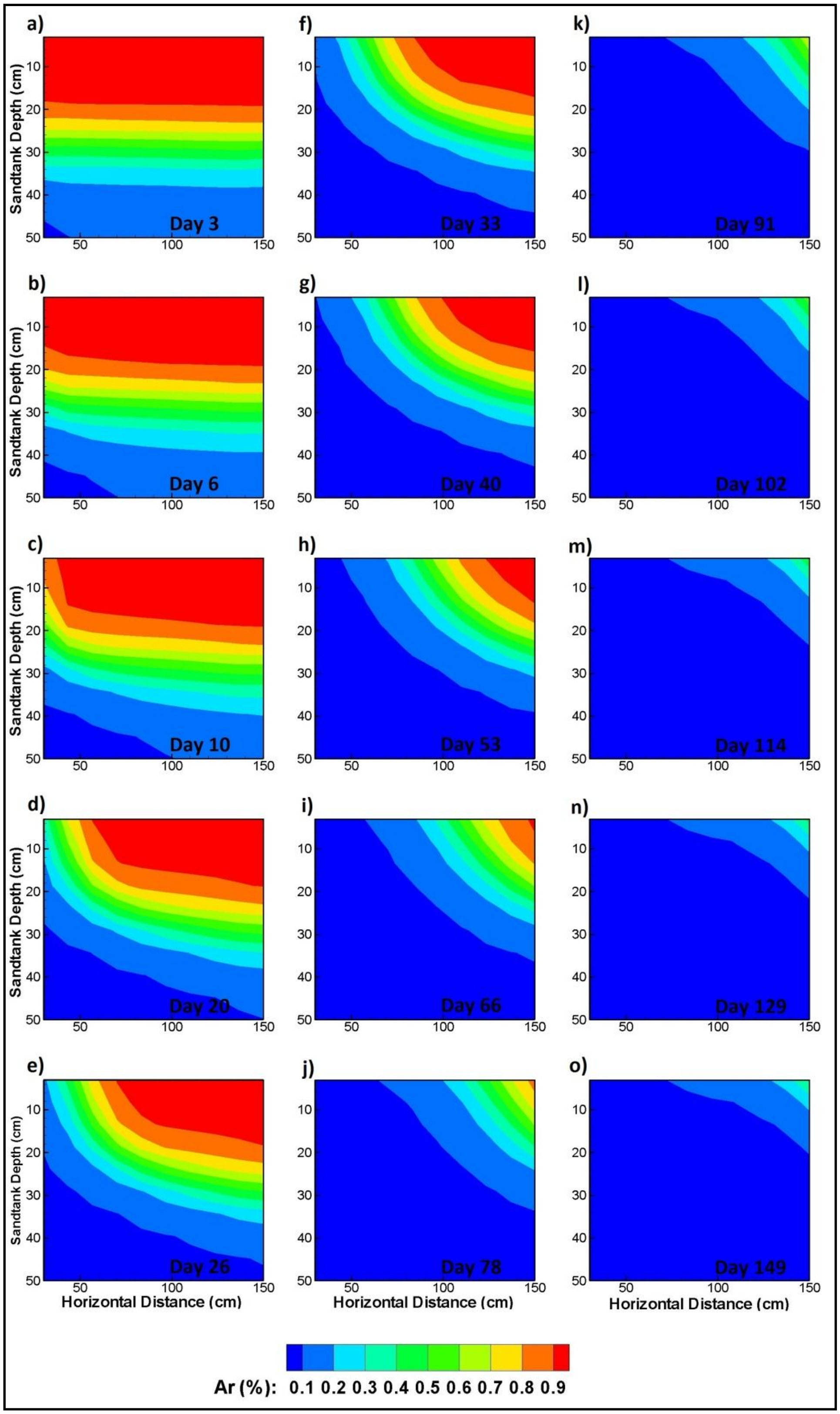

Figure 4.8 MIN3P 45 cm air-entrapment simulation results for argon

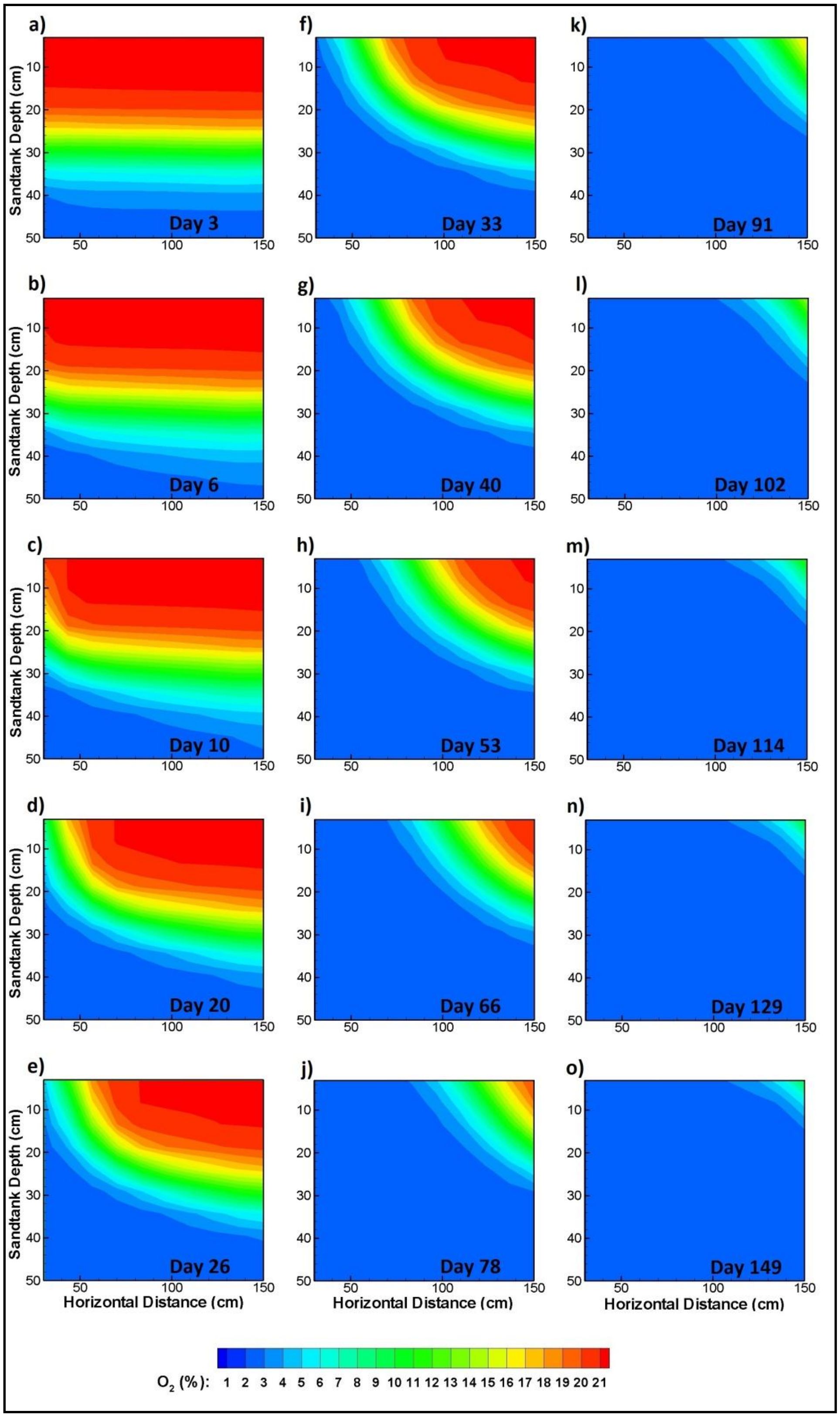

Figure 4.9 MIN3P 45 cm air-entrapment simulation results for oxygen

The model was effective in capturing the enhanced depletion of argon and oxygen at the inflow end, at greater depths and at the leading edge of the gas-water equilibrium front. The model accurately captured the position of the equilibrium front and the timing of argon and oxygen depletion.

The consistency between the model and experimental results allowed an appreciation of the air entrapment equations and the model set up with regard to modelling an air-entrapment experiment. The van Genuchten parameters of the water content-pressure head curve were adjusted to fit the Kaluarachchi and Parker (1992) equations to ensure that the experimental results were better represented. These equations were used for the bubble-entrapment simulations; therefore the adjusted van Genuchten parameters probably played an important role in ensuring that MIN3P simulated the experimental results well. Given this consistency, the sand may not have the same soil properties as the 'same' soil used by Williams and Oostrom (2000).

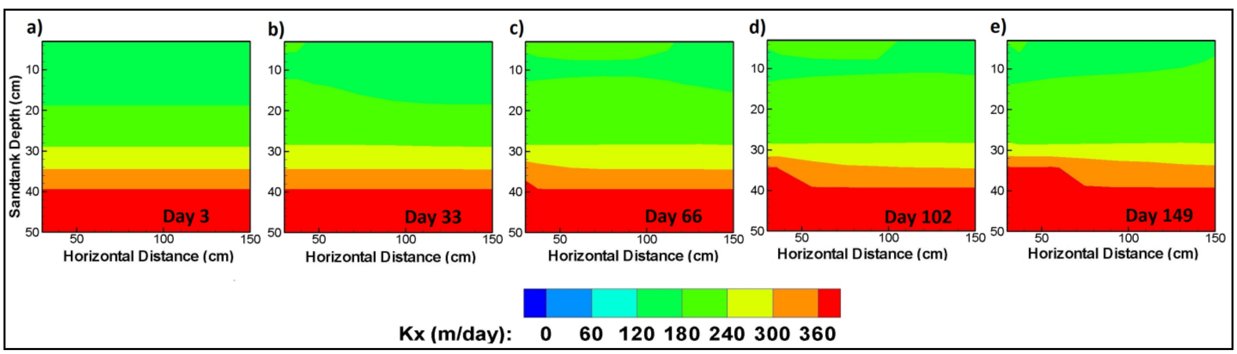

Figure 4.10 Change in Hydraulic Conductivity as simulated by MIN3P

In Chapter 3, it was identified that the hydraulic conductivity decreased as the air entrapment increased. However, the simulations did not show too much of a change in the conductivity over the course of the experiment (Figure 4.10). Initially the conductivity is horizontally stratified, but with time, the conductivity increases at the inflow end. The change in conductivity does not follow an evolving gradient as was seen with the gas concentrations. It was expected that a conductivity gradient would travel through the sand tank with time due to the dissolution of gas bubbles and the subsequent re-saturation of the previously air filled pores. Similarly, the velocity did not change much over the course of the simulation (Figure 4.11).

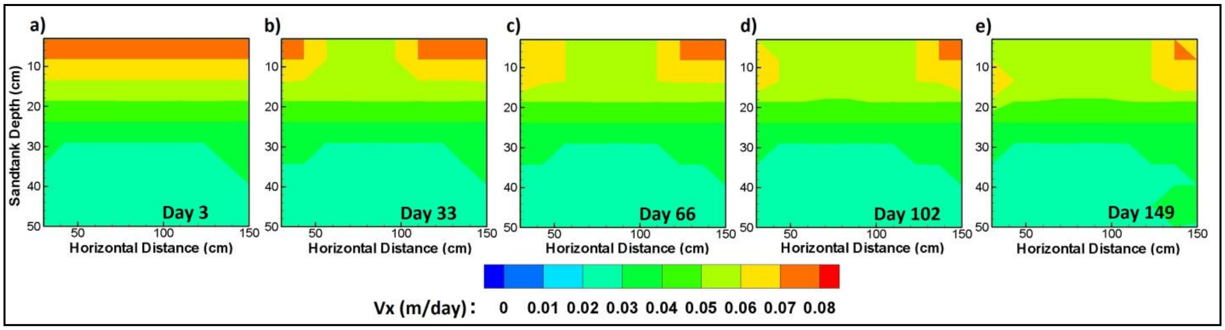

Figure 4.11 Change in Velocity as simulated by MIN3P

The simulation results for water saturation (Figure 4.12) captured the initial horizontal stratification due to the decrease in the water content (increase in air entrapment) when progressing from the capillary fringe to the water surface. The water saturation changed from fully saturated below 38 cm and progressively decreased to the minimum of 85 % at the top of the water surface. Over the course of the experiment, the water saturation in the sand tank gradually increased at the inflow end. As the anaerobic input water encountered the air bubbles, oxygen and argon from the bubbles dissolved into the water until the gas bubbles were stripped of these two gases, leaving nitrogen within these bubbles. The simulation results show that initially, the sand tank was fully saturated below a depth of 42 cm. However, by the final sampling event, the saturated zone extended below a depth of 32 cm from the inflow to the middle of the sand tank and below a depth of 36 cm from the middle to the outflow end of the sand tank. Overall, the simulation shows that there was only a slight increase in the water saturation during this experiment, particularly within the shallow 20 cm, which helps explain why the hydraulic conductivity and velocity were essentially unchanged over the course of the simulation.

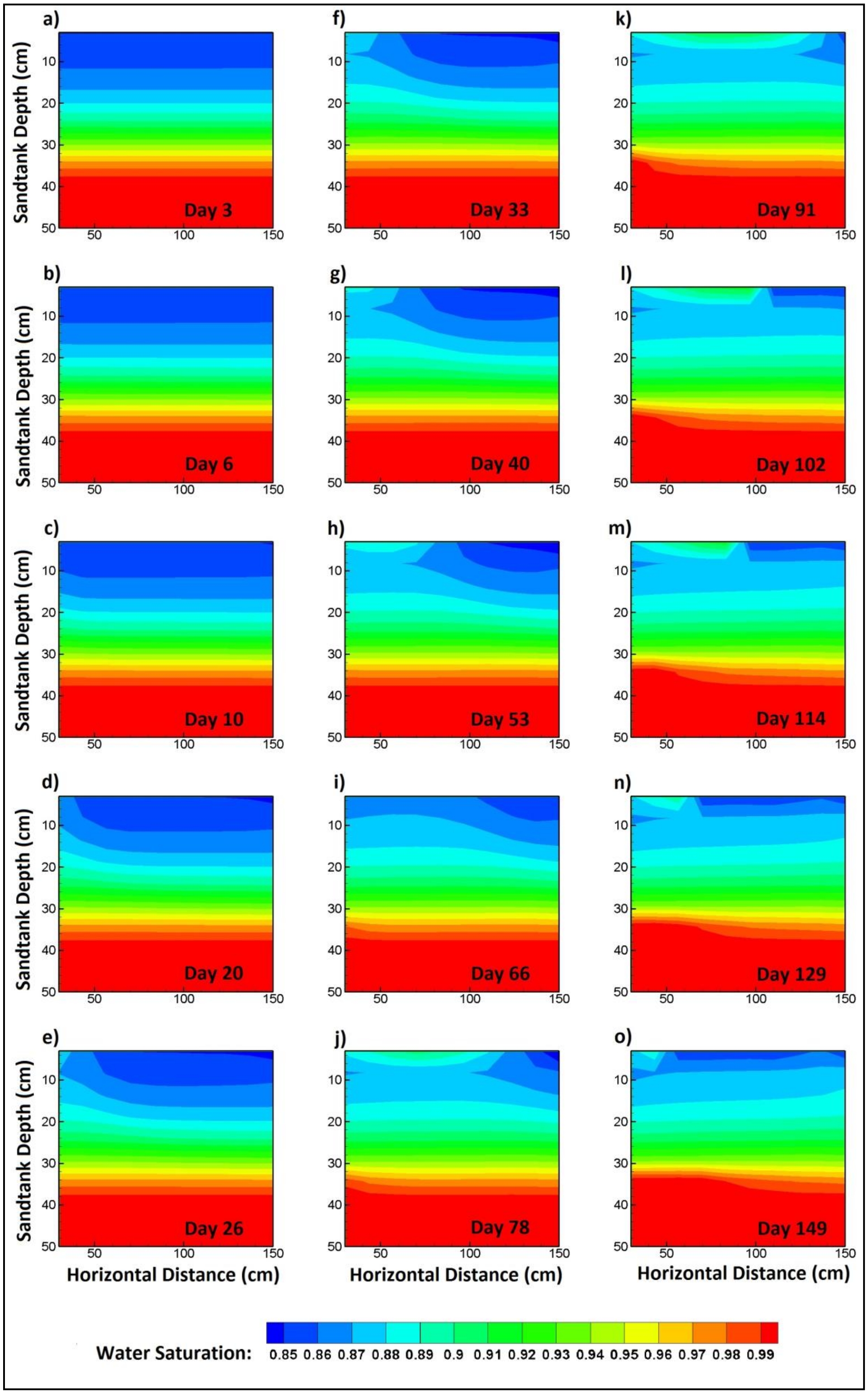

Figure 4.12 The change in water saturation across the sand tank over the course of the 45 cm air-entrapment experiment

4.4 Conclusions

Water table fluctuations result in the entrapment of air below the water surface. The entrapment of air alters the flow field resulting in a decrease in the hydraulic conductivity and flow velocity in the vicinity of the trapped-gas bubbles. Anaerobic water flowing past the entrapped-air bubbles will dissolve some of the gases present, obeying Henry's law of equilibrium partitioning. Some bubbles may decrease in size resulting in a slight increase in the overall water saturation. We have shown that fluctuating water tables can provide a reasonable amount of oxygen to a groundwater system as long as the amplitude of the fluctuating cycle is significant enough to entrap air bubbles into the groundwater. As the gases dissolve into the anaerobic input water, a concentration front develops whose shape, travel path and transport are directly dependent on the quantity of bubbles and the equilibration between these gas bubbles and the flowing groundwater.

5. Conclusion

5.1 Summary of Contributions

The main goal of this research was to identify the effects of entrapped-air bubbles on the physical properties of a sand media and to capture the change in dissolved-gas concentrations over time. In order to accomplish this goal, physical properties were quantified under saturated and fluctuating water-table conditions. These included hydraulic conductivity, water content, dispersivity and groundwater velocities. Hydraulic conductivity experiments were effective in quantifying the changes in hydraulic conductivity with depth. As the amount of entrapped air increased, the water content decreased which resulted in a reduction of the hydraulic conductivity progressing from the saturated zone to the zone of greatest air-bubble entrapment. Bromide tracer tests performed under fully-saturated and variably-saturated conditions identified a decrease in dispersivity within the sand tank which was consistent with the results of Orlob and Radhakrishna (1958). However, stratified velocity profiles were observed which resulted in preferential flow across the bottom of the tank. The overall horizontal velocity of the sand tank, however, was consistent with the calculated average linear groundwater velocity based on Darcy flux calculations (from hydraulic conductivity, hydraulic gradient and input flow velocity). Although the sand was the same kind used by Williams and Oostrom (2000), experimental results suggested that the sand behaved differently. The Brooks-Corey parameters identified by Williams and Oostrom (2000) did not match the soil well especially when the experimental measurements were tested against the model by Kaluarachchi and Parker (1992). In order to fit the model better, soil parameters were adjusted to allow for a better fit between the measurements and the model. As a result, the experimental sand, which was supposed to be well sorted, appeared to resemble poorly sorted sand, as was evident by the adjusted water content – pressure head curves.

Three experiments were performed to try and identify the effect of air entrapment on dissolved-air concentrations in groundwater. The fully-saturated experiment was intended to measure the ingress of air through diffusion across the top of the water surface. However, due to sampling limitations, it was not possible to quantify the influence of diffusion on the groundwater concentrations, though the effects were possibly small. The 29 cm and 45 cm fluctuating water-table experiments provided insight into the rate of dissolution and depletion of dissolved gas concentrations. There is increasing entrapment of air from the top of the saturated zone (and the capillary fringe) to the top of the water surface. If the fluctuation amplitude is significant enough, sufficient gas bubbles will be entrapped that can contribute dissolved oxygen to a groundwater system. The gas in the bubbles will partition into the anaerobic water until they are in equilibrium with one another. As a result, greater depletion of the dissolved argon and oxygen concentrations can be seen closer to the inflow end of the sand tank at early times, along with a mobile gas-water concentration front which progresses to the outflow, depleting the argon and oxygen concentrations from all the air bubbles it encounters. The rate at which the concentration front travels is dependent on the hydraulic conductivity and the groundwater velocity, but the quantity of entrapped-gas bubbles and the equilibration between the gas and aqueous phase has the most significant impact. The model simulations using MIN3P provided insight regarding the effectiveness of the sampling procedure due to the similarity between the experimental and simulation results. The model results showed that the depletion of argon and oxygen concentrations were primarily controlled by the quantity of gas bubbles and the equilibration between the gaseous and aqueous phases, rather than the changes in hydraulic conductivity and velocity. Additionally the combination of the equations formulated by Kaluarachchi and Parker (1992), Henry's law and the bubble entrapment model modification, described this system well.

5.2 Future Considerations

These experiments have provided an understanding of the physical properties of the sand, and have helped to understand the differences between saturated and variably-saturated flow through this sand media. The experimental results were tested against analytical and numerical models and fit them reasonably well. The next logical step would be to perform experiments that simulate a real world situation where the biogeochemistry also plays an important role. Physical flow through sand can deplete the gas concentrations in bubbles from a groundwater system, but in reality the influence of bacteria on oxygen depletion would be more significant. An aerobically degraded organic contaminant should be used to test the rate of contaminant degradation and oxygen depletion.

Additionally, all of the experiments performed during the course of this research can be repeated on sand tanks with soils of different grain sizes. It would be interesting to run all of these experiments in a sand tank with a silt or clay soil. The amount of air that can be entrapped will vary which can provide additional information on the effectiveness of fluctuating water-tables as a source for oxygen in non-coarse soil. The introduction of heterogeneities into this sand tank like silt or clay lenses will also provide some additional insight.

References

Adam, K.M., 1967. Diffusion of entrapped gas from porous media, PhD dissertation, Colorado State University, Fort Collins, Colorado.

Adam, K.M., Bloomsburg, G.L. and Corey, A.T., 1969. Diffusion of trapped gas from porous media. Water Resources Research 5: 840–849.

Amos, R.T., Mayer, K.U., Bekins, B.A., Delin, G.N. and Williams, R.L., 2005. Use of dissolved and vapor-phase gases to investigate methanogenic degradation of petroleum hydrocarbon contamination in the subsurface. Water Resources Research 41. DOI: 10.1029/2004WR003433

Amos, R.T., and Mayer K.U., 2006. Investigating the role of gas bubble formation and entrapment in contaminated aquifers: Reactive transport modelling. Journal of Contaminant Hydrology 87:123–154

Amos, R.T., Bekins, B.A., Delin, G.N., Cozzarelli, I.M., Blowes, D.W. and Kirshtein, J.D., 2011. Methane oxidation in a crude oil contaminated aquifer: delineation of aerobic reactions at the plume fringes. Journal of Contaminant Hydrology 125: 13–25

Berkowitz, B., Silliman, S.E. and Dunn, A.M., 2004. Impact of the capillary fringe on local flow, chemical migration, and microbiology. Vadose Zone Journal 3: 534–548.

Blicher-Mathiesen, G., McCarty, G.W. and Nielsen, L.P., 1998. Denitrification and degassing in groundwater estimated from dissolved dinitrogen and argon. Journal of Hydrology 208: 16–24

Bloomsburg, G.L., 1964. Diffusion of entrapped air from porous media, PhD dissertation, Colorado State University, Fort Collins, Colorado.

Bloomsburg, G.L., and Corey, A.T., 1964. Diffusion of Entrapped Air from Porous Media. Hydrology Papers No. 5, Colorado State University, Fort Collins, Colorado.

Boutt, D.F., and Fleming, B.J., 2009. Implications of anthropogenic river stage fluctuations on mass transport in a valley fill aquifer. Water Resources Research 45. DOI: 10.1029/2007WR006526

Brooks, R.H., and Corey, A.T., 1964. Hydraulic properties of porous media. Hydrology Papers No. 3, Department of Civil Engineering, Colorado State University, Fort Collins, Colorado.

Christiansen, J.E., 1944. Effect of entrapped air upon the permeability of soils. Soil Science 58: 355–365.

Cirpka, O.A., and Kitanidis, P.K., 2001. Transport of volatile compounds in porous media in the presence of a trapped gas phase. Journal of Contaminant Hydrology 49: 263–285.

Dror, I., Berkowitz, B., and Gorelick, S.M., 2004. Effects of air injection on flow through porous media: observations and analyses of laboratory-scale processes. Water Resources Research 40. DOI: 10.1029/2003WR002960

Faybishenko, B.A., 1995. Hydraulic behavior of quasi-saturated soils in the presence of entrapped air: Laboratory experiments. Water Resources Research 31: 2421–2435.

Fortuin, N.P.M., and Willemsen, A., 2005. Exsolution of nitrogen and argon by methanogenesis in Dutch ground water. Journal of Hydrology 301: 1–13.

Freitas, J.G., 2009. Impacts of ethanol in gasoline on subsurface contamination, PhD dissertation, University of Waterloo, Waterloo, Ontario.

Fry, V.A., Istok, J.D., Semprini, L., O'Reilly, K.T., and Buscheck, T.E., 1995. Retardation of dissolved oxygen due to a trapped gas phase in porous media. Ground Water 33: 391–398.

Fry, V.A., Istok, J.D., and O'Reilly, K.T., 1996. Effect of trapped gas on dissolved oxygen transport—implications for in situ bioremediation. Ground Water 34: 200–210.

Fry, V.A., Selker, J.S., and Gorelick, S.M., 1997. Experimental investigations for trapping oxygen gas in saturated porous media for in situ bioremediation. Water Resources Research 33: 2687–2696.

Haberer, C.M., Rolle, M., Cirpka, O.A., and Grathwohl, P., 2012. Oxygen transfer in a fluctuating capillary fringe. Vadose Zone Journal 11. DOI: 10.2136/vzj2011.0056

Haberer, C.M., Rolle, M., Liu, S., Cirpka, O.A., Grathwohl, P. 2011. A high-resolution non-invasive approach to quantify oxygen transport across the capillary fringe and within the underlying groundwater. Journal of Contaminant Hydrology 122: 26–39.

Kaluarachchi, J.J., and Parker, J.C., 1992. Multiple flow with a simplified model of oil entrapment. Transport in Porous Media 7: 1–14.

Lenhard, R.J., 1992. Measurement and modeling of three-phase saturation pressure hysteresis. Journal of Contaminant Hydrology 9: 243–269.

Marinas, M., Roy, J.W., and Smith, J.E., 2013. Changes in entrapped gas content and hydraulic conductivity with pressure. Ground Water 51: 41–50.

Mayer, K.U., Frind, E.O., and Blowes, D.W., 2002. A numerical model for the investigation of reactive transport in variably saturated media using a generalized formulation for kinetically controlled reactions. Water Resources Research 38: 1174–1194.

Orlob, G.T., and Radhakrishna, G.N., 1958. The effects of entrapped gases on the hydraulic characteristics of porous media. Eos Transactions of the AGU 39, No. 4: 648–659.

Parker, J.C., and Lenhard, R.J., 1987. A model for hysteretic constitutive relations governing multiphase flow 1. Saturation–pressure relations. Water Resources Research 23: 2187–2196.

Ronen, D., Berkowitz, B., and Magaritz, M., 1989. The development and influence of gas bubbles in phreatic aquifers under natural flow conditions. Transport in Porous Media 4: 295–306.

Ryan, M.C., MacQuarrie, K.T.B., Harman, J., and McLellan, J., 2000. Field and modeling evidence for a "stagnant flow" zone in the upper meter of sandy phreatic aquifers. Journal of Hydrology 233: 233–240.

Sakaguchi, A., Nishimura, T., and Kato, M., 2005. The effect of entrapped air on the quasi-saturated soil hydraulic conductivity and comparison with the unsaturated hydraulic conductivity. Vadose Zone Journal 4: 139–144.

Sudicky, E.A., Cherry, J.A., and Frind, E.O.,1983. Migration of contaminants in groundwater at a landfill; a case study.4.. Journal of Hydrology 63: 81–108

Tang, G., Mayes, M.A., Parker, J.C., and Jardine, P.M., 2010. CXTFIT/Excel – a modular adaptable code for parameter estimation, sensitivity analysis, and uncertainty analysis for laboratory and field tracer experiments. Computers & Geosciences 36: 1200-1209.

van Genuchten, M.Th., 1980. A closed-form equation for predicting the hydraulic conductivity of unsaturated soils. Soil Science Society of America Journal 44: 892–898.

Williams, M.D., and Oostrom, M., 2000. Oxygenation of anoxic water in a fluctuating water table system: an experimental and numerical study. Journal of Hydrology 230: 70–85.

Appendix A – Dispersivity Data and Figures

N1-3 Saturated

	Estimate
Velocity (cm/day)	8.3066
Dispersion	32.3022
R^2	0.9832

Concentration (ppm)				
Distance (m)	Time (days)	Observation	Prediction	Residual
30	0	0.0000	0.0000	0.0000
30	2	0.0509	0.1028	-0.0519
30	4	0.6420	0.5737	0.0683
30	6	0.7768	0.8498	-0.0730
30	8	0.9554	0.9519	0.0035

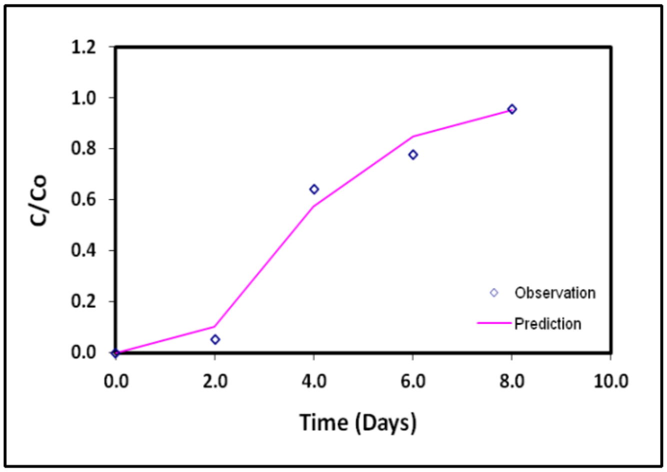

N1-5 Saturated

	Estimate
Velocity (cm/day)	9.9607
Dispersion	51.4001
R^2	0.9643

Concentration (ppm)				
Distance (m)	Time (days)	Observation	Prediction	Residual
30	0	0.0000	0.0000	0.0000
30	2	0.1688	0.2160	-0.0472
30	4	0.7902	0.6861	0.1041
30	6	0.7902	0.8934	-0.1032
30	8	0.9268	0.9648	-0.0380

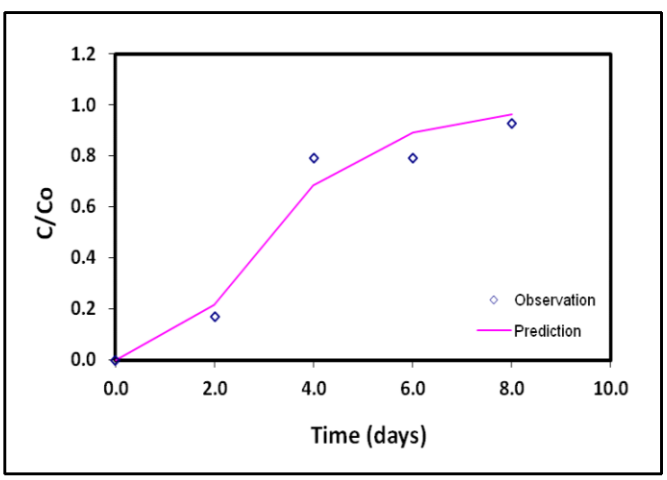

N1-7 Saturated

	Estimate
Velocity (cm/day)	23.0727
Dispersion	1002.8192
R^2	0.9690

Concentration (ppm)				
Distance (m)	Time (days)	Observation	Prediction	Residual
30	0	0.0000	0.0000	0.0000
30	2	0.4982	0.5343	-0.0361
30	4	0.8518	0.7475	0.1043
30	6	0.8143	0.8502	-0.0359
30	8	0.8491	0.9067	-0.0576

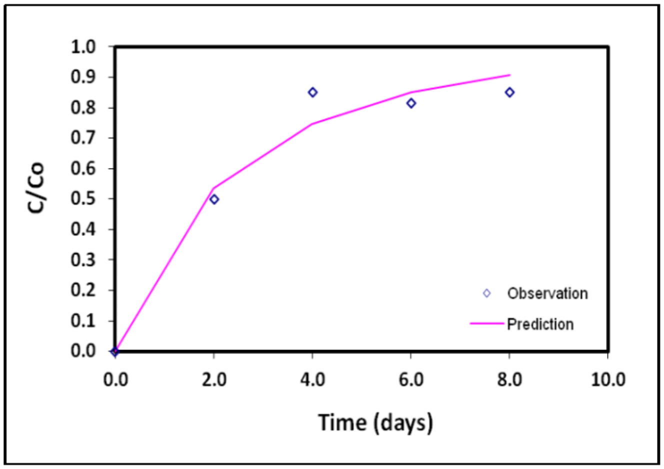

N1-9 Saturated

	Estimate
Velocity (cm/day)	7.0000
Dispersion	75.0000
R^2	0.8886

Concentration (ppm)				
Distance (m)	Time (days)	Observation	Prediction	Residual
30	0	0.0000	0.0000	0.0000
30	6	0.7902	0.6459	0.1443
30	8	0.8705	0.7787	0.0918
30	10	0.7536	0.8605	-0.1069
30	12	0.8491	0.9112	-0.0621
30	15	0.8188	0.9541	-0.1353

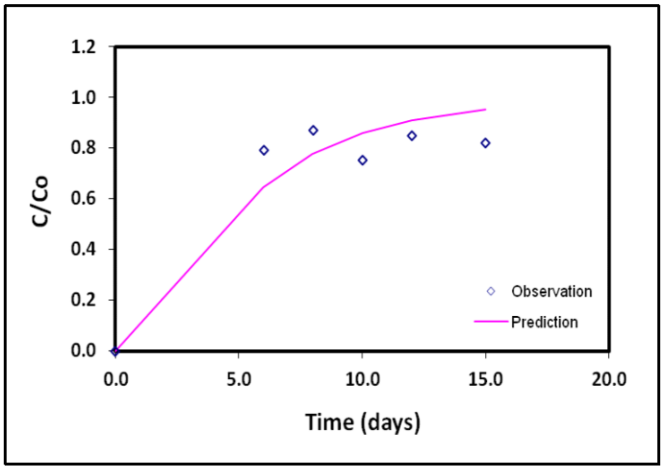

N1-11 Saturated

	Estimate
Velocity (cm/day)	6.0000
Dispersion	36.0000
R^2	0.8435

Concentration (ppm)				
Distance (m)	Time (days)	Observation	Prediction	Residual
30	0	0.0000	0.0000	0.0000
30	6	0.8589	0.6067	0.2522
30	8	0.8143	0.7789	0.0354
30	10	0.7661	0.8777	-0.1116
30	12	0.8491	0.9326	-0.0835
30	15	0.8839	0.9724	-0.0885

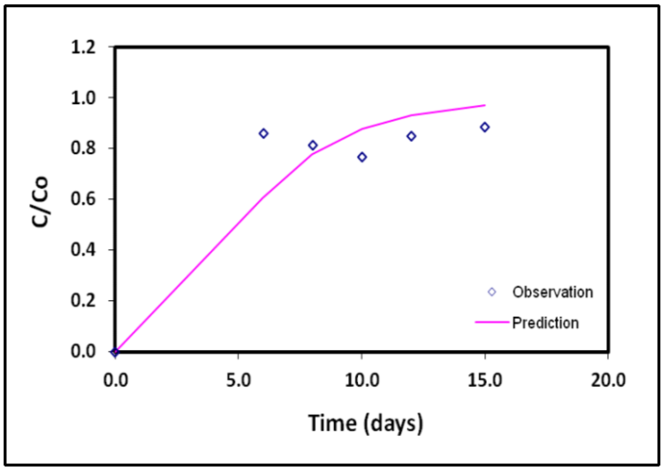

N1-13 Saturated

	Estimate
Velocity (cm/day)	7.0000
Dispersion	105.0000
R^2	0.8845

Concentration (ppm)				
Distance (m)	Time (days)	Observation	Prediction	Residual
30	0	0.0000	0.0000	0.0000
30	6	0.8348	0.6128	0.2220
30	8	0.6946	0.7357	-0.0411
30	10	0.7536	0.8172	-0.0636
30	12	0.7902	0.8720	-0.0818
30	15	0.8884	0.9236	-0.0352

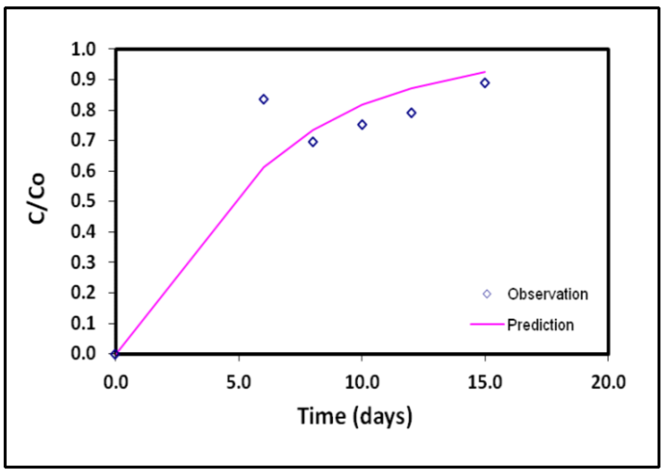

N2-3 Saturated

	Estimate
Velocity (cm/day)	7.6251
Dispersion	8.0060
R^2	0.9913

Concentration (ppm)				
Distance (m)	**Time (days)**	**Observation**	**Prediction**	**Residual**
60	0	0.0000	0.0000	0.0000
60	2	0.0661	0.0000	0.0661
60	4	0.0259	0.0001	0.0258
60	6	0.0929	0.0711	0.0218
60	8	0.5205	0.5349	-0.0144
60	11	1.0000	0.9651	0.0349

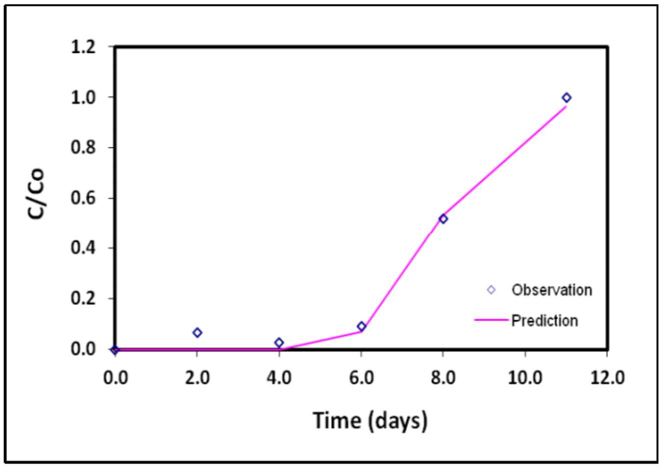

N2-5 Saturated

	Estimate
Velocity (cm/day)	9.2955
Dispersion	6.6604
R^2	0.9930

Concentration (ppm)				
Distance (m)	**Time (days)**	**Observation**	**Prediction**	**Residual**
60	0	0.0000	0.0000	0.0000
60	2	0.0580	0.0000	0.0580
60	4	0.0330	0.0008	0.0322
60	6	0.3161	0.3169	-0.0008
60	8	0.9205	0.9190	0.0015
60	11	0.9500	0.9998	-0.0498

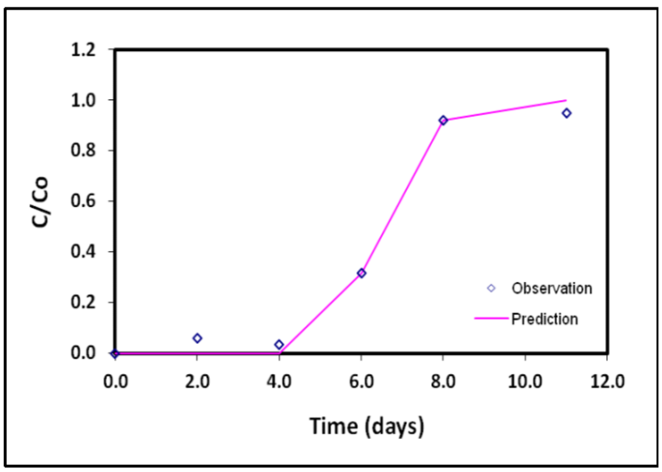

N2-7 Saturated

	Estimate
Velocity (cm/day)	10.7341
Dispersion	15.0270
R^2	0.9926

Concentration (ppm)				
Distance (m)	Time (days)	Observation	Prediction	Residual
60	0	0.0000	0.0000	0.0000
60	2	0.0545	0.0000	0.0545
60	4	0.0821	0.0575	0.0246
60	6	0.6107	0.6291	-0.0184
60	8	0.9955	0.9540	0.0415

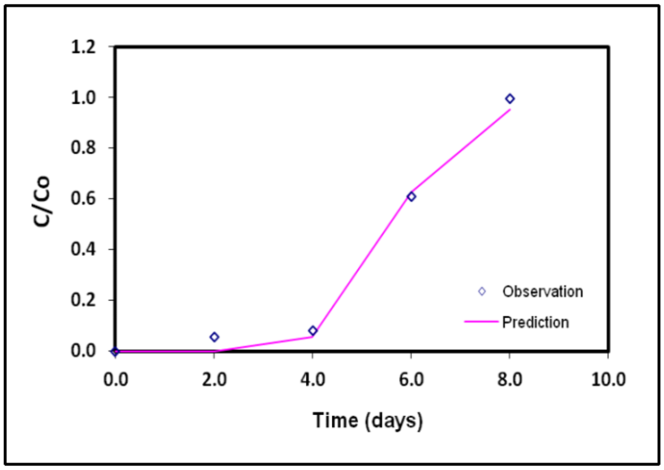

N2-9 Saturated

	Estimate
Velocity (cm/day)	15.5334
Dispersion	135.1328
R^2	0.9847

Concentration (ppm)				
Distance (m)	Time (days)	Observation	Prediction	Residual
60	0	0.0000	0.0000	0.0000
60	2	0.0661	0.0893	-0.0232
60	4	0.5571	0.5160	0.0411
60	6	0.7268	0.8009	-0.0741
60	8	0.9813	0.9241	0.0572

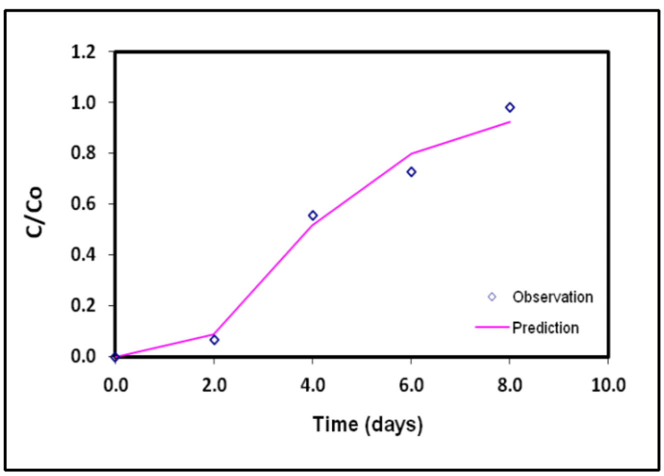

N2-11 Saturated

	Estimate
Velocity (cm/day)	20.7143
Dispersion	250.1783
R^2	0.9784

Concentration (ppm)				
Distance (m)	**Time (days)**	**Observation**	**Prediction**	**Residual**
60	0	0.0000	0.0000	0.0000
60	2	0.2179	0.2500	-0.0321
60	4	0.7750	0.6952	0.0798
60	6	0.7991	0.8893	-0.0902
60	8	0.9750	0.9602	0.0148
60	11	0.9438	0.9913	-0.0475

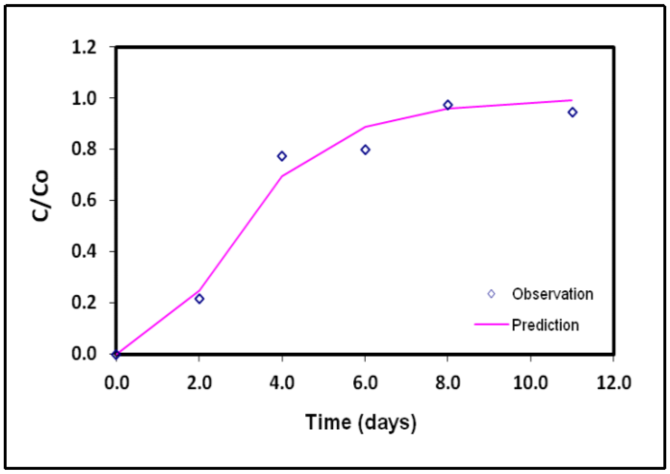

N2-13 Saturated

	Estimate
Velocity (cm/day)	12.0000
Dispersion	118.0000
R^2	0.9095

Concentration (ppm)				
Distance (m)	**Time (days)**	**Observation**	**Prediction**	**Residual**
60	0	0.0000	0.0000	0.0000
60	6	0.7875	0.6208	0.1667
60	8	0.7875	0.8026	-0.0151
60	10	0.7473	0.9001	-0.1528
60	12	0.9839	0.9500	0.0339

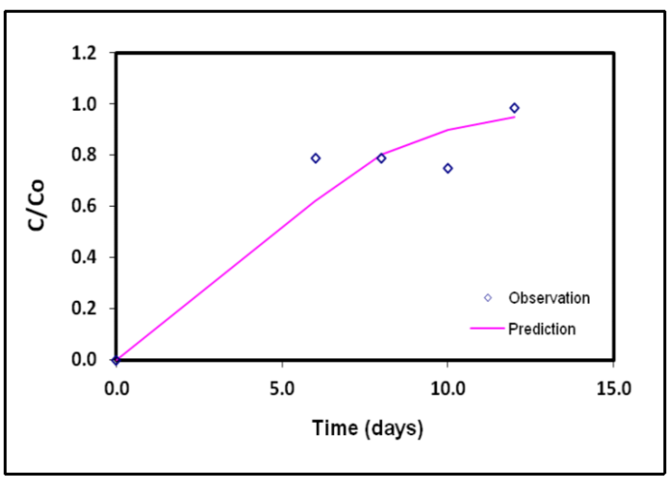

N3-3 Saturated

	Estimate
Velocity (cm/day)	6.0613
Dispersion	42.7958
R^2	0.9937

Concentration (ppm)				
Distance (m)	Time (days)	Observation	Prediction	Residual
90	0	0.0000	0.0000	0.0000
90	2	0.0000	0.0000	0.0000
90	4	0.0166	0.0001	0.0165
90	6	0.0205	0.0070	0.0135
90	8	0.0143	0.0492	-0.0349
90	11	0.2313	0.2120	0.0193
90	17	0.6277	0.6336	-0.0059

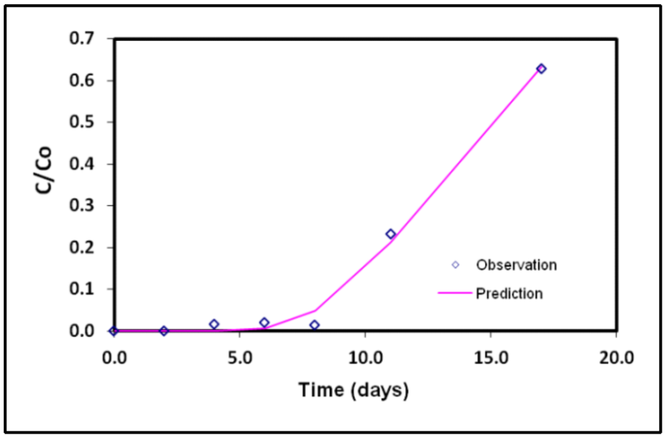

N3-5 Saturated

	Estimate
Velocity (cm/day)	7.5993
Dispersion	52.7028
R^2	0.9375

Concentration (ppm)				
Distance (m)	Time (days)	Observation	Prediction	Residual
90	0	0.0000	0.0000	0.0000
90	2	0.0161	0.0000	0.0161
90	4	0.0170	0.0013	0.0157
90	6	0.0188	0.0332	-0.0144
90	8	0.0304	0.1463	-0.1159
90	11	0.5438	0.4180	0.1258
90	17	0.7464	0.8278	-0.0814

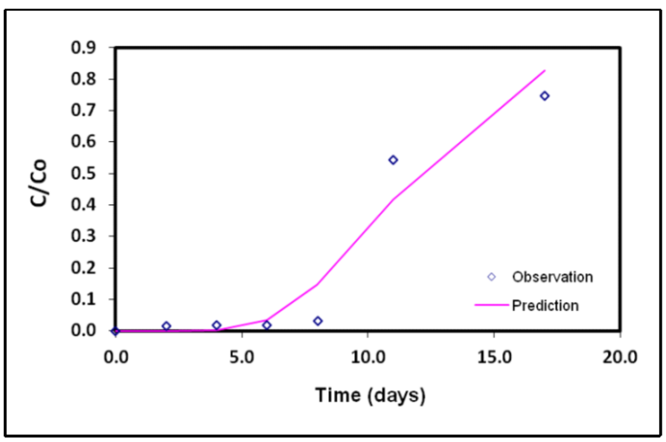

N3-7 Saturated

	Estimate
Velocity (cm/day)	9.4335
Dispersion	9.3333
R^2	0.9976

Concentration (ppm)				
Distance (m)	Time (days)	Observation	Prediction	Residual
90	0	0.0000	0.0000	0.0000
90	2	0.0241	0.0000	0.0241
90	4	0.0152	0.0000	0.0152
90	6	0.0232	0.0008	0.0224
90	8	0.1152	0.1158	-0.0006
90	11	0.8330	0.8328	0.0002

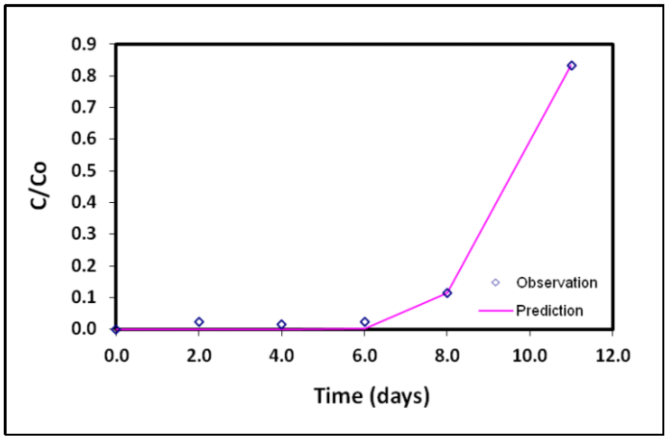

N3-9 Saturated

	Estimate
Velocity (cm/day)	10.7400
Dispersion	35.8158
R^2	0.9780

Concentration (ppm)				
Distance (m)	Time (days)	Observation	Prediction	Residual
90	0	0.0000	0.0000	0.0000
90	2	0.0196	0.0000	0.0196
90	4	0.0241	0.0023	0.0218
90	6	0.0759	0.1040	-0.0281
90	8	0.4491	0.4294	0.0197
90	11	0.8384	0.8451	-0.0067
90	17	0.8929	0.9965	-0.1036

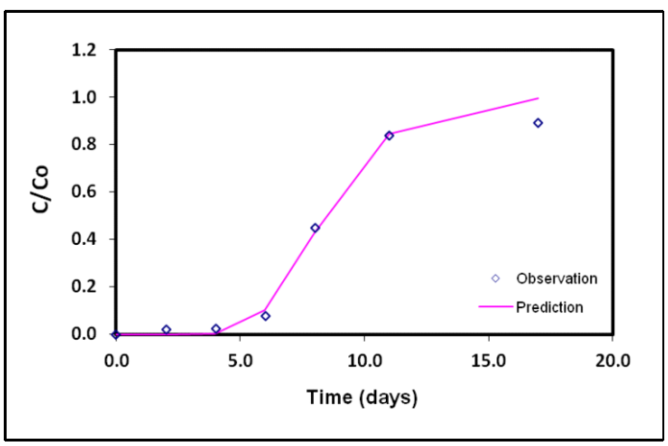

N3-11 Saturated

	Estimate
Velocity (cm/day)	14.5755
Dispersion	19.7957
R^2	0.9984

Concentration (ppm)				
Distance (m)	Time (days)	Observation	Prediction	Residual
90	0	0.0000	0.0000	0.0000
90	2	0.0241	0.0000	0.0241
90	4	0.0268	0.0056	0.0212
90	6	0.4313	0.4334	-0.0021
90	8	0.9375	0.9338	0.0037

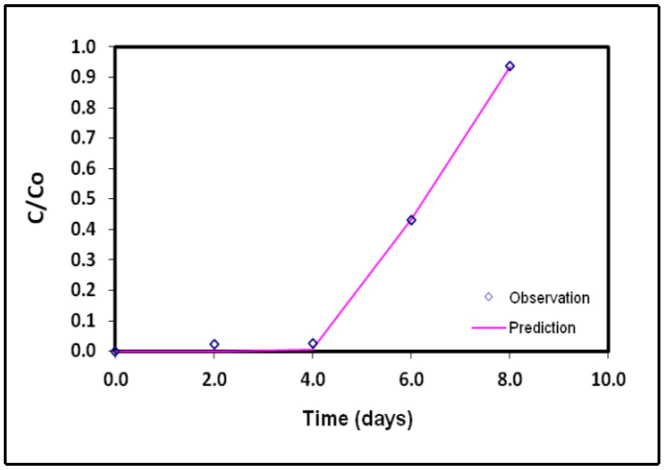

N3-13 Saturated

	Estimate
Velocity (cm/day)	18.0911
Dispersion	106.3826
R^2	0.9980

Concentration (ppm)				
Distance (m)	Time (days)	Observation	Prediction	Residual
90	0	0.0000	0.0000	0.0000
90	2	0.0321	0.0036	0.0285
90	4	0.2554	0.2636	-0.0082
90	6	0.7143	0.7001	0.0142
90	8	0.8964	0.9124	-0.0160

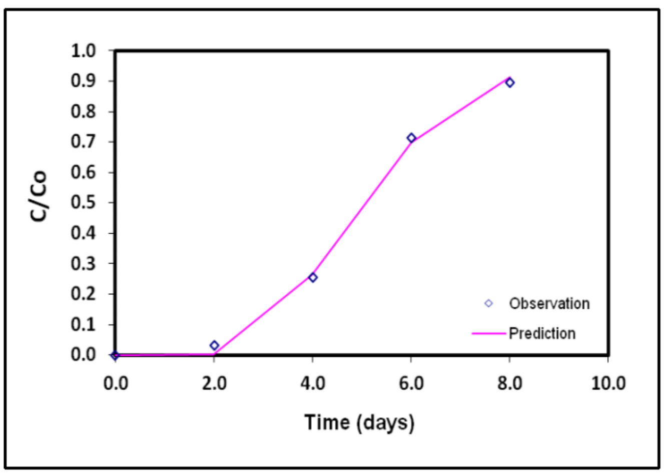

N4-3 Saturated

	Estimate
Velocity (cm/day)	4.8820
Dispersion	51.7094
R^2	0.9990

Concentration (ppm)				
Distance (m)	Time (days)	Observation	Prediction	Residual
120	0	0.0000	0.0000	0.0000
120	2	0.0000	0.0000	0.0000
120	4	0.0000	0.0000	0.0000
120	6	0.0000	0.0001	-0.0001
120	8	0.0000	0.0017	-0.0017
120	11	0.0098	0.0201	-0.0103
120	17	0.1813	0.1758	0.0055
120	22	0.3839	0.3862	-0.0023

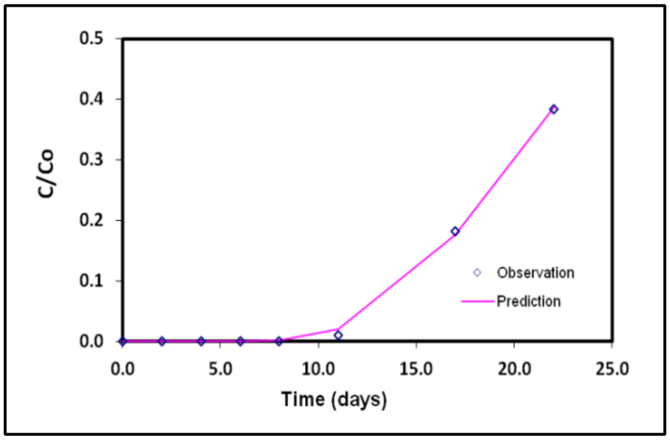

N4-5 Saturated

	Estimate
Velocity (cm/day)	7.1222
Dispersion	16.0242
R^2	0.9999

Concentration (ppm)				
Distance (m)	Time (days)	Observation	Prediction	Residual
120	0	0.0000	0.0000	0.0000
120	2	0.0000	0.0000	0.0000
120	4	0.0000	0.0000	0.0000
120	6	0.0000	0.0000	0.0000
120	8	0.0054	0.0000	0.0054
120	11	0.0125	0.0125	0.0000
120	17	0.5179	0.5179	0.0000

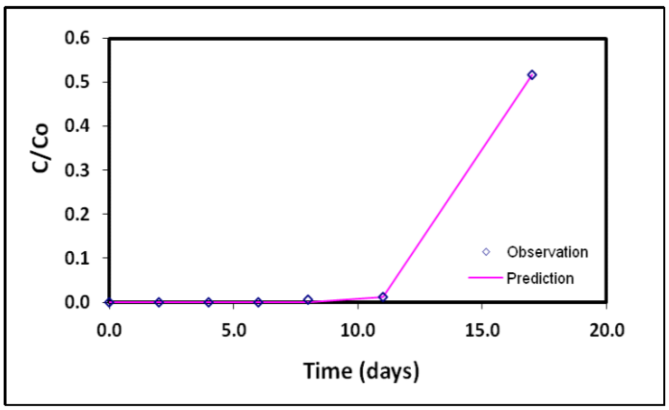

N4-7 Saturated

	Estimate
Velocity (cm/day)	7.3720
Dispersion	1.1966
R^2	0.9958

Concentration (ppm)				
Distance (m)	**Time (days)**	**Observation**	**Prediction**	**Residual**
120	0	0.0000	0.0000	0.0000
120	2	0.0250	0.0000	0.0250
120	8	0.0063	0.0000	0.0063
120	11	0.0375	0.0000	0.0375
120	17	0.7982	0.7982	0.0000

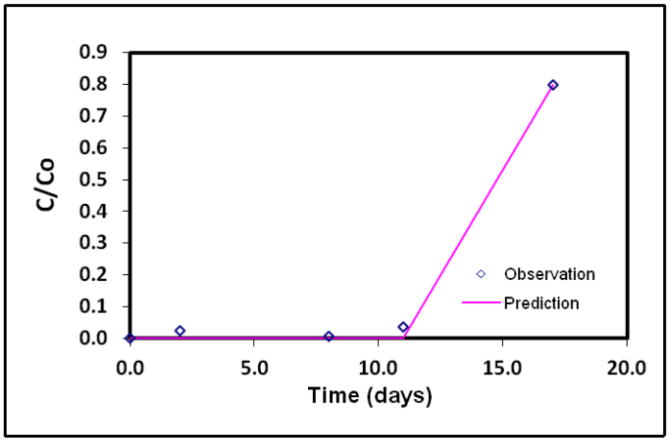

N4-9 Saturated

	Estimate
Velocity (cm/day)	9.2097
Dispersion	30.6440
R^2	0.9991

Concentration (ppm)				
Distance (m)	**Time (days)**	**Observation**	**Prediction**	**Residual**
120	0	0.0000	0.0000	0.0000
120	2	0.0000	0.0000	0.0000
120	4	0.0232	0.0000	0.0232
120	8	0.0125	0.0169	-0.0044
120	11	0.2330	0.2319	0.0011
120	17	0.8732	0.8739	-0.0007

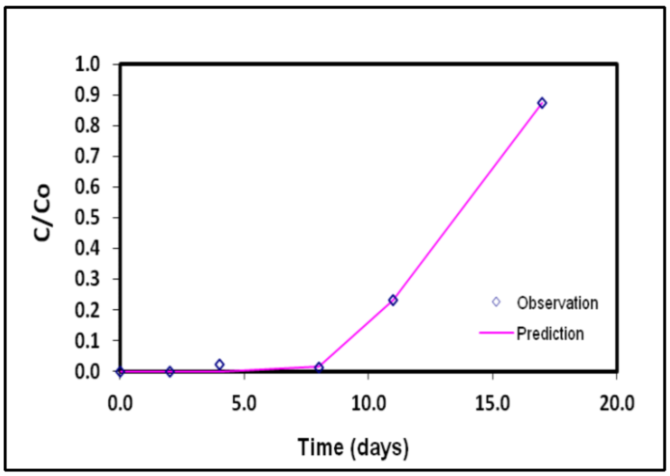

N4-11 Saturated

	Estimate
Velocity (cm/day)	11.7944
Dispersion	13.3246
R^2	0.9912

Concentration (ppm)				
Distance (m)	Time (days)	Observation	Prediction	Residual
120	0	0.0000	0.0000	0.0000
120	2	0.0277	0.0000	0.0277
120	8	0.0384	0.0388	-0.0004
120	11	0.7161	0.7159	0.0002
120	17	0.9214	0.9999	-0.0785
120	22	0.9482	1.0000	-0.0518

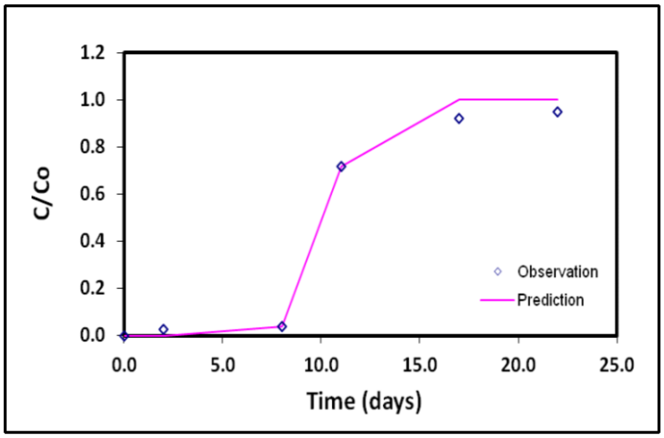

N4-13 Saturated

	Estimate
Velocity (cm/day)	13.6117
Dispersion	29.8179
R^2	0.9790

Concentration (ppm)				
Distance (m)	Time (days)	Observation	Prediction	Residual
120	0	0.0000	0.0000	0.0000
120	2	0.0188	0.0000	0.0188
120	4	0.0170	0.0000	0.0170
120	6	0.0214	0.0204	0.0010
120	8	0.3027	0.3034	-0.0007
120	11	0.8804	0.8789	0.0015
120	17	0.8634	0.9998	-0.1364
120	22	0.9098	1.0000	-0.0902

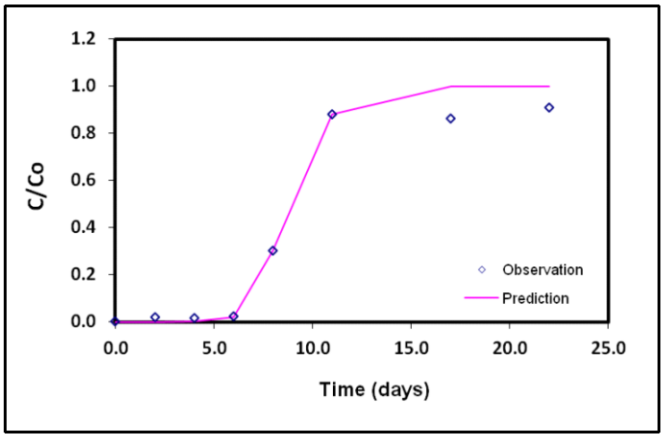

N5-3 Saturated

	Estimate
Velocity (cm/day)	5.8157
Dispersion	12.9675
R^2	1.0000

Concentration (ppm)				
Distance (m)	**Time (days)**	**Observation**	**Prediction**	**Residual**
150	0	0.0000	0.0000	0.0000
150	2	0.0000	0.0000	0.0000
150	4	0.0000	0.0000	0.0000
150	6	0.0000	0.0000	0.0000
150	8	0.0000	0.0000	0.0000
150	17	0.0071	0.0071	0.0000
150	22	0.1759	0.1759	0.0000

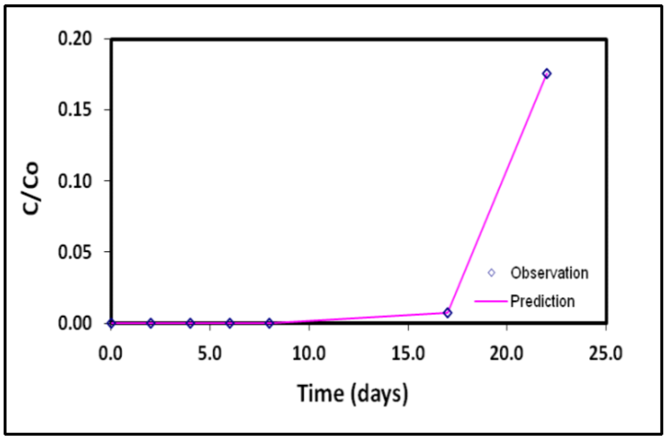

N5-5 Saturated

	Estimate
Velocity (cm/day)	6.7578
Dispersion	7.4550
R^2	1.0000

Concentration (ppm)				
Distance (m)	**Time (days)**	**Observation**	**Prediction**	**Residual**
150	0	0.0000	0.0000	0.0000
150	2	0.0000	0.0000	0.0000
150	4	0.0000	0.0000	0.0000
150	6	0.0000	0.0000	0.0000
150	8	0.0000	0.0000	0.0000
150	17	0.0134	0.0134	0.0000
150	22	0.4705	0.4705	0.0000

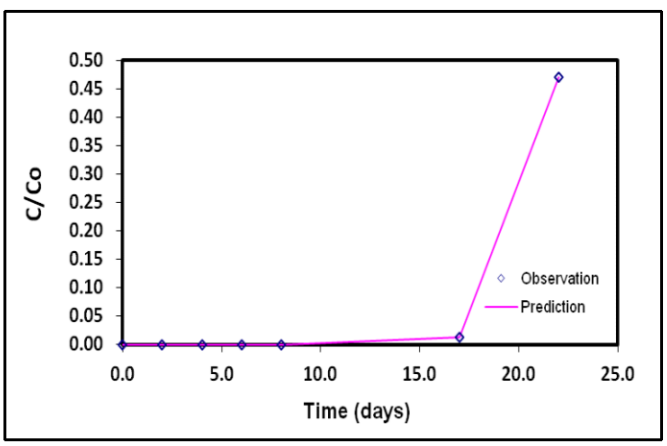

N5-7 Saturated

	Estimate
Velocity (cm/day)	7.2319
Dispersion	5.5326
R^2	1.0000

Concentration (ppm)				
Distance (m)	Time (days)	Observation	Prediction	Residual
150	0	0.0000	0.0000	0.0000
150	2	0.0000	0.0000	0.0000
150	4	0.0000	0.0000	0.0000
150	6	0.0000	0.0000	0.0000
150	8	0.0000	0.0000	0.0000
150	17	0.0241	0.0240	0.0001
150	22	0.7205	0.7206	-0.0001

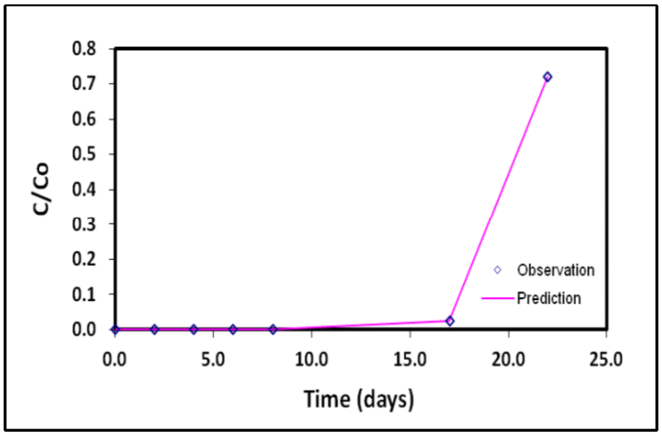

N5-9 Saturated

	Estimate
Velocity (cm/day)	8.0468
Dispersion	12.3559
R^2	1.0000

Concentration (ppm)				
Distance (m)	Time (days)	Observation	Prediction	Residual
150	0	0.0000	0.0000	0.0000
150	2	0.0000	0.0000	0.0000
150	4	0.0000	0.0000	0.0000
150	6	0.0000	0.0000	0.0000
150	8	0.0000	0.0000	0.0000
150	17	0.2589	0.2584	0.0005
150	22	0.8777	0.8779	-0.0002

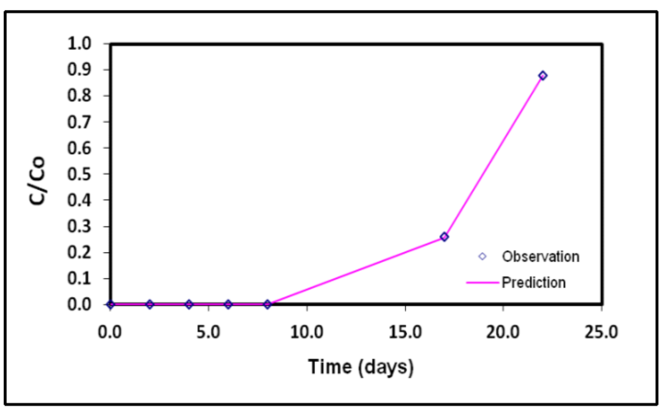

N5-11 Saturated

	Estimate
Velocity (cm/day)	10.2807
Dispersion	81.8235
R^2	0.9978

Concentration (ppm)				
Distance (m)	Time (days)	Observation	Prediction	Residual
150	0	0.0000	0.0000	0.0000
150	2	0.0000	0.0000	0.0000
150	4	0.0000	0.0000	0.0000
150	6	0.0000	0.0019	-0.0019
150	8	0.0000	0.0272	-0.0272
150	17	0.7018	0.6822	0.0196
150	22	0.8723	0.9020	-0.0297

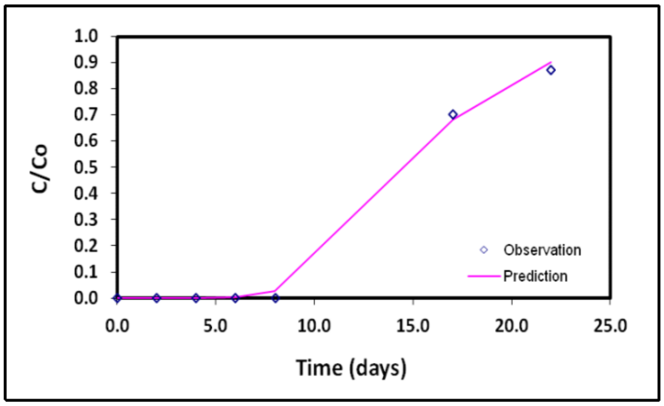

N5-13 Saturated

	Estimate
Velocity (cm/day)	11.2760
Dispersion	67.0625
R^2	0.9945

Concentration (ppm)				
Distance (m)	Time (days)	Observation	Prediction	Residual
150	0	0.0000	0.0000	0.0000
150	2	0.0000	0.0000	0.0000
150	4	0.0000	0.0000	0.0000
150	6	0.0000	0.0015	-0.0015
150	8	0.0071	0.0312	-0.0241
150	17	0.8375	0.8118	0.0257
150	22	0.8982	0.9666	-0.0684

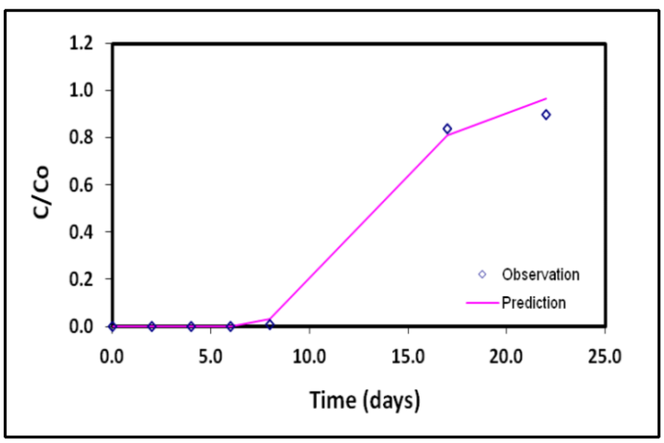

N1-3; 29 cm Fluctuation

	Estimate
Velocity (cm/day)	16.2831
Dispersion	0.5027
R^2	0.9984

Concentration (ppm)				
Distance (m)	Time (days)	Observation	Prediction	Residual
30	0	0.0000	0.0000	0.0000
30	2	0.9649	0.9649	0.0000
30	4	1.0000	1.0000	0.0000
30	5	0.9658	1.0000	-0.0342

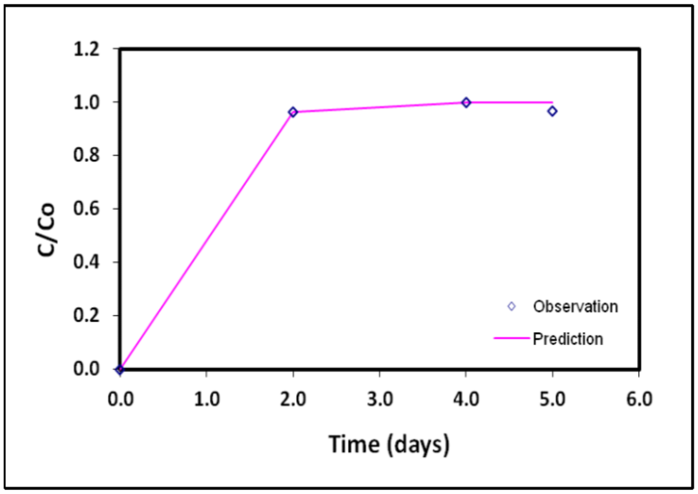

N1-5; 29 cm Fluctuation

	Estimate
Velocity (cm/day)	16.0125
Dispersion	0.4000
R^2	1.0000

Concentration (ppm)				
Distance (m)	Time (days)	Observation	Prediction	Residual
30	0	0.0000	0.0000	0.0000
30	2	0.9459	0.9454	0.0005
30	4	1.0000	1.0000	0.0000
30	5	1.0000	1.0000	0.0000

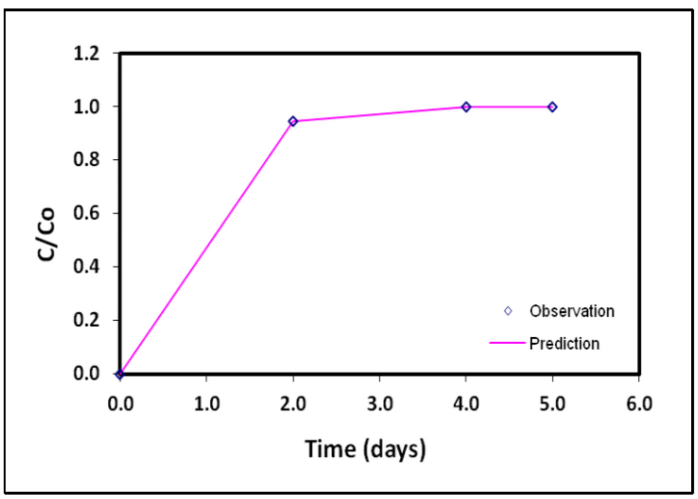

N1-7; 29 cm Fluctuation

	Estimate
Velocity (cm/day)	15.9192
Dispersion	0.4000
R^2	1.0000

Concentration (ppm)				
Distance (m)	Time (days)	Observation	Prediction	Residual
30	0	0.0000	0.0000	0.0000
30	2	0.9270	0.9270	0.0000
30	4	1.0000	1.0000	0.0000
30	5	1.0000	1.0000	0.0000

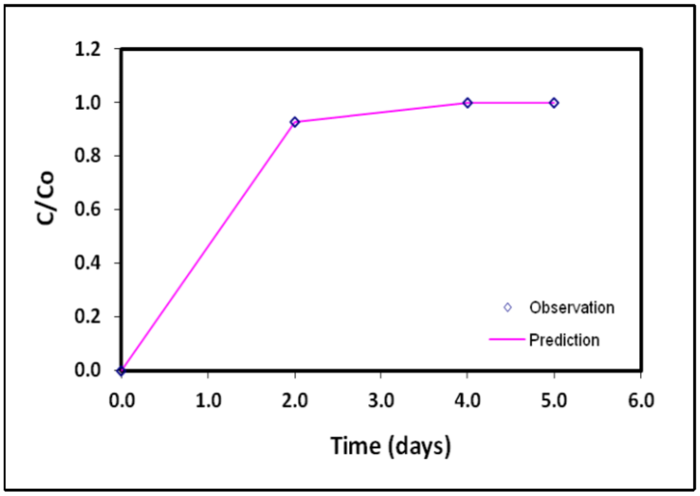

N1-9; 29 cm Fluctuation

	Estimate
Velocity (cm/day)	16.0085
Dispersion	0.6000
R^2	1.0000

Concentration (ppm)				
Distance (m)	Time (days)	Observation	Prediction	Residual
30	0	0.0000	0.0000	0.0000
30	2	0.9036	0.9037	-0.0001
30	4	1.0000	1.0000	0.0000
30	5	1.0000	1.0000	0.0000

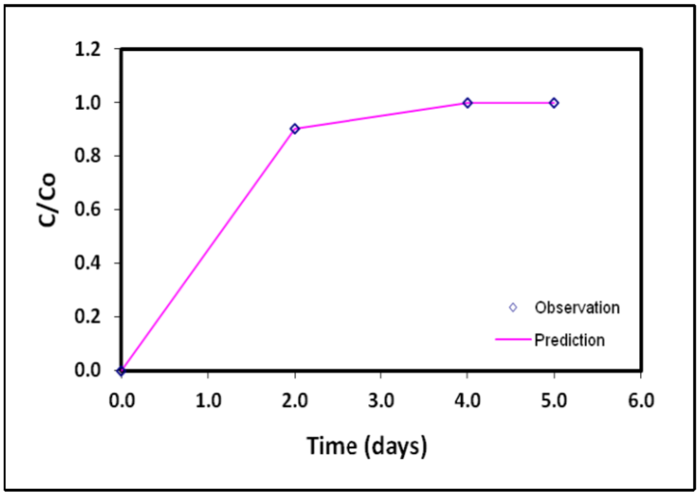

N1-11; 29 cm Fluctuation

	Estimate
Velocity (cm/day)	14.9798
Dispersion	1.0000
R^2	1.0000

Concentration (ppm)				
Distance (m)	**Time (days)**	**Observation**	**Prediction**	**Residual**
30	0	0.0000	0.0000	0.0000
30	2	0.4919	0.4919	0.0000
30	4	1.0000	1.0000	0.0000
30	5	1.0000	1.0000	0.0000

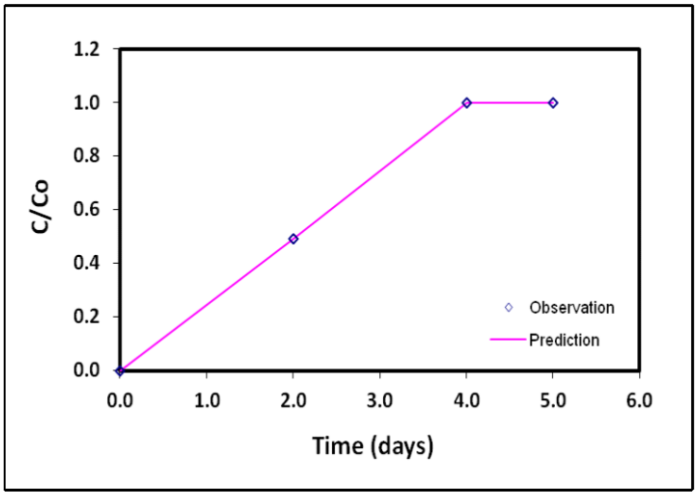

N1-13; 29 cm Fluctuation

	Estimate
Velocity (cm/day)	16.0236
Dispersion	1.9999
R^2	0.9894

Concentration (ppm)				
Distance (m)	**Time (days)**	**Observation**	**Prediction**	**Residual**
30	0	0.0000	0.0000	0.0000
30	2	0.7658	0.7658	0.0000
30	4	1.0000	1.0000	0.0000
30	5	0.9577	1.0000	-0.0423
30	6	0.9252	1.0000	-0.0748

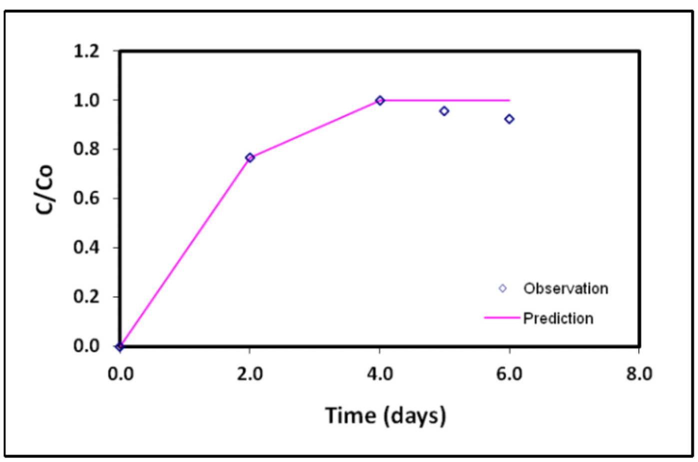

N2-3; 29 cm Fluctuation

	Estimate
Velocity (cm/day)	17.8016
Dispersion	27.7088
R^2	0.9994

Concentration (ppm)				
Distance (m)	Time (days)	Observation	Prediction	Residual
60	0	0.0000	0.0000	0.0000
60	2	0.0000	0.0094	-0.0094
60	4	0.7802	0.7762	0.0040
60	5	0.9468	0.9609	-0.0141
60	6	1.0135	0.9953	0.0182
60	7	0.9946	0.9995	-0.0049

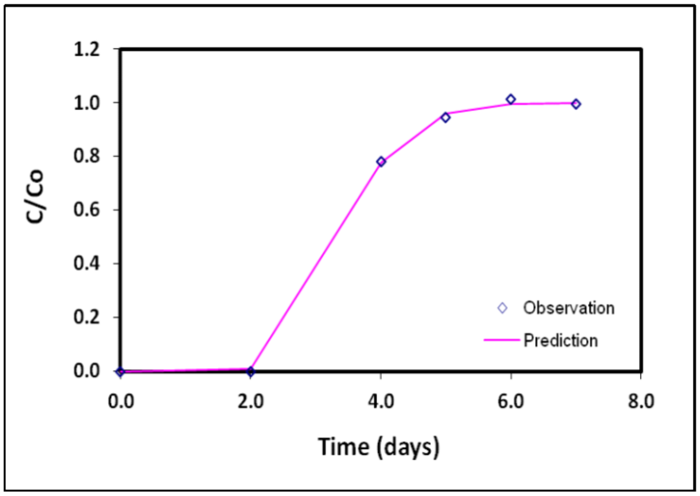

N2-5; 29 cm Fluctuation

	Estimate
Velocity (cm/day)	27.8038
Dispersion	0.9632
R^2	0.9999

Concentration (ppm)				
Distance (m)	Time (days)	Observation	Prediction	Residual
60	0	0.0000	0.0000	0.0000
60	2	0.0126	0.0126	0.0000
60	4	1.0099	1.0000	0.0099
60	5	1.0000	1.0000	0.0000
60	6	1.0000	1.0000	0.0000
60	7	1.0000	1.0000	0.0000

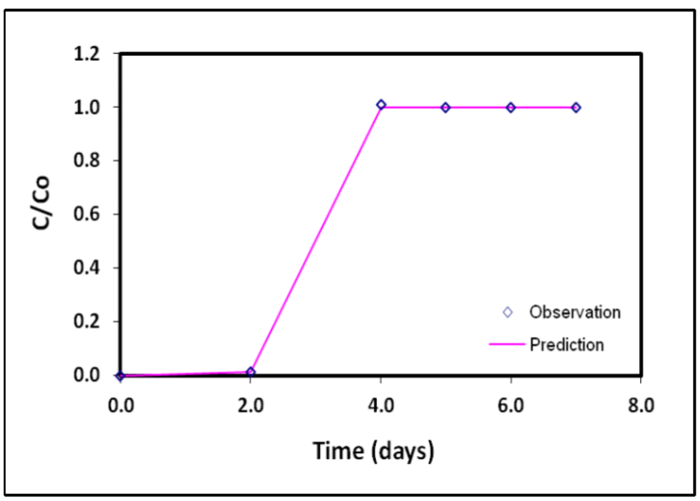

N2-7; 29 cm Fluctuation

	Estimate
Velocity (cm/day)	22.3990
Dispersion	0.9796
R^2	0.9995

Concentration (ppm)				
Distance (m)	Time (days)	Observation	Prediction	Residual
60	0	0.0000	0.0000	0.0000
60	2	0.0000	0.0000	0.0000
60	4	1.0252	1.0000	0.0252
60	5	1.0000	1.0000	0.0000
60	6	1.0000	1.0000	0.0000
60	7	1.0000	1.0000	0.0000

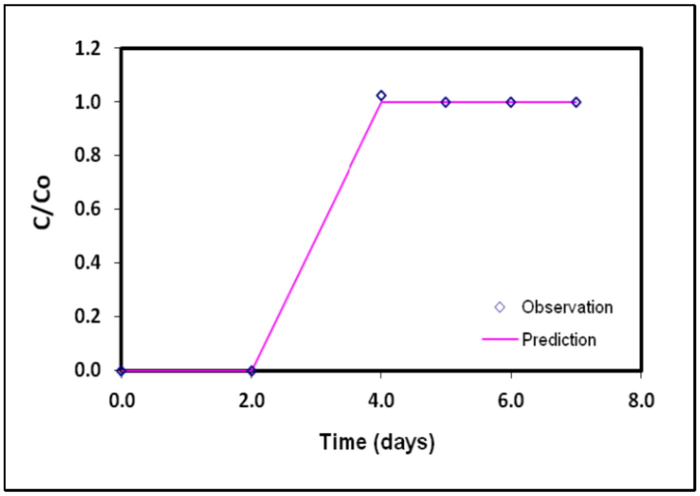

N2-9; 29 cm Fluctuation

	Estimate
Velocity (cm/day)	22.1000
Dispersion	0.9824
R^2	0.9995

Concentration (ppm)				
Distance (m)	Time (days)	Observation	Prediction	Residual
60	0	0.0000	0.0000	0.0000
60	2	0.0000	0.0000	0.0000
60	4	1.0225	1.0000	0.0225
60	5	1.0000	1.0000	0.0000
60	6	1.0000	1.0000	0.0000
60	7	1.0000	1.0000	0.0000

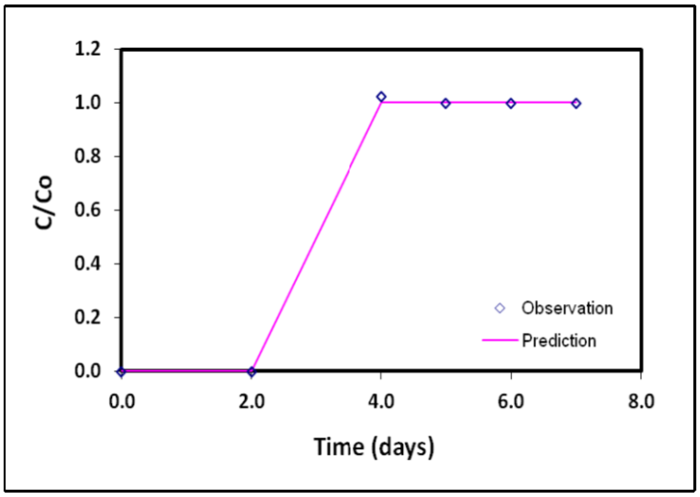

N2-11; 29 cm Fluctuation

	Estimate
Velocity (cm/day)	16.5750
Dispersion	1.0015
R^2	0.9995

Concentration (ppm)				
Distance (m)	**Time (days)**	**Observation**	**Prediction**	**Residual**
60	0	0.0000	0.0000	0.0000
60	2	0.0000	0.0000	0.0000
60	4	0.9865	0.9870	-0.0005
60	5	1.0000	1.0000	0.0000
60	6	1.0000	1.0000	0.0000
60	7	1.0000	1.0000	0.0000

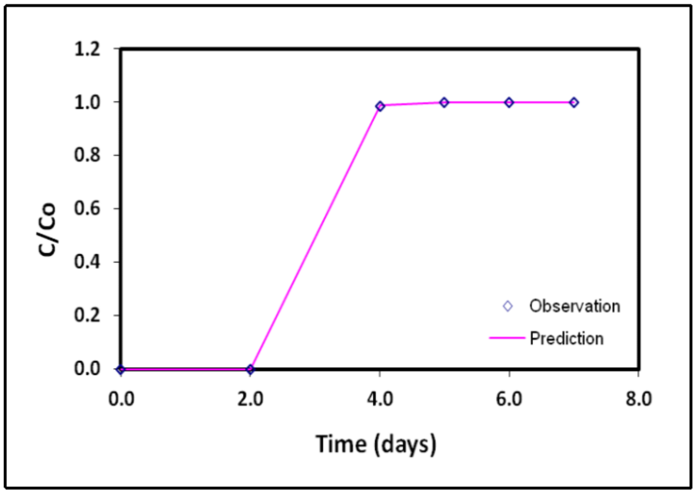

N2-13; 29 cm Fluctuation

	Estimate
Velocity (cm/day)	19.1596
Dispersion	63.4656
R^2	0.9829

Concentration (ppm)				
Distance (m)	**Time (days)**	**Observation**	**Prediction**	**Residual**
60	0	0.0000	0.0000	0.0000
60	2	0.0450	0.0804	-0.0354
60	4	0.8441	0.7732	0.0709
60	5	0.8207	0.9263	-0.1056
60	6	0.9667	0.9789	-0.0122
60	7	0.9748	0.9944	-0.0196

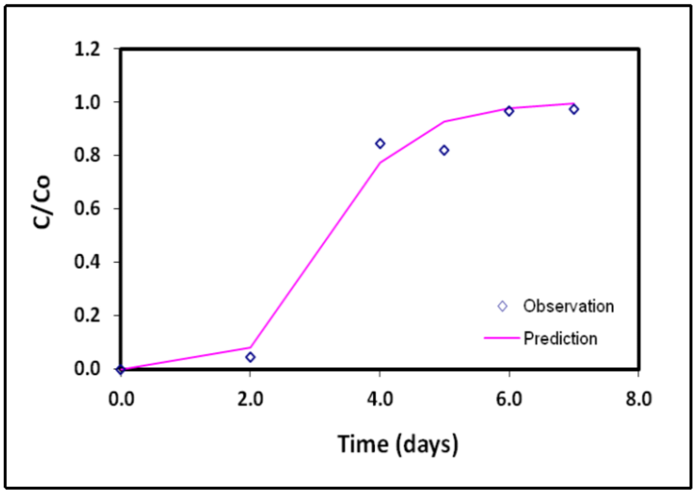

N3-3; 29 cm Fluctuation

	Estimate
Velocity (cm/day)	14.6066
Dispersion	7.4332
R^2	0.9972

Concentration (ppm)				
Distance (m)	**Time (days)**	**Observation**	**Prediction**	**Residual**
90	0	0.0000	0.0000	0.0000
90	2	0.0000	0.0000	0.0000
90	4	0.0000	0.0000	0.0000
90	5	0.0207	0.0242	-0.0035
90	6	0.4045	0.4009	0.0036
90	7	0.8739	0.8856	-0.0117
90	8	1.0505	0.9932	0.0573

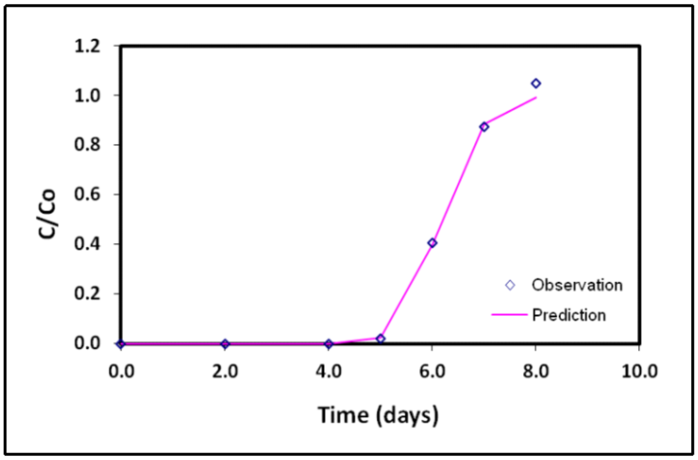

N3-5; 29 cm Fluctuation

	Estimate
Velocity (cm/day)	16.2132
Dispersion	3.3283
R^2	0.9997

Concentration (ppm)				
Distance (m)	**Time (days)**	**Observation**	**Prediction**	**Residual**
90	0	0.0000	0.0000	0.0000
90	2	0.0000	0.0000	0.0000
90	4	0.0117	0.0000	0.0117
90	5	0.0604	0.0605	-0.0001
90	6	0.8757	0.8755	0.0002
90	7	0.9838	0.9997	-0.0159
90	8	1.0000	1.0000	0.0000

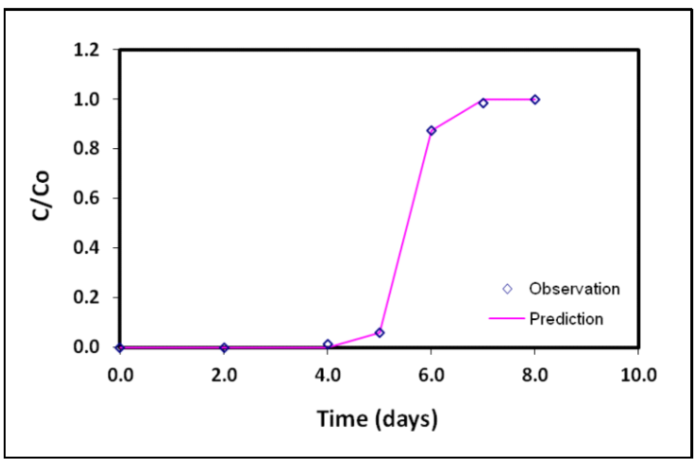

N3-7; 29 cm Fluctuation

	Estimate
Velocity (cm/day)	17.1807
Dispersion	3.5018
R^2	0.9997

Concentration (ppm)				
Distance (m)	Time (days)	Observation	Prediction	Residual
90	0	0.0000	0.0000	0.0000
90	2	0.0000	0.0000	0.0000
90	4	0.0171	0.0000	0.0171
90	5	0.2441	0.2441	0.0000
90	6	0.9784	0.9783	0.0001
90	7	0.9946	1.0000	-0.0054
90	8	1.0000	1.0000	0.0000

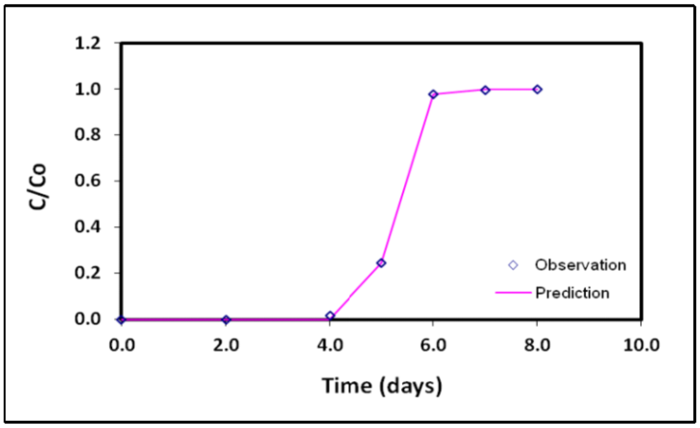

N3-9; 29 cm Fluctuation

	Estimate
Velocity (cm/day)	19.6438
Dispersion	12.1628
R^2	0.9980

Concentration (ppm)				
Distance (m)	Time (days)	Observation	Prediction	Residual
90	0	0.0000	0.0000	0.0000
90	2	0.0000	0.0000	0.0000
90	4	0.1198	0.1225	-0.0027
90	5	0.7766	0.7726	0.0040
90	6	0.9667	0.9897	-0.0230
90	7	0.9532	0.9999	-0.0467
90	8	1.0000	1.0000	0.0000

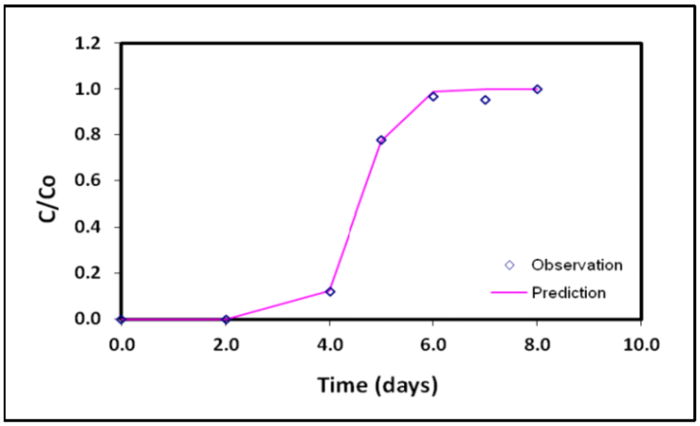

N3-11; 29 cm Fluctuation

	Estimate
Velocity (cm/day)	21.8643
Dispersion	87.5410
R^2	0.9929

Concentration (ppm)				
Distance (m)	Time (days)	Observation	Prediction	Residual
90	0	0.0000	0.0000	0.0000
90	2	0.0000	0.0058	-0.0058
90	4	0.4775	0.4586	0.0189
90	5	0.6919	0.7456	-0.0537
90	6	0.9667	0.9017	0.0650
90	7	0.9423	0.9665	-0.0242
90	8	1.0000	0.9895	0.0105

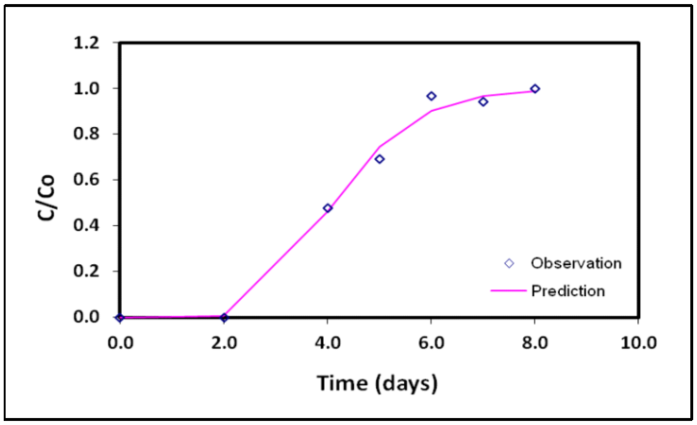

N3-13; 29 cm Fluctuation

	Estimate
Velocity (cm/day)	23.9729
Dispersion	4.0003
R^2	0.9587

Concentration (ppm)				
Distance (m)	Time (days)	Observation	Prediction	Residual
90	0	0.0000	0.0000	0.0000
90	2	0.0000	0.0000	0.0000
90	4	0.8514	0.8514	0.0000
90	5	0.8009	1.0000	-0.1991
90	6	0.9468	1.0000	-0.0532
90	7	0.9171	1.0000	-0.0829
90	8	1.0207	1.0000	0.0207

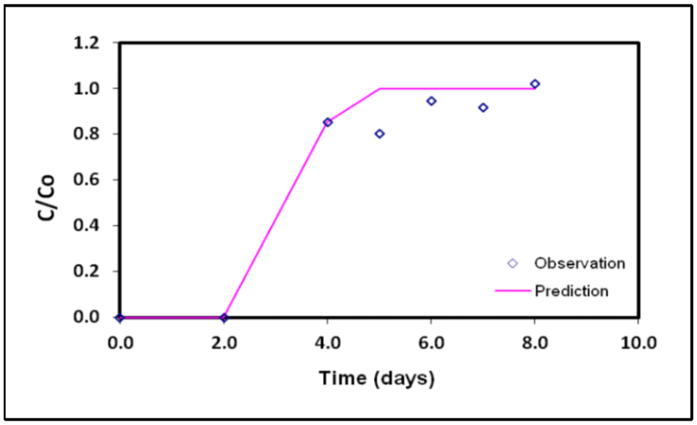

N4-3; 29 cm Fluctuation

	Estimate
Velocity (cm/day)	11.4984
Dispersion	119.3138
R^2	0.9133

Concentration (ppm)				
Distance (m)	Time (days)	Observation	Prediction	Residual
120	0	0.0000	0.0000	0.0000
120	4	0.0000	0.0063	-0.0063
120	5	0.0000	0.0294	-0.0294
120	6	0.0090	0.0789	-0.0699
120	7	0.0423	0.1544	-0.1121
120	8	0.4288	0.2482	0.1806
120	11	0.5315	0.5466	-0.0151
120	13	0.6703	0.7038	-0.0335

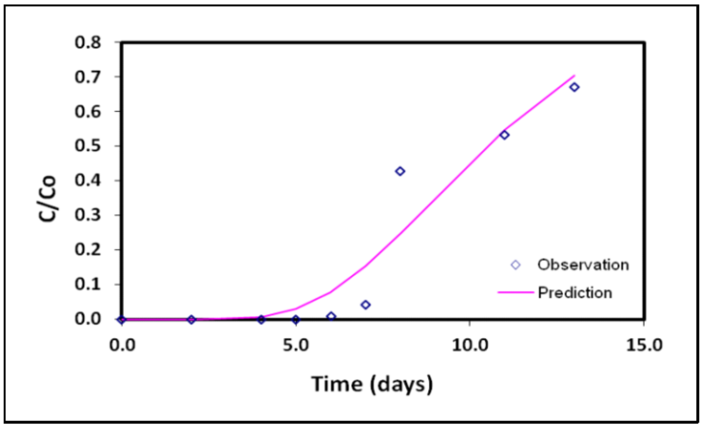

N4-5; 29 cm Fluctuation

	Estimate
Velocity (cm/day)	15.9628
Dispersion	4.7291
R^2	0.9984

Concentration (ppm)				
Distance (m)	Time (days)	Observation	Prediction	Residual
120	0	0.0000	0.0000	0.0000
120	2	0.0000	0.0000	0.0000
120	4	0.0000	0.0000	0.0000
120	5	0.0000	0.0000	0.0000
120	6	0.0297	0.0006	0.0291
120	7	0.1541	0.1547	-0.0006
120	8	0.8126	0.8123	0.0003

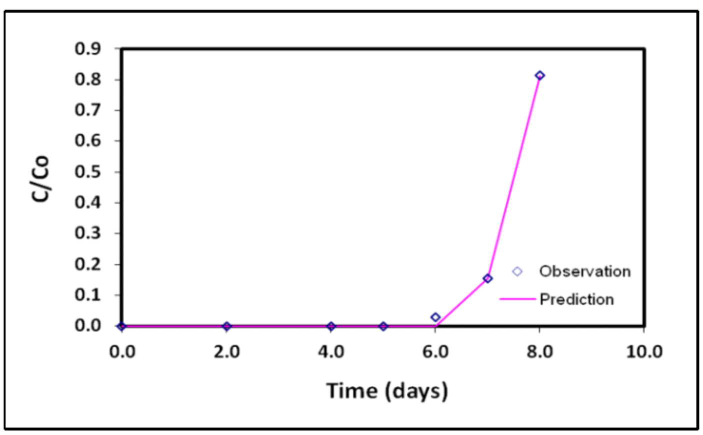

N4-7; 29 cm Fluctuation

	Estimate
Velocity (cm/day)	17.3300
Dispersion	9.7903
R^2	0.9966

Concentration (ppm)				
Distance (m)	Time (days)	Observation	Prediction	Residual
120	0	0.0000	0.0000	0.0000
120	2	0.0000	0.0000	0.0000
120	4	0.0000	0.0000	0.0000
120	5	0.0000	0.0004	-0.0004
120	6	0.1009	0.0692	0.0317
120	7	0.5216	0.5446	-0.0230
120	8	0.9694	0.9322	0.0372

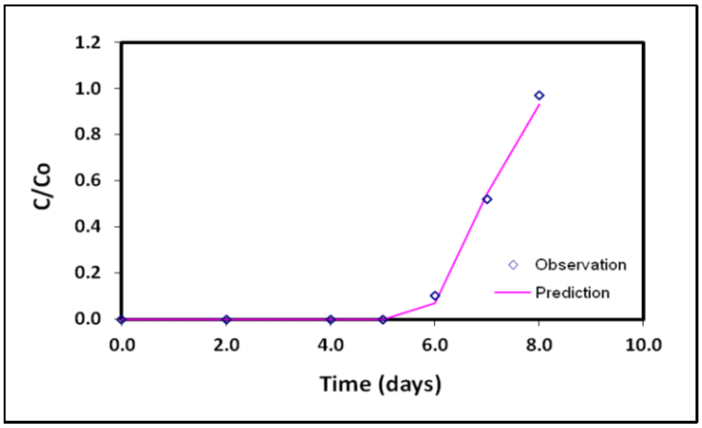

N4-9; 29 cm Fluctuation

	Estimate
Velocity (cm/day)	19.0350
Dispersion	12.9230
R^2	0.9994

Concentration (ppm)				
Distance (m)	Time (days)	Observation	Prediction	Residual
120	0	0.0000	0.0000	0.0000
120	2	0.0000	0.0000	0.0000
120	4	0.0000	0.0000	0.0000
120	5	0.0000	0.0143	-0.0143
120	6	0.3252	0.3204	0.0048
120	7	0.8306	0.8382	-0.0076
120	8	1.0090	0.9878	0.0212

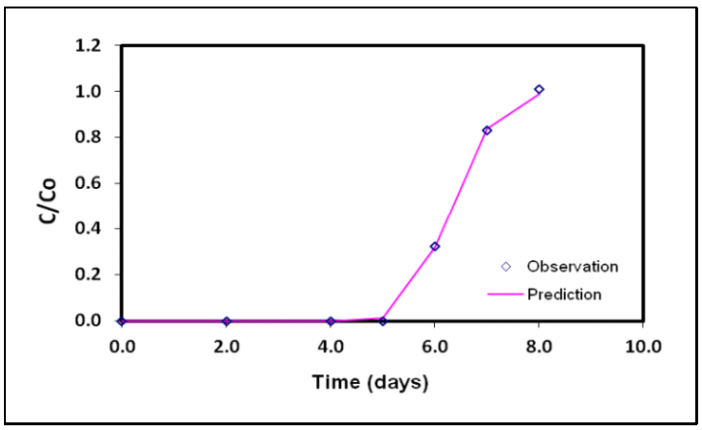

N4-11; 29 cm Fluctuation

	Estimate
Velocity (cm/day)	20.3321
Dispersion	26.7298
R^2	0.9449

Concentration (ppm)				
Distance (m)	Time (days)	Observation	Prediction	Residual
120	0	0.0000	0.0000	0.0000
120	2	0.0000	0.0000	0.0000
120	4	0.0000	0.0039	-0.0039
120	5	0.0000	0.1295	-0.1295
120	6	0.6928	0.5442	0.1486
120	7	0.7297	0.8769	-0.1472
120	8	0.9523	0.9809	-0.0286

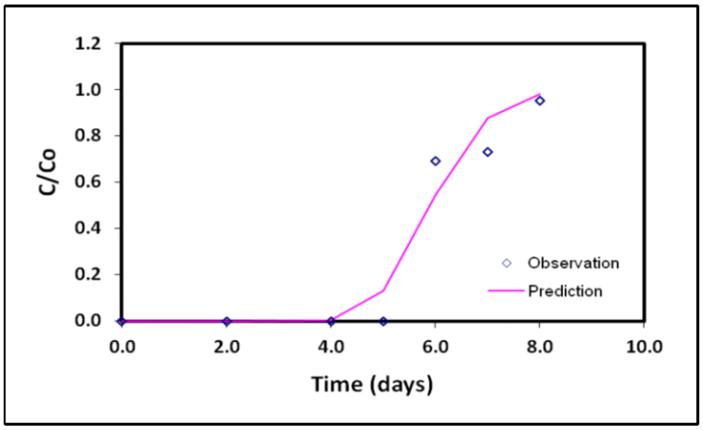

N4-13; 29 cm Fluctuation

	Estimate
Velocity (cm/day)	21.1103
Dispersion	4.6161
R^2	0.9632

Concentration (ppm)				
Distance (m)	Time (days)	Observation	Prediction	Residual
120	0	0.0000	0.0000	0.0000
120	2	0.0000	0.0000	0.0000
120	4	0.0063	0.0000	0.0063
120	5	0.0126	0.0166	-0.0040
120	6	0.8162	0.8148	0.0014
120	7	0.8036	0.9997	-0.1961
120	8	0.9198	1.0000	-0.0802

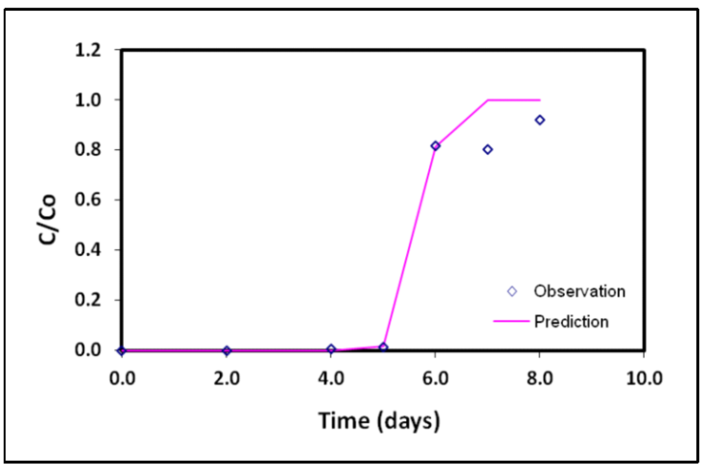

N5-3; 29 cm Fluctuation

	Estimate
Velocity (cm/day)	11.3603
Dispersion	87.5905
R^2	0.9810

Concentration (ppm)				
Distance (m)	Time (days)	Observation	Prediction	Residual
150	0	0.0000	0.0000	0.0000
150	5	0.0000	0.0006	-0.0006
150	6	0.0000	0.0048	-0.0048
150	7	0.0000	0.0194	-0.0194
150	8	0.0000	0.0523	-0.0523
150	11	0.2865	0.2772	0.0093
150	13	0.5604	0.4773	0.0831
150	14	0.5216	0.5714	-0.0498
150	15	0.6288	0.6556	-0.0268

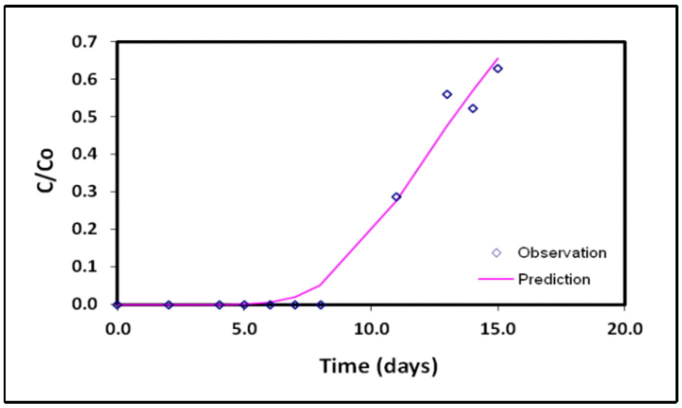

N5-5; 29 cm Fluctuation

	Estimate
Velocity (cm/day)	13.9879
Dispersion	3.0000
R^2	1.0000

Concentration (ppm)				
Distance (m)	Time (days)	Observation	Prediction	Residual
150	0	0.0000	0.0000	0.0000
150	2	0.0000	0.0000	0.0000
150	4	0.0000	0.0000	0.0000
150	5	0.0000	0.0000	0.0000
150	6	0.0000	0.0000	0.0000
150	7	0.0000	0.0000	0.0000
150	8	0.0000	0.0000	0.0000
150	11	0.6829	0.6830	-0.0001

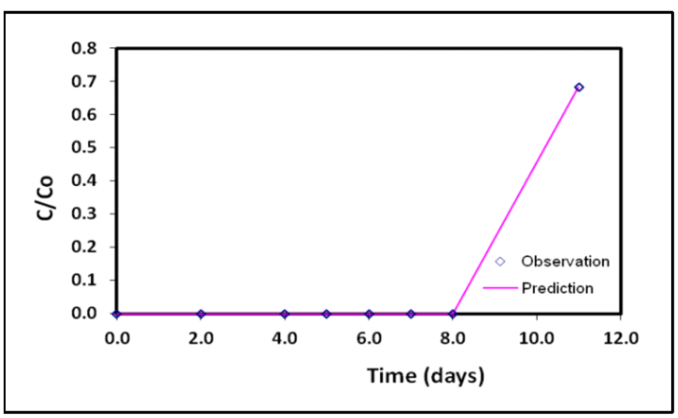

N5-7; 29 cm Fluctuation

	Estimate
Velocity (cm/day)	15.1087
Dispersion	16.0544
R^2	1.0000

Concentration (ppm)				
Distance (m)	Time (days)	Observation	Prediction	Residual
150	0	0.0000	0.0000	0.0000
150	2	0.0000	0.0000	0.0000
150	4	0.0000	0.0000	0.0000
150	5	0.0000	0.0000	0.0000
150	6	0.0000	0.0000	0.0000
150	7	0.0000	0.0015	-0.0015
150	8	0.0342	0.0341	0.0001
150	11	0.8063	0.8063	0.0000

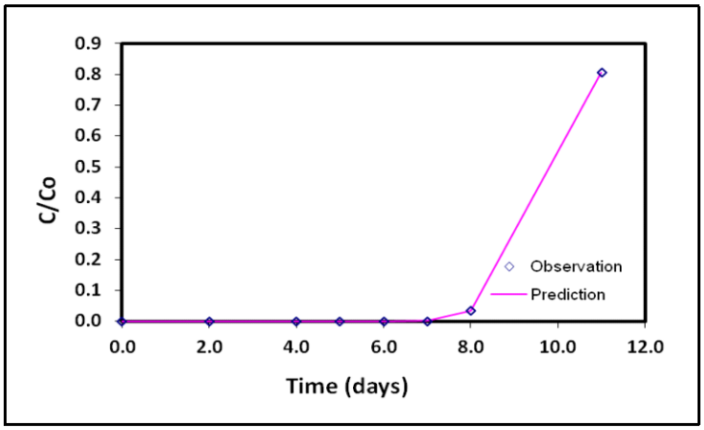

N5-9; 29 cm Fluctuation

	Estimate
Velocity (cm/day)	15.7122
Dispersion	29.3948
R^2	1.0000

Concentration (ppm)				
Distance (m)	Time (days)	Observation	Prediction	Residual
150	0	0.0000	0.0000	0.0000
150	2	0.0000	0.0000	0.0000
150	4	0.0000	0.0000	0.0000
150	5	0.0000	0.0000	0.0000
150	6	0.0000	0.0014	-0.0014
150	7	0.0090	0.0236	-0.0146
150	8	0.1351	0.1296	0.0055
150	11	0.8153	0.8166	-0.0013

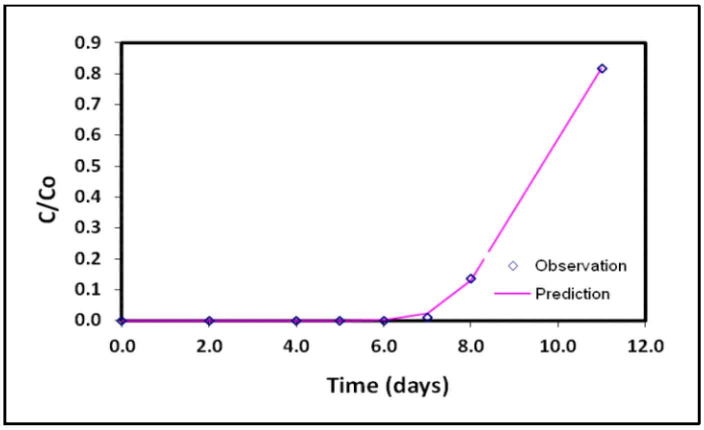

N5-11; 29 cm Fluctuation

	Estimate
Velocity (cm/day)	17.2476
Dispersion	66.8719
R^2	0.9623

Concentration (ppm)				
Distance (m)	Time (days)	Observation	Prediction	Residual
150	0	0.0000	0.0000	0.0000
150	4	0.0000	0.0002	-0.0002
150	5	0.0000	0.0062	-0.0062
150	6	0.0000	0.0480	-0.0480
150	7	0.0396	0.1658	-0.1262
150	8	0.4928	0.3539	0.1389
150	11	0.8090	0.8522	-0.0432
150	13	0.9009	0.9640	-0.0631

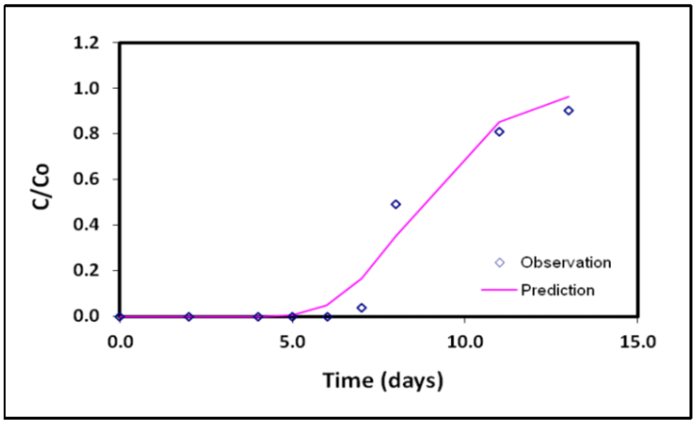

N5-13; 29 cm Fluctuation

	Estimate
Velocity (cm/day)	20.5582
Dispersion	19.2872
R^2	0.9508

Concentration (ppm)				
Distance (m)	Time (days)	Observation	Prediction	Residual
150	0	0.0000	0.0000	0.0000
150	2	0.0000	0.0000	0.0000
150	4	0.0000	0.0000	0.0000
150	5	0.0000	0.0003	-0.0003
150	6	0.0360	0.0394	-0.0034
150	7	0.3559	0.3548	0.0011
150	8	0.7955	0.7955	0.0000
150	11	0.7613	0.9999	-0.2386
150	13	0.9234	1.0000	-0.0766

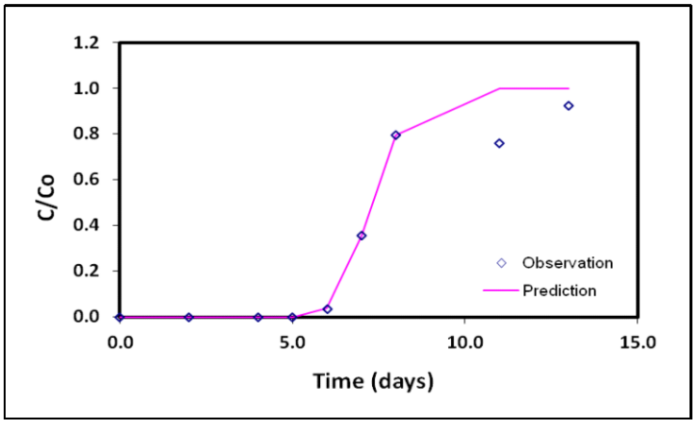

N1-5; 45 cm Fluctuation

	Estimate
Velocity (cm/day)	16.0000
Dispersion	13.0000
R^2	0.9828

Concentration (ppm)				
Distance (m)	Time (days)	Observation	Prediction	Residual
30	0	0.0000	0.0000	0.0000
30	1	0.0014	0.0027	-0.0013
30	2	0.5829	0.6095	-0.0266
30	3	1.1090	0.9804	0.1286
30	4	0.9225	0.9996	-0.0771
30	5	0.9838	1.0000	-0.0162
30	7	1.0036	1.0000	0.0036

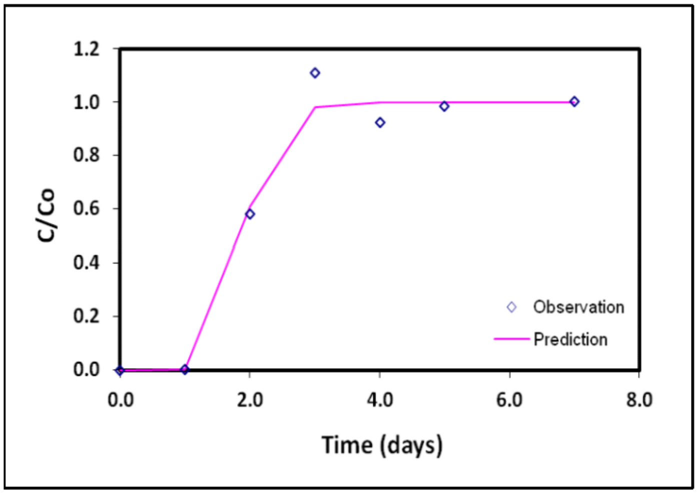

N1-7; 45 cm Fluctuation

	Estimate
Velocity (cm/day)	15.5593
Dispersion	1.3139
R^2	0.9780

Concentration (ppm)				
Distance (m)	Time (days)	Observation	Prediction	Residual
30	0	0.0000	0.0000	0.0000
30	1	0.0016	0.0000	0.0016
30	2	0.6874	0.6874	0.0000
30	3	1.1198	1.0000	0.1198
30	4	0.9495	1.0000	-0.0505
30	5	0.8901	1.0000	-0.1099
30	7	0.9856	1.0000	-0.0144

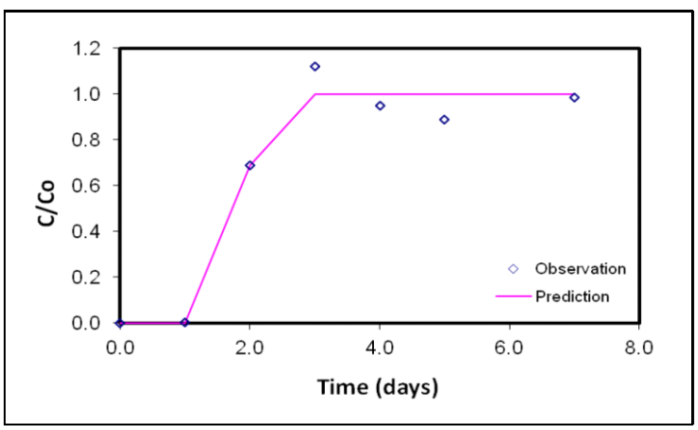

N1-9; 45 cm Fluctuation

	Estimate
Velocity (cm/day)	15.4683
Dispersion	1.7648
R^2	0.9768

Concentration (ppm)				
Distance (m)	Time (days)	Observation	Prediction	Residual
30	0	0.0000	0.0000	0.0000
30	1	0.0026	0.0000	0.0026
30	2	0.6378	0.6380	-0.0002
30	3	1.1027	1.0000	0.1027
30	4	0.9586	1.0000	-0.0414
30	5	0.8694	1.0000	-0.1306
30	7	0.9739	1.0000	-0.0261

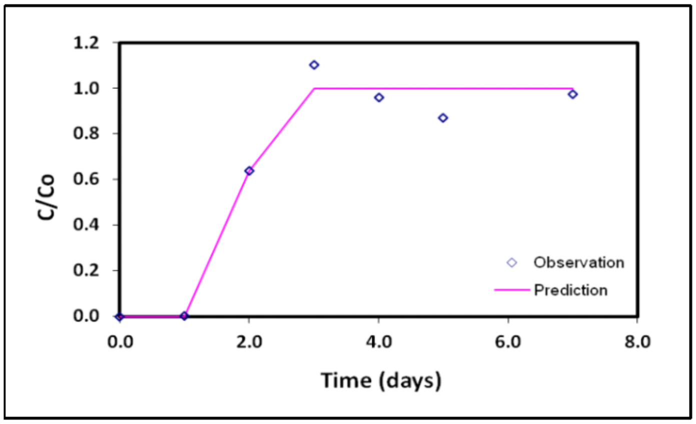

N1-11; 45 cm Fluctuation

	Estimate
Velocity (cm/day)	16.0000
Dispersion	12.0000
R^2	0.9578

Concentration (ppm)				
Distance (m)	Time (days)	Observation	Prediction	Residual
30	0	0.0000	0.0000	0.0000
30	1	0.0023	0.0019	0.0004
30	2	0.5964	0.6139	-0.0175
30	3	1.0820	0.9840	0.0980
30	4	0.9144	0.9998	-0.0854
30	5	0.8135	1.0000	-0.1865
30	7	0.9856	1.0000	-0.0144

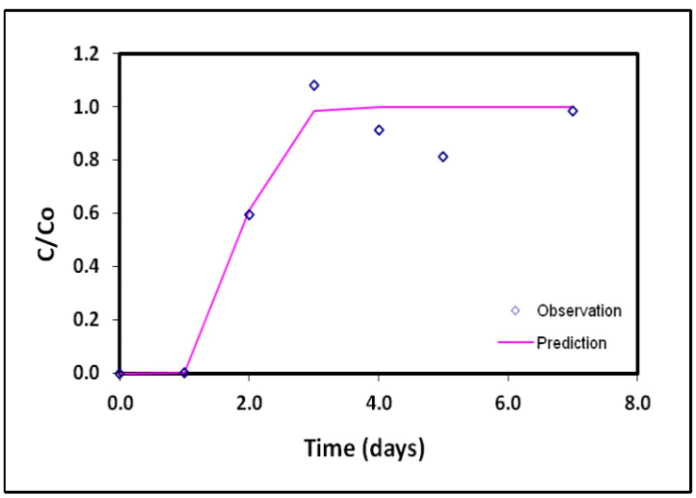

N1-13; 45 cm Fluctuation

	Estimate
Velocity (cm/day)	16.9863
Dispersion	4.0009
R^2	0.9346

Concentration (ppm)				
Distance (m)	**Time (days)**	**Observation**	**Prediction**	**Residual**
30	0	0.0000	0.0000	0.0000
30	1	0.0027	0.0000	0.0027
30	2	0.8405	0.8405	0.0000
30	3	0.9757	1.0000	-0.0243
30	4	0.8000	1.0000	-0.2000
30	5	0.8613	1.0000	-0.1387
30	7	0.9126	1.0000	-0.0874
30	8	0.9009	1.0000	-0.0991

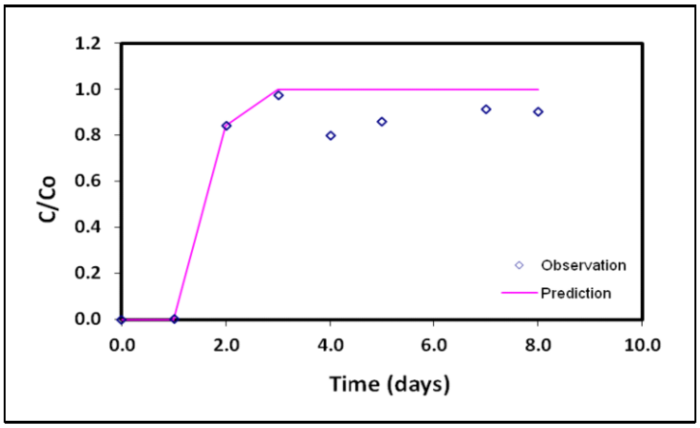

N2-5; 45 cm Fluctuation

	Estimate
Velocity (cm/day)	13.8012
Dispersion	4.2077
R^2	0.9993

Concentration (ppm)				
Distance (m)	**Time (days)**	**Observation**	**Prediction**	**Residual**
60	0	0.0000	0.0000	0.0000
60	3	0.0036	0.0001	0.0035
60	4	0.2036	0.2036	0.0000
60	5	0.9180	0.9180	0.0000
60	7	0.9829	1.0000	-0.0171
60	8	1.0009	1.0000	0.0009
60	10	1.0324	1.0000	0.0324

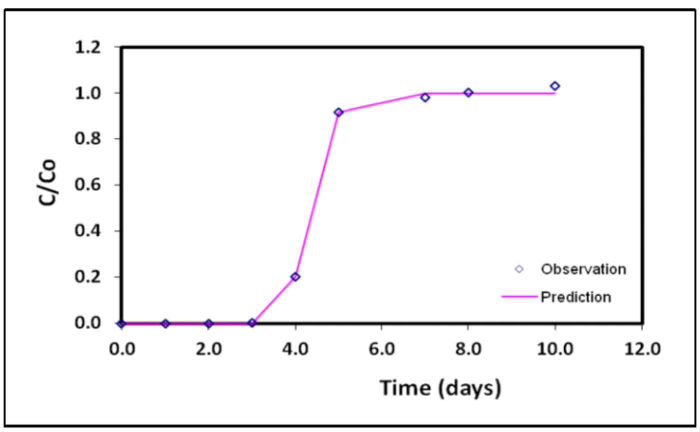

N2-7; 45 cm Fluctuation

	Estimate
Velocity (cm/day)	14.5845
Dispersion	5.1001
R^2	1.0000

Concentration (ppm)				
Distance (m)	**Time (days)**	**Observation**	**Prediction**	**Residual**
60	0	0.0000	0.0000	0.0000
60	3	0.0189	0.0016	0.0173
60	4	0.3964	0.3969	-0.0005
60	5	0.9667	0.9652	0.0015
60	7	1.0072	1.0000	0.0072
60	8	1.0090	1.0000	0.0090
60	10	1.0000	1.0000	0.0000

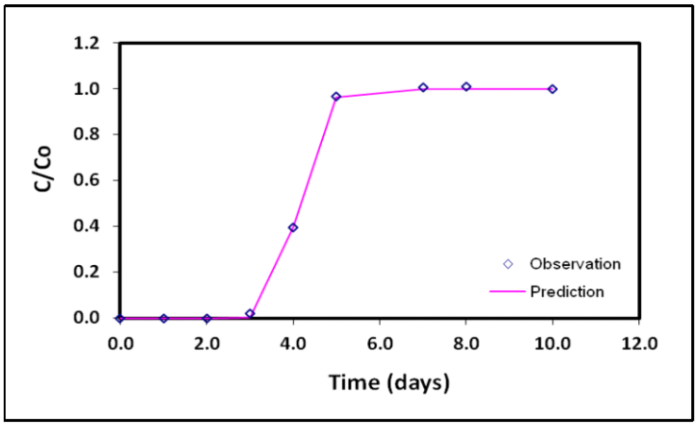

N2-9; 45 cm Fluctuation

	Estimate
Velocity (cm/day)	16.6058
Dispersion	15.7009
R^2	1.0000

Concentration (ppm)				
Distance (m)	**Time (days)**	**Observation**	**Prediction**	**Residual**
60	0	0.0000	0.0000	0.0000
60	2	0.0000	0.0003	-0.0003
60	3	0.1459	0.1449	0.0010
60	4	0.7162	0.7178	-0.0016
60	5	0.9721	0.9679	0.0042
60	7	0.9775	0.9999	-0.0224
60	8	0.9856	1.0000	-0.0144
60	10	0.9901	1.0000	-0.0099

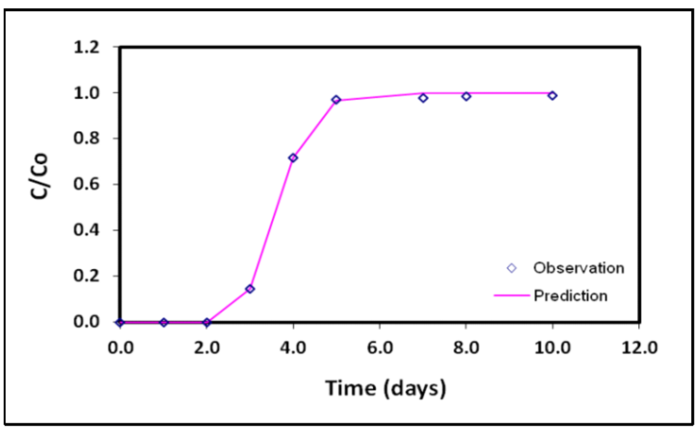

N2-11; 45 cm Fluctuation

	Estimate
Velocity (cm/day)	19.3948
Dispersion	65.7705
R^2	0.9799

Concentration (ppm)				
Distance (m)	Time (days)	Observation	Prediction	Residual
60	0	0.0000	0.0000	0.0000
60	2	0.0000	0.0886	-0.0886
60	3	0.5568	0.4594	0.0974
60	4	0.6793	0.7818	-0.1025
60	5	0.9811	0.9293	0.0518
60	7	0.9477	0.9946	-0.0469
60	8	0.9793	0.9986	-0.0193
60	10	1.0000	0.9999	0.0001

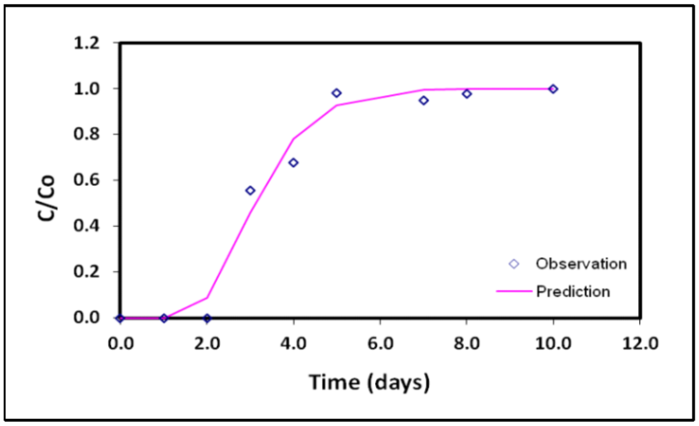

N2-13; 45 cm Fluctuation

	Estimate
Velocity (cm/day)	22.8616
Dispersion	7.4631
R^2	0.9650

Concentration (ppm)				
Distance (m)	Time (days)	Observation	Prediction	Residual
60	0	0.0000	0.0000	0.0000
60	2	0.0038	0.0044	-0.0006
60	3	0.9009	0.9008	0.0001
60	4	0.8883	1.0000	-0.1117
60	5	0.8982	1.0000	-0.1018
60	7	0.8216	1.0000	-0.1784
60	8	0.9405	1.0000	-0.0595
60	10	1.0261	1.0000	0.0261

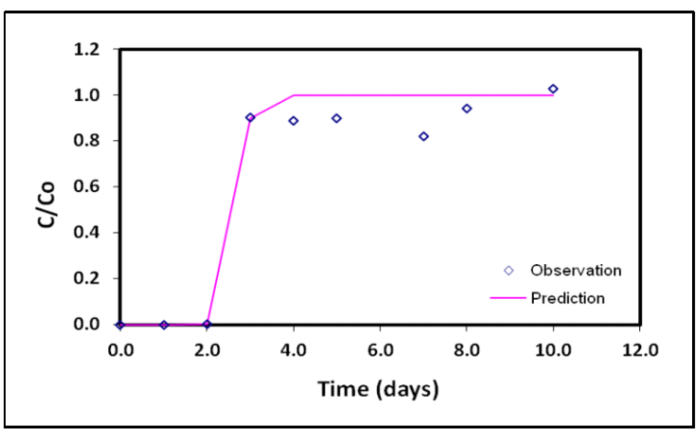

N3-5; 45 cm Fluctuation

	Estimate
Velocity (cm/day)	11.7479
Dispersion	2.7930
R^2	0.9947

Concentration (ppm)				
Distance (m)	Time (days)	Observation	Prediction	Residual
90	0	0.0000	0.0000	0.0000
90	5	0.0000	0.0000	0.0000
90	7	0.1072	0.1069	0.0003
90	8	0.7243	0.7246	-0.0003
90	10	1.0829	0.9999	0.0830

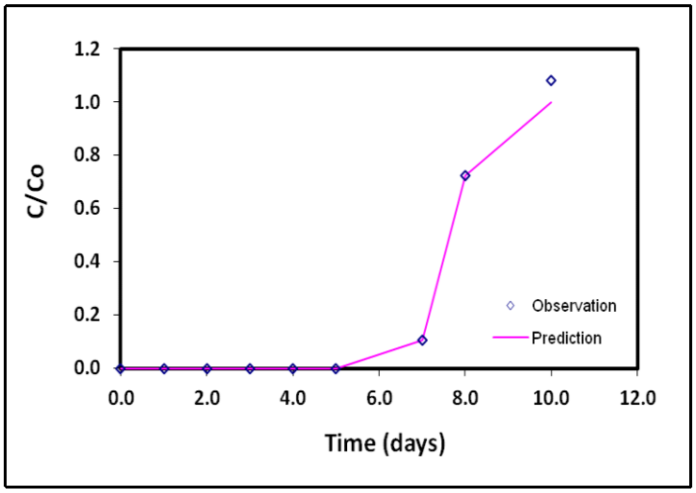

N3-7; 45 cm Fluctuation

	Estimate
Velocity (cm/day)	12.5410
Dispersion	4.4312
R^2	0.9964

Concentration (ppm)				
Distance (m)	Time (days)	Observation	Prediction	Residual
90	0	0.0000	0.0000	0.0000
90	5	0.0086	0.0000	0.0086
90	7	0.3892	0.3891	0.0001
90	8	0.8901	0.8904	-0.0003
90	10	1.0721	0.9999	0.0722

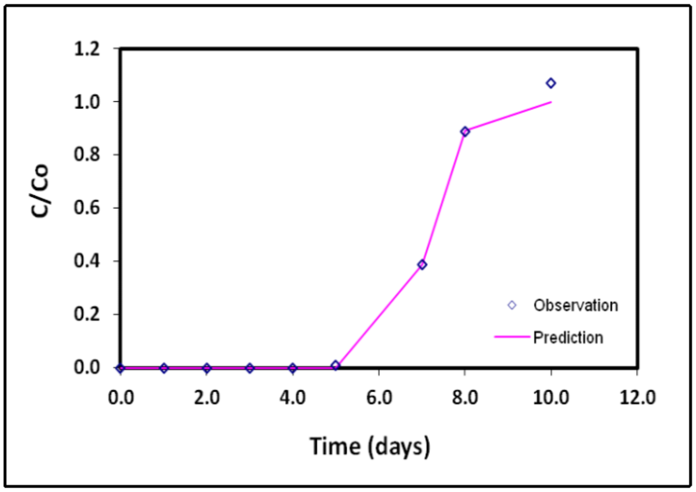

N3-9; 45 cm Fluctuation

	Estimate
Velocity (cm/day)	14.4814
Dispersion	11.5949
R^2	0.9976

Concentration (ppm)				
Distance (m)	Time (days)	Observation	Prediction	Residual
90	0	0.0000	0.0000	0.0000
90	4	0.0000	0.0004	-0.0004
90	5	0.0423	0.0503	-0.0080
90	7	0.8261	0.8148	0.0113
90	8	0.9378	0.9717	-0.0339
90	10	1.0541	0.9998	0.0543

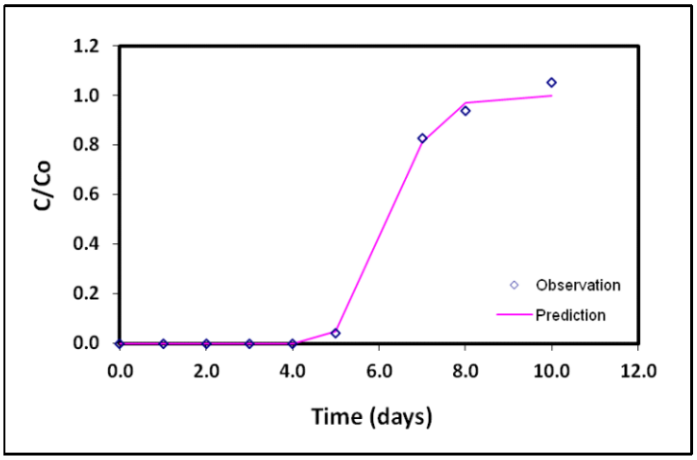

N3-11; 45 cm Fluctuation

	Estimate
Velocity (cm/day)	16.7205
Dispersion	32.5223
R^2	0.9932

Concentration (ppm)				
Distance (m)	Time (days)	Observation	Prediction	Residual
90	0	0.0000	0.0000	0.0000
90	3	0.0000	0.0020	-0.0020
90	4	0.0068	0.0735	-0.0667
90	5	0.3973	0.3592	0.0381
90	7	0.8937	0.8995	-0.0058
90	8	0.9099	0.9736	-0.0637
90	10	1.0387	0.9989	0.0398

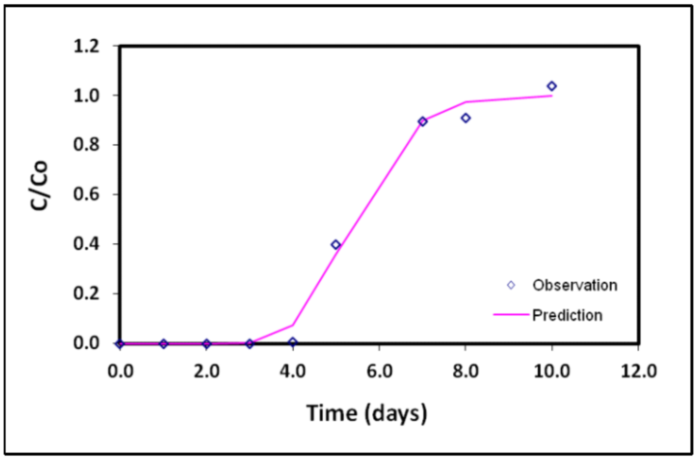

N3-13; 45 cm Fluctuation

	Estimate
Velocity (cm/day)	20.7421
Dispersion	30.0182
R^2	0.9637

Concentration (ppm)				
Distance (m)	**Time (days)**	**Observation**	**Prediction**	**Residual**
90	0	0.0000	0.0000	0.0000
90	3	0.0029	0.0185	-0.0156
90	4	0.3216	0.3232	-0.0016
90	5	0.7964	0.7870	0.0094
90	7	0.8775	0.9967	-0.1192
90	8	0.7973	0.9998	-0.2025
90	10	0.9901	1.0000	-0.0099

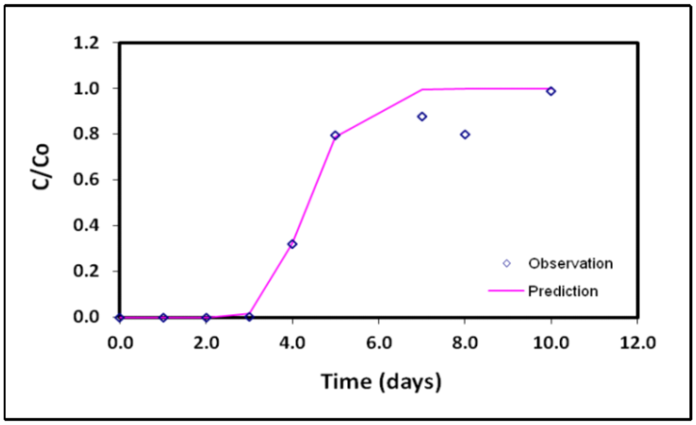

N4-5; 45 cm Fluctuation

	Estimate
Velocity (cm/day)	10.3336
Dispersion	31.7099
R^2	0.9565

Concentration (ppm)				
Distance (m)	**Time (days)**	**Observation**	**Prediction**	**Residual**
120	0	0.0000	0.0000	0.0000
120	5	0.0000	0.0001	-0.0001
120	7	0.0000	0.0110	-0.0110
120	8	0.0000	0.0465	-0.0465
120	9	0.0775	0.1258	-0.0483
120	10	0.2054	0.2506	-0.0452
120	11	0.5324	0.4031	0.1293
120	14	0.7252	0.7983	-0.0731

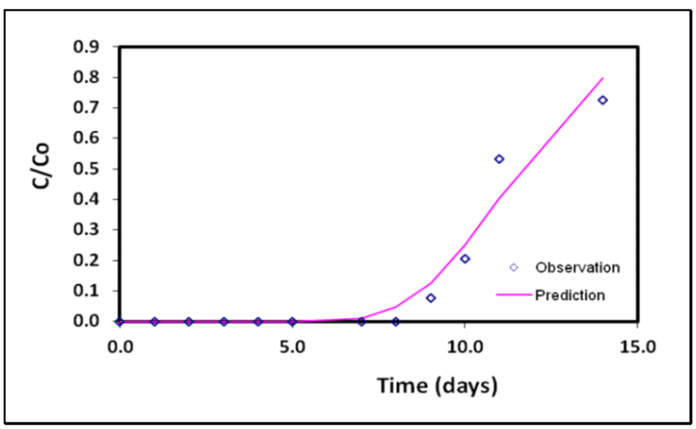

N4-7; 45 cm Fluctuation

	Estimate
Velocity (cm/day)	12.3272
Dispersion	12.9466
R^2	0.9887

Concentration (ppm)				
Distance (m)	Time (days)	Observation	Prediction	Residual
120	0	0.0000	0.0000	0.0000
120	5	0.0000	0.0000	0.0000
120	7	0.0000	0.0059	-0.0059
120	8	0.0022	0.0678	-0.0656
120	9	0.3369	0.2755	0.0614
120	10	0.5450	0.5807	-0.0357
120	11	0.8315	0.8232	0.0083

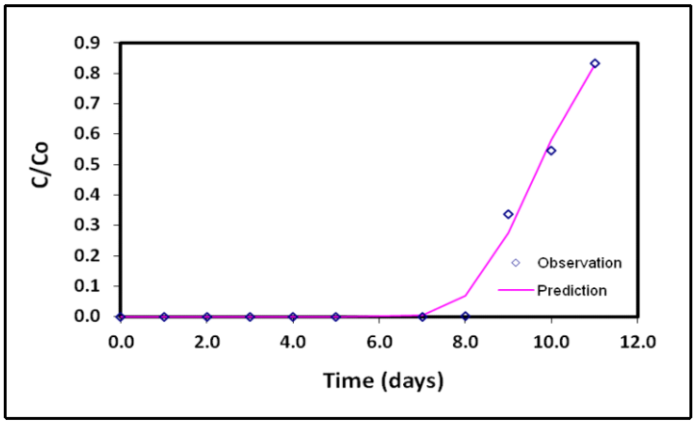

N4-9; 45 cm Fluctuation

	Estimate
Velocity (cm/day)	14.0626
Dispersion	4.8671
R^2	0.9957

Concentration (ppm)				
Distance (m)	Time (days)	Observation	Prediction	Residual
120	0	0.0000	0.0000	0.0000
120	5	0.0000	0.0000	0.0000
120	7	0.0068	0.0044	0.0024
120	8	0.1937	0.1973	-0.0036
120	9	0.7649	0.7587	0.0062
120	10	0.9631	0.9818	-0.0187
120	11	0.9180	0.9996	-0.0816

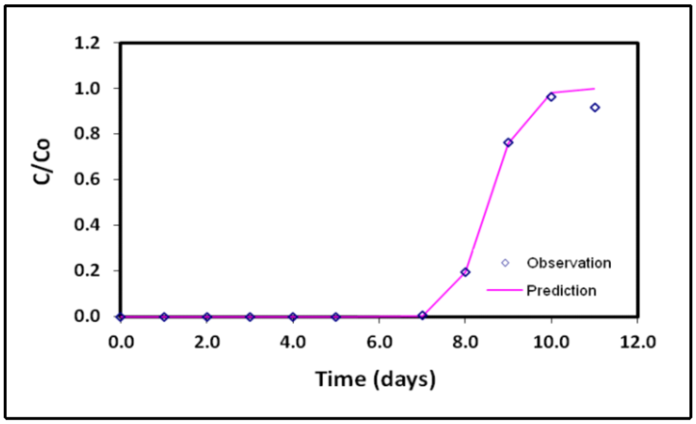

N4-11; 45 cm Fluctuation

	Estimate
Velocity (cm/day)	15.2611
Dispersion	6.3871
R^2	0.9928

Concentration (ppm)				
Distance (m)	Time (days)	Observation	Prediction	Residual
120	0	0.0000	0.0000	0.0000
120	5	0.0000	0.0000	0.0000
120	7	0.0459	0.0814	-0.0355
120	8	0.6117	0.5819	0.0298
120	9	0.8874	0.9475	-0.0601
120	10	1.0324	0.9981	0.0343
120	11	0.9153	1.0000	-0.0847

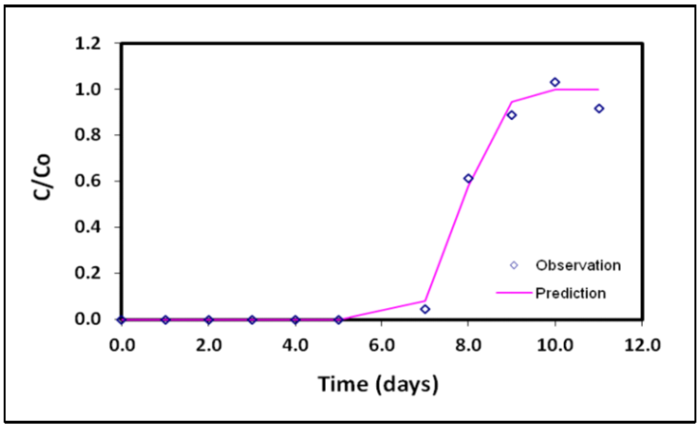

N4-13; 45 cm Fluctuation

	Estimate
Velocity (cm/day)	17.1889
Dispersion	37.0364
R^2	0.9646

Concentration (ppm)				
Distance (m)	Time (days)	Observation	Prediction	Residual
120	0	0.0000	0.0000	0.0000
120	4	0.0000	0.0013	-0.0013
120	5	0.0000	0.0370	-0.0370
120	7	0.4766	0.5050	-0.0284
120	8	0.8766	0.7655	0.1111
120	9	0.8081	0.9121	-0.1040
120	10	0.9748	0.9727	0.0021
120	11	0.8414	0.9926	-0.1512
120	14	0.8405	0.9999	-0.1594

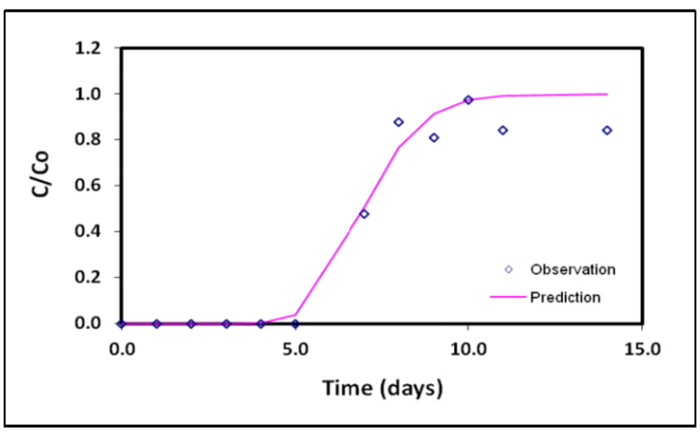

N5-5; 45 cm Fluctuation

	Estimate
Velocity (cm/day)	11.0000
Dispersion	2.0000
R^2	0.9965

Concentration (ppm)				
Distance (m)	Time (days)	Observation	Prediction	Residual
150	0	0.0000	0.0000	0.0000
150	4	0.0000	0.0013	-0.0013
150	11	0.0054	0.0000	0.0054
150	14	0.6595	0.7036	-0.0441
150	15	1.0225	0.9737	0.0488

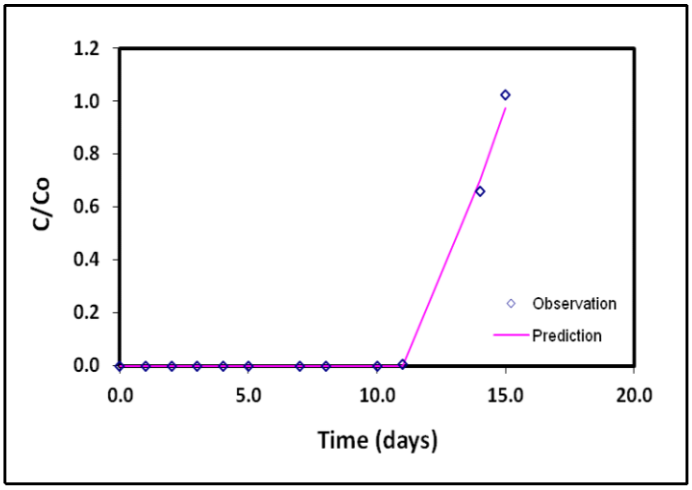

N5-7; 45 cm Fluctuation

	Estimate
Velocity (cm/day)	11.2624
Dispersion	4.6423
R^2	1.0000

Concentration (ppm)				
Distance (m)	Time (days)	Observation	Prediction	Residual
150	0	0.0000	0.0000	0.0000
150	8	0.0000	0.0000	0.0000
150	10	0.0000	0.0001	-0.0001
150	11	0.0108	0.0048	0.0060
150	14	0.7486	0.7498	-0.0012
150	15	0.9486	0.9459	0.0027

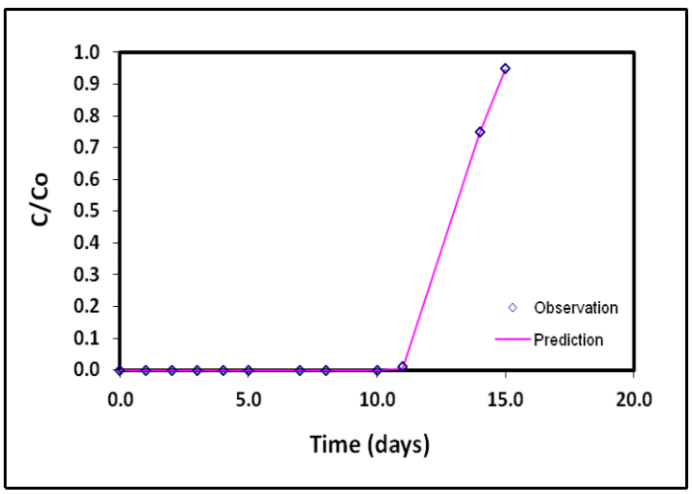

N5-9; 45 cm Fluctuation

	Estimate
Velocity (cm/day)	12.1399
Dispersion	13.4630
R^2	0.9988

Concentration (ppm)				
Distance (m)	Time (days)	Observation	Prediction	Residual
150	0	0.0000	0.0000	0.0000
150	8	0.0036	0.0001	0.0035
150	10	0.0065	0.0401	-0.0336
150	11	0.1856	0.1684	0.0172
150	14	0.8387	0.8488	-0.0101
150	15	0.9541	0.9455	0.0086

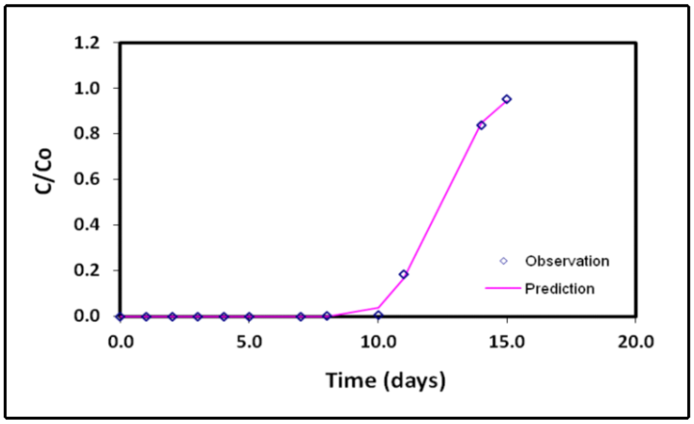

N5-11; 45 cm Fluctuation

	Estimate
Velocity (cm/day)	13.9247
Dispersion	7.3641
R^2	0.9883

Concentration (ppm)				
Distance (m)	Time (days)	Observation	Prediction	Residual
150	0	0.0000	0.0000	0.0000
150	7	0.0047	0.0000	0.0047
150	8	0.0351	0.0002	0.0349
150	10	0.1838	0.1873	-0.0035
150	11	0.6018	0.5985	0.0033
150	14	0.8856	0.9991	-0.1135
150	15	0.9432	1.0000	-0.0568

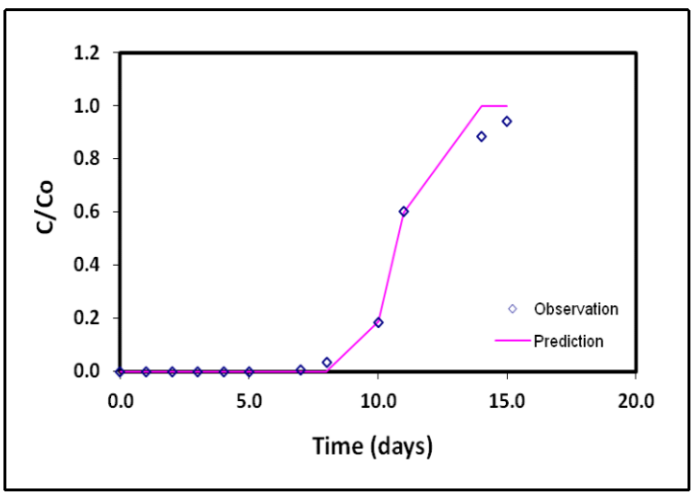

N5-13; 45 cm Fluctuation

	Estimate
Velocity (cm/day)	17.3141
Dispersion	39.2123
R^2	0.9917

Concentration (ppm)				
Distance (m)	**Time (days)**	**Observation**	**Prediction**	**Residual**
150	0	0.0000	0.0000	0.0000
150	5	0.0000	0.0006	-0.0006
150	7	0.1027	0.1076	-0.0049
150	8	0.3135	0.3216	-0.0081
150	10	0.8405	0.7971	0.0434
150	11	0.8667	0.9172	-0.0505
150	14	0.9063	0.9975	-0.0912

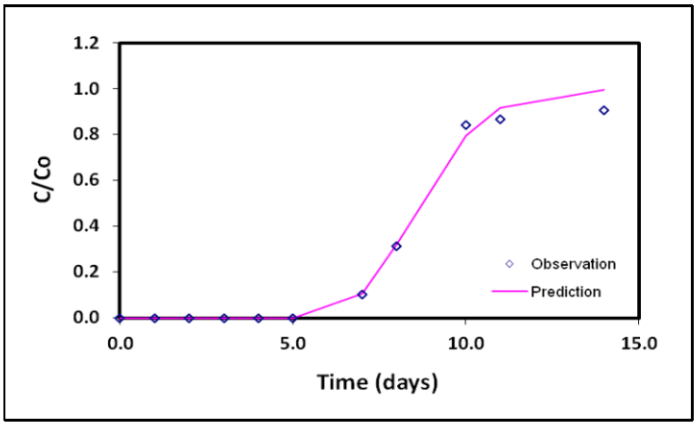

Appendix B – Air Entrapment Data

Saturated Experiment

4-May-13					
Sample ID	**Parameter**	**Retention (min)**	**Area**	**Height**	**External (%)**
Cal01	Oxygen	4.096	3.0898	0.132	21.1854
	Argon	0.583	3.6070	1.287	0.9253
Cal02	Oxygen*	4.056	2.4078	0.117	16.5092
	Argon	0.586	3.4940	1.234	0.9065
Cal03	Oxygen	4.053	2.9370	0.128	20.0996
	Argon	0.576	3.5468	1.274	0.9294
N1-3	Oxygen	4.100	0.5828	0.028	3.9884
	Argon	0.593	0.4951	0.180	0.1297
N1-5	Oxygen	4.113	0.2746	0.021	1.8792
	Argon	0.593	0.4088	0.145	0.1071
N1-7	Oxygen	4.083	0.2920	0.023	1.9983
	Argon	0.593	0.4228	0.158	0.1108
N1-9	Oxygen	4.053	0.5200	0.027	3.5587
	Argon	0.590	0.5006	0.179	0.1312
N1-11	Oxygen	4.170	0.1410	0.017	0.9649
	Argon	0.590	0.3860	0.130	0.1011
N1-13	Oxygen	4.100	0.2960	0.023	2.0257
	Argon	0.586	0.3584	0.124	0.0939
N2-3	Oxygen	4.176	0.2032	0.022	1.3906
	Argon	0.590	0.3524	0.129	0.0923
N2-5	Oxygen	4.160	0.2168	0.018	1.4837
	Argon	0.586	0.4078	0.121	0.1069
N2-7	Oxygen	4.110	0.5446	0.033	3.7270
	Argon	0.590	0.6186	0.213	0.1621
N2-9	Oxygen	4.056	0.2116	0.026	1.4481
	Argon	0.590	0.5536	0.196	0.1451
N2-11	Oxygen	4.110	0.2260	0.024	1.5466
	Argon	0.593	0.5084	0.178	0.1332
N2-13	Oxygen	4.086	0.2302	0.019	1.5754
	Argon	0.593	0.5356	0.173	0.1403
N3-3	Oxygen	4.110	0.8612	0.038	5.8937
	Argon	0.586	0.7820	0.293	0.2049
N3-5	Oxygen	4.123	0.3132	0.026	2.1434
	Argon	0.590	0.3814	0.148	0.0999

N3-7	Oxygen	4.106	0.2304	0.025	1.5768
	Argon	0.583	0.2911	0.125	0.0763
N3-9	Oxygen	4.040	0.1534	0.017	1.0498
	Argon	0.590	0.2492	0.098	0.0653
N3-11	Oxygen	4.130	0.1818	0.022	1.2442
	Argon	0.593	0.4373	0.170	0.1146
N3-13	Oxygen	4.020	0.3690	0.024	2.9267
	Argon	0.543	0.5132	0.171	0.1357
Cal04	Oxygen	4.040	2.5348	0.121	20.1045
	Argon	0.580	3.5105	1.312	0.9283
Cal05	Oxygen	4.030	2.4524	0.118	19.4510
	Argon	0.580	3.5566	1.296	0.9404
N4-3	Oxygen	4.043	0.3924	0.027	3.1123
	Argon	0.586	0.9068	0.320	0.2398
N4-5	Oxygen	4.103	0.3172	0.024	2.5158
	Argon	0.583	0.6932	0.248	0.1833
N4-7	Oxygen	4.033	0.4954	0.034	3.9276
	Argon	0.583	0.7364	0.244	0.1947
N4-9	Oxygen	4.056	0.2652	0.026	2.1034
	Argon	0.586	0.4722	0.173	0.1249
N4-11	Oxygen	4.103	0.2684	0.027	2.1288
	Argon	0.593	0.4844	0.156	0.1281
N4-13	Oxygen	4.036	0.2062	0.024	1.6355
	Argon	0.590	0.3756	0.135	0.0993
N5-3	Oxygen	4.073	0.3728	0.034	2.9568
	Argon	0.583	0.6481	0.228	0.1714
N5-5	Oxygen	4.040	0.5444	0.037	4.3179
	Argon	0.580	0.7350	0.270	0.1944
N5-7	Oxygen	4.080	0.8988	0.051	7.1287
	Argon	0.583	1.2934	0.441	0.3420
N5-11	Oxygen	4.013	0.3142	0.022	2.4920
	Argon	0.590	0.5646	0.180	0.1497
N5-13	Oxygen	4.106	0.2020	0.021	1.6021
	Argon	0.590	0.6170	0.172	0.1631

7-May-13					
Sample ID	**Parameter**	**Retention (min)**	**Area**	**Height**	**External (%)**
Cal01	Oxygen	4.053	2.4960	0.125	20.9634
	Argon	0.583	3.1219	1.171	0.8557

Cal02	Oxygen	4.060	2.7194	0.118	22.9317
	Argon	0.576	3.3675	1.206	0.9395
Cal03	Oxygen	4.040	2.8278	0.130	22.7023
	Argon	0.580	3.5023	1.273	0.9780
N1-2	Oxygen	4.010	0.3984	0.030	3.1985
	Argon	0.586	0.6151	0.230	0.1718
N1-3	Oxygen	4.096	0.2428	0.026	1.9493
	Argon	0.586	0.5215	0.189	0.1456
N1-4	Oxygen	3.993	0.2764	0.021	2.2190
	Argon	0.583	0.3939	0.129	0.1100
N1-5	Oxygen	4.013	0.2766	0.020	2.2206
	Argon	0.590	0.3492	0.120	0.0975
N1-6	Oxygen	4.053	0.2504	0.019	2.0103
	Argon	0.586	0.4284	0.148	0.1196
N1-7	Oxygen	4.070	0.2034	0.023	1.6329
	Argon	0.580	0.4816	0.159	0.1345
N1-9	Oxygen	4.006	0.3806	0.025	3.0556
	Argon	0.586	0.4096	0.150	0.1144
N1-11	Oxygen	4.050	0.1744	0.024	1.4001
	Argon	0.580	0.3809	0.147	0.1064
N1-13	Oxygen	4.043	0.2518	0.018	2.0215
	Argon	0.590	0.3816	0.112	0.1066
N2-2	Oxygen	4.070	0.4352	0.028	3.4939
	Argon	0.586	0.6910	0.228	0.1929
N2-3	Oxygen	4.080	0.4322	0.030	3.4698
	Argon	0.590	0.4529	0.158	0.1265
N2-5	Oxygen	4.050	0.6228	0.032	5.3134
	Argon	0.563	0.6382	0.224	0.1632
N2-6	Oxygen	4.113	0.2228	0.019	1.9008
	Argon	0.580	0.4160	0.141	0.1064
N2-7	Oxygen	4.173	0.2007	0.022	1.7123
	Argon	0.590	0.3596	0.134	0.0919
N2-9	Oxygen	4.153	0.3057	0.023	2.6081
	Argon	0.586	0.4252	0.135	0.1087
N2-11	Oxygen	4.053	0.3308	0.028	2.8222
	Argon	0.583	0.5290	0.172	0.1352
N2-13	Oxygen	4.130	0.1640	0.017	1.3992
	Argon	0.586	0.3864	0.137	0.0988
Cal04	Oxygen	4.026	2.5784	0.120	20.4844

	Argon	0.573	3.3340	1.231	0.9116
Cal05	Oxygen	4.016	2.4280	0.119	19.4787
	Argon	0.580	3.6488	1.248	0.9709
Cal06	Oxygen	4.013	2.3604	0.122	20.1378
	Argon	0.573	3.9303	1.332	1.0048
N3-2	Oxygen	4.070	0.2204	0.021	1.8803
	Argon	0.583	0.4778	0.160	0.1222
N3-3	Oxygen	4.086	0.2250	0.024	1.9196
	Argon	0.586	0.5344	0.168	0.1366
N3-4	Oxygen	4.080	0.2707	0.026	2.3095
	Argon	0.590	0.4840	0.155	0.1237
N3-5	Oxygen	4.090	0.2252	0.024	1.9213
	Argon	0.590	0.4856	0.160	0.1241
N3-6	Oxygen	4.160	0.2662	0.028	2.2711
	Argon	0.590	0.5750	0.176	0.1470
N3-7	Oxygen	4.176	0.3352	0.025	2.8598
	Argon	0.586	0.4616	0.156	0.1180
N3-9	Oxygen	4.050	0.2108	0.029	1.7984
	Argon	0.583	0.6364	0.224	0.1627
N3-11	Oxygen	4.093	0.2224	0.021	1.8974
	Argon	0.593	0.3544	0.113	0.0906
N3-13	Oxygen	4.126	0.1758	0.020	1.4998
	Argon	0.590	0.4828	0.135	0.1234
N4-2	Oxygen	4.026	0.3476	0.027	2.9656
	Argon	0.583	0.7910	0.270	0.2022
N4-3	Oxygen	4.060	0.5236	0.035	4.4671
	Argon	0.580	0.7392	0.250	0.1890
N4-4	Oxygen	4.056	0.2300	0.021	1.9622
	Argon	0.580	0.5290	0.174	0.1352
N4-5	Oxygen	4.116	0.2572	0.026	2.1943
	Argon	0.580	0.6260	0.219	0.1600
N4-6	Oxygen	4.073	0.1792	0.019	1.5288
	Argon	0.583	0.4447	0.143	0.1137
N4-7	Oxygen	4.073	0.2218	0.022	1.8923
	Argon	0.580	0.5020	0.168	0.1283
N4-9	Oxygen	4.163	0.2690	0.021	2.2950
	Argon	0.580	0.3710	0.148	0.0948
N4-11	Oxygen	4.050	0.2474	0.022	2.1107
	Argon	0.580	0.3940	0.127	0.1007

N4-13	Oxygen	4.063	0.2027	0.019	1.7293
	Argon	0.576	0.4308	0.140	0.1101
N5-2	Oxygen	4.070	0.5143	0.028	4.3878
	Argon	0.580	0.6926	0.232	0.1771
N5-3	Oxygen	4.010	0.5472	0.031	4.6684
	Argon	0.570	0.6486	0.227	0.1658
N5-4	Oxygen	4.090	0.4804	0.034	4.0985
	Argon	0.573	0.8968	0.287	0.2293
N5-5	Oxygen	4.053	0.6256	0.039	5.3373
	Argon	0.580	0.7864	0.252	0.2010
N5-6	Oxygen	4.033	0.4582	0.032	3.9091
	Argon	0.576	0.8738	0.303	0.2234
N5-7	Oxygen	4.030	0.6640	0.042	5.6649
	Argon	0.576	0.9404	0.323	0.2404
N5-9	Oxygen	4.043	0.3104	0.025	2.6482
	Argon	0.580	0.5964	0.200	0.1525
N5-11	Oxygen	4.013	0.4692	0.035	4.0030
	Argon	0.576	0.7082	0.254	0.1811
N5-13	Oxygen	4.006	0.1756	0.019	1.4981
	Argon	0.580	0.2459	0.080	0.0629

11-May-13					
Sample ID	**Parameter**	**Retention (min)**	**Area**	**Height**	**External (%)**
Cal01	Oxygen	4.010	2.9396	0.136	23.9071
	Argon	0.576	3.4130	1.231	0.8663
Cal02	Oxygen	4.006	2.8902	0.128	22.1788
	Argon	0.570	3.3682	1.210	0.8773
Cal03	Oxygen	4.010	2.6558	0.128	19.6706
	Argon	0.573	3.4510	1.257	0.9410
N1-2	Oxygen	4.026	0.6010	0.035	4.4514
	Argon	0.580	0.8182	0.330	0.2231
N1-3	Oxygen	4.046	0.4820	0.034	3.5700
	Argon	0.580	0.5428	0.223	0.1480
N1-4	Oxygen	4.046	0.1858	0.024	1.3910
	Argon	0.583	0.4024	0.146	0.1097
N1-5	Oxygen	4.073	0.3116	0.026	2.3079
	Argon	0.586	0.6192	0.195	0.1688
N1-6	Oxygen	4.133	0.1752	0.020	1.2976
	Argon	0.580	0.4544	0.159	0.1239

N1-7	Oxygen	4.093	0.1666	0.022	1.2340
	Argon	0.586	0.5516	0.194	0.1504
N1-9	Oxygen	4.100	0.1765	0.019	1.3073
	Argon	0.583	0.3487	0.117	0.0951
N1-13	Oxygen	4.036	0.2092	0.024	1.5495
	Argon	0.580	0.4024	0.168	0.1097
N2-2	Oxygen	4.176	0.3476	0.029	2.5746
	Argon	0.583	0.6257	0.236	0.1706
N2-3	Oxygen	4.126	0.2084	0.023	1.5435
	Argon	0.583	0.3820	0.153	0.1042
N2-4	Oxygen	4.083	0.1704	0.018	1.2621
	Argon	0.586	0.3812	0.140	0.1039
N2-5	Oxygen	4.076	0.1717	0.024	1.2717
	Argon	0.590	0.3490	0.124	0.0952
N2-6	Oxygen	4.090	0.2005	0.019	1.4850
	Argon	0.583	0.5584	0.203	0.1523
N2-7	Oxygen	4.093	0.1690	0.020	1.2517
	Argon	0.580	0.3484	0.125	0.0950
N2-9	Oxygen	4.140	0.2440	0.024	1.9613
	Argon	0.583	0.3764	0.142	0.1007
N2-11	Oxygen	4.130	0.1644	0.017	1.3215
	Argon	0.583	0.3080	0.120	0.0824
N2-13	Oxygen	4.093	0.2488	0.022	1.9999
	Argon	0.590	0.4006	0.139	0.1071
Cal04	Oxygen	4.033	2.5844	0.121	19.9781
	Argon	0.576	3.4901	1.262	0.9445
Cal05	Oxygen	4.030	2.5666	0.120	20.6629
	Argon	0.573	3.5293	1.270	0.9404
Cal06	Oxygen	4.043	2.6680	0.128	21.4457
	Argon	0.576	3.4128	1.247	0.9127
N3-2	Oxygen	4.070	0.4470	0.035	3.5930
	Argon	0.583	0.6960	0.251	0.1861
N3-3	Oxygen	4.126	0.1718	0.015	1.3809
	Argon	0.583	0.3409	0.127	0.0912
N3-4	Oxygen	4.036	0.2614	0.030	2.1012
	Argon	0.583	0.5528	0.192	0.1478
N3-5	Oxygen	4.116	0.1580	0.020	1.2700
	Argon	0.580	0.2228	0.085	0.0596
N3-6	Oxygen	4.136	0.2448	0.021	1.9677

	Argon	0.583	0.4524	0.153	0.1210
N3-7	Oxygen	4.086	0.1688	0.017	1.3568
	Argon	0.580	0.4089	0.137	0.1094
N3-9	Oxygen	4.140	0.1485	0.020	1.1937
	Argon	0.580	0.3866	0.151	0.1034
N3-11	Oxygen	4.093	0.3287	0.027	2.6421
	Argon	0.583	0.4888	0.176	0.1307
N3-13	Oxygen	4.066	0.1082	0.021	0.8697
	Argon	0.583	0.2712	0.100	0.0725
N4-2	Oxygen	4.033	0.2816	0.026	2.2635
	Argon	0.583	0.6455	0.225	0.1726
N4-3	Oxygen	4.113	0.2002	0.024	1.6092
	Argon	0.586	0.4236	0.150	0.1133
N4-4	Oxygen	4.196	0.2120	0.020	1.7041
	Argon	0.580	0.3072	0.107	0.0822
N4-5	Oxygen	4.150	0.2688	0.025	2.1606
	Argon	0.583	0.3712	0.124	0.0993
N4-6	Oxygen	4.056	0.3188	0.029	2.3556
	Argon	0.580	0.4396	0.155	0.1177
N4-7	Oxygen	4.086	0.2380	0.023	1.7586
	Argon	0.590	0.2844	0.092	0.0762
N4-9	Oxygen	4.100	0.1758	0.017	1.2990
	Argon	0.583	0.3132	0.108	0.0839
N4-11	Oxygen	4.210	0.1056	0.013	0.7803
	Argon	0.593	0.2232	0.078	0.0598
N4-13	Oxygen	4.076	0.3350	0.030	2.4753
	Argon	0.583	0.4672	0.171	0.1251
Cal07	Oxygen	4.050	2.7198	0.119	21.4899
	Argon	0.573	3.4326	1.206	0.9231
Cal08	Oxygen	4.050	2.7652	0.127	21.3164
	Argon	0.573	3.5197	1.263	0.9474
Cal09	Oxygen	4.070	3.0210	0.129	22.3219
	Argon	0.570	3.4674	1.235	0.9284
N4-2	Oxygen	4.033	0.2816	0.026	2.2635
	Argon	0.583	0.6455	0.225	0.1726
N4-3	Oxygen	4.113	0.2002	0.024	1.6092
	Argon	0.586	0.4236	0.150	0.1133
N4-4	Oxygen	4.196	0.2120	0.020	1.7041
	Argon	0.580	0.3072	0.107	0.0822

N4-5	Oxygen	4.150	0.2688	0.025	2.1606
	Argon	0.583	0.3712	0.124	0.0993
N4-6	Oxygen	4.056	0.3188	0.029	2.3556
	Argon	0.580	0.4396	0.155	0.1177
N4-7	Oxygen	4.086	0.2380	0.023	1.7586
	Argon	0.590	0.2844	0.092	0.0762
N4-9	Oxygen	4.100	0.1758	0.017	1.2990
	Argon	0.583	0.3132	0.108	0.0839
N4-11	Oxygen	4.210	0.1056	0.013	0.7803
	Argon	0.593	0.2232	0.078	0.0598
N4-13	Oxygen	4.076	0.3350	0.030	2.4753
	Argon	0.583	0.4672	0.171	0.1251
N5-2	Oxygen	4.073	0.7734	0.043	5.7142
	Argon	0.580	0.9668	0.335	0.2589
N5-3	Oxygen	4.090	0.3708	0.031	2.7398
	Argon	0.573	0.7434	0.266	0.1991
N5-4	Oxygen	4.043	0.3116	0.026	2.3024
	Argon	0.583	0.5700	0.174	0.1526
N5-5	Oxygen	4.206	0.3824	0.032	2.8255
	Argon	0.583	0.6232	0.206	0.1669
N5-6	Oxygen	4.073	0.3644	0.024	2.6925
	Argon	0.580	0.5494	0.184	0.1471
N5-7	Oxygen	4.090	0.3369	0.028	2.4893
	Argon	0.580	0.6108	0.190	0.1635
N5-9	Oxygen	4.113	0.1379	0.021	1.0189
	Argon	0.583	0.3125	0.113	0.0837
N5-11	Oxygen	4.110	0.1732	0.020	1.2798
	Argon	0.586	0.4313	0.152	0.1155
N5-13	Oxygen	4.160	0.1062	0.016	0.7847
	Argon	0.593	0.1896	0.068	0.0508

14-May-13

Sample ID	**Parameter**	**Retention (min)**	**Area**	**Height**	**External (%)**
Cal01	Oxygen	4.073	2.6368	0.119	19.6750
	Argon	0.580	3.3330	1.164	0.9011
Cal02	Oxygen	4.026	2.6664	0.119	20.7297
	Argon	0.576	0.3632	1.187	0.9232
Cal03	Oxygen	4.090	2.6894	0.121	21.8029
	Argon	0.576	3.1084	1.117	0.8845

N1-2	Oxygen	4.106	0.6957	0.033	5.6400
	Argon	0.583	0.9023	0.311	0.2568
N1-3	Oxygen	4.096	0.5192	0.032	4.2091
	Argon	0.586	0.7564	0.254	0.2152
N1-4	Oxygen	4.166	0.3536	0.022	2.8666
	Argon	0.590	0.6573	0.202	0.1870
N1-5	Oxygen	4.053	0.3514	0.030	2.8488
	Argon	0.586	0.4704	0.165	0.1339
N1-6	Oxygen	4.066	0.3044	0.024	2.4678
	Argon	0.586	0.5321	0.165	0.1514
N1-7	Oxygen	4.126	0.2128	0.023	1.7252
	Argon	0.586	0.4748	0.143	0.1351
N1-11	Oxygen	4.066	0.1195	0.019	0.9688
	Argon	0.586	0.3688	0.101	0.1049
N1-13	Oxygen	4.153	0.1042	0.015	0.8496
	Argon	0.586	0.3705	0.122	0.1054
N2-2	Oxygen	4.096	0.7232	0.033	5.8630
	Argon	0.580	0.6716	0.230	0.1911
N2-3	Oxygen	4.046	0.1152	0.016	0.9339
	Argon	0.583	0.4262	0.144	0.1213
N2-4	Oxygen	4.030	0.2852	0.019	2.3121
	Argon	0.586	0.2850	0.096	0.0811
N2-5	Oxygen	4.060	0.2152	0.020	1.7446
	Argon	0.590	0.3524	0.124	0.1003
N2-6	Oxygen	4.160	0.2964	0.024	2.4029
	Argon	0.586	0.3710	0.134	0.1056
N2-7	Oxygen	4.136	0.1048	0.014	0.8496
	Argon	0.590	0.3489	0.117	0.0993
N2-9	Oxygen	4.140	0.1720	0.020	1.3944
	Argon	0.590	0.3008	0.111	0.0856
N2-11	Oxygen	4.073	0.2693	0.025	2.1832
	Argon	0.586	0.4336	0.161	0.1234
N2-13	Oxygen	4.076	0.1526	0.015	1.2371
	Argon	0.590	0.3438	0.098	0.0978
N3-2	Oxygen	4.063	0.4804	0.032	3.7776
	Argon	0.576	0.7508	0.284	0.2136
N3-3	Oxygen	4.126	0.2606	0.025	2.0492
	Argon	0.586	0.5156	0.168	0.1467
N3-4	Oxygen	4.036	0.2386	0.024	1.8762

	Argon	0.583	0.3629	0.126	0.1033
N3-5	Oxygen	<DL	<DL	<DL	<DL
	Argon	0.590	0.2830	0.083	0.0805
N3-6	Oxygen	4.083	0.1916	0.019	1.5067
	Argon	0.583	0.4838	0.150	0.1377
N3-7	Oxygen	4.193	0.2370	0.024	1.8637
	Argon	0.580	0.3068	0.111	0.0873
N3-9	Oxygen	4.140	0.2330	0.023	1.8322
	Argon	0.586	0.3458	0.106	0.0984
N3-11	Oxygen	4.093	0.2218	0.020	1.7441
	Argon	0.580	0.4782	0.175	0.1361
N3-13	Oxygen	4.086	0.2247	0.023	1.7669
	Argon	0.586	0.4542	0.139	0.1292
N4-2	Oxygen	4.120	0.1860	0.020	1.4626
	Argon	0.583	0.5693	0.188	0.1620
N4-3	Oxygen	4.160	0.3972	0.033	3.1234
	Argon	0.590	0.6066	0.178	0.1726
N4-4	Oxygen	4.123	0.2336	0.221	1.8579
	Argon	0.583	0.4202	0.124	0.1171
N4-5	Oxygen	4.046	0.2107	0.023	1.6758
	Argon	0.586	0.2776	0.087	0.0774
N4-6	Oxygen	4.103	0.2297	0.019	1.8269
	Argon	0.590	0.3844	0.139	0.1071
N4-7	Oxygen	4.090	0.1577	0.015	1.2543
	Argon	0.586	0.4032	0.133	0.1124
N4-9	Oxygen	4.096	0.2460	0.022	1.9566
	Argon	0.586	0.4808	0.148	0.1340
N4-11	Oxygen	4.263	0.1200	0.018	0.9544
	Argon	0.593	0.3168	0.108	0.0883
N4-13	Oxygen	4.153	0.2429	0.020	1.9319
	Argon	0.586	0.5259	0.176	0.1466
Cal04	Oxygen	4.080	2.5464	0.120	20.2527
	Argon	0.580	3.5404	1.213	0.9866
N5-2	Oxygen	4.050	0.4534	0.033	3.6061
	Argon	0.580	0.7468	0.244	0.2081
N5-3	Oxygen	4.066	0.3030	0.028	2.4099
	Argon	0.563	0.3920	0.144	0.1092
N5-4	Oxygen	4.290	0.1367	0.017	1.0872
	Argon	0.586	0.2528	0.087	0.0704

N5-5	Oxygen	4.096	0.1791	0.024	1.4245
	Argon	0.590	0.4448	0.134	0.1240
N5-6	Oxygen	4.153	0.1709	0.017	1.3592
	Argon	0.583	0.2449	0.090	0.0682
N5-7	Oxygen	4.096	0.2082	0.020	1.6559
	Argon	0.593	0.3456	0.088	0.0963
N5-9	Oxygen	4.066	0.3632	0.029	2.8887
	Argon	0.576	0.5278	0.194	0.1471
N5-11	Oxygen	4.070	0.1248	0.018	0.9926
	Argon	0.593	0.3300	0.122	0.0920
N5-13	Oxygen	4.110	0.1910	0.019	1.5191
	Argon	0.593	0.4421	0.150	0.1232

29 cm Fluctuation Experiment

28-May-13					
Sample ID	**Parameter**	**Retention (min)**	**Area**	**Height**	**External (%)**
Cal01	Oxygen	4.040	2.9864	0.124	22.8279
	Argon	0.573	3.3956	1.169	0.9432
Cal02	Oxygen	4.033	2.6036	0.116	20.1116
	Argon	0.580	3.3213	1.184	0.9034
Cal03	Oxygen	4.056	2.4676	0.108	19.2475
	Argon	0.573	3.0567	1.084	0.8726
N1-2	Oxygen	4.076	1.6870	0.078	13.1588
	Argon	0.580	1.9698	0.706	0.5623
N1-3	Oxygen	4.076	0.9882	0.046	7.7080
	Argon	0.576	1.2348	0.441	0.3525
N1-4	Oxygen	4.090	0.9124	0.046	7.1168
	Argon	0.583	1.0016	0.348	0.2859
N1-5	Oxygen	4.110	0.4496	0.029	3.5069
	Argon	0.583	0.8759	0.302	0.2500
N1-6	Oxygen	4.053	0.6288	0.031	4.9047
	Argon	0.580	0.6732	0.229	0.1922
N1-7	Oxygen	4.183	0.2700	0.017	2.1060
	Argon	0.586	0.3684	0.131	0.1052
N1-8	Oxygen	4.036	0.2503	0.022	1.9524
	Argon	0.583	0.4264	0.145	0.1217
N1-9	Oxygen	4.126	0.1892	0.020	1.4758
	Argon	0.590	0.3184	0.110	0.0909

N1-10	Oxygen	4.050	0.1672	0.016	1.3042
	Argon	0.586	0.2916	0.108	0.0832
N1-11	Oxygen	4.166	0.2358	0.021	1.8393
	Argon	0.580	0.4517	0.171	0.1289
N1-13	Oxygen	4.036	0.1092	0.016	0.8518
	Argon	0.580	0.2892	0.105	0.0826
Cal04	Oxygen	4.040	2.2176	0.100	19.1220
	Argon	0.573	3.1296	1.082	0.9184
N2-2	Oxygen	4.050	1.1072	0.061	9.5472
	Argon	0.570	1.8767	0.666	0.5507
N2-3	Oxygen	4.083	1.0196	0.053	8.7918
	Argon	0.576	1.6792	0.587	0.4928
N2-4	Oxygen	4.116	0.4458	0.034	3.8441
	Argon	0.580	0.6836	0.248	0.2006
N2-5	Oxygen	4.146	0.1959	0.020	1.6892
	Argon	0.583	0.3892	0.144	0.1142
N2-6	Oxygen	4.076	0.2140	0.017	1.8453
	Argon	0.590	0.3030	0.111	0.0889
N2-7	Oxygen	4.166	0.1372	0.012	1.1831
	Argon	0.586	0.3176	0.116	0.0932
N2-8	Oxygen	4.110	0.2713	0.024	2.3394
	Argon	0.586	0.4329	0.169	0.1270
N2-9	Oxygen	4.186	0.1672	0.020	1.4417
	Argon	0.583	0.3015	0.105	0.0885
N2-11	Oxygen	4.133	0.1366	0.015	1.1779
	Argon	0.586	0.3356	0.119	0.0985
N2-13	Oxygen	4.100	0.2736	0.020	2.3592
	Argon	0.583	0.3971	0.151	0.1165
Cal05	Oxygen	4.036	2.0732	0.105	19.2798
	Argon	0.573	3.2620	1.148	0.9632
N3-2	Oxygen	4.066	1.7448	0.090	16.2258
	Argon	0.573	2.6676	0.940	0.7877
N3-3	Oxygen	4.003	1.1048	0.056	10.2741
	Argon	0.580	1.8501	0.649	0.5463
N3-4	Oxygen	4.083	0.9576	0.046	8.9052
	Argon	0.580	1.2240	0.443	0.3610
N3-5	Oxygen	4.086	0.1658	0.019	1.5419
	Argon	0.583	0.3978	0.118	0.1175
N3-6	Oxygen	4.140	2.4160	0.022	2.2468

	Argon	0.580	0.4240	0.128	0.1252
N3-7	Oxygen	4.130	0.2916	0.027	2.7117
	Argon	0.586	0.5204	0.180	0.1537
N3-8	Oxygen	<DL	<DL	<DL	<DL
	Argon	0.586	0.2958	0.113	0.0873
N3-9	Oxygen	4.113	0.3286	0.027	3.0558
	Argon	0.586	0.4915	0.169	0.1451
N3-11	Oxygen	4.203	0.3612	0.026	3.3590
	Argon	0.580	0.5404	0.172	0.1596
N3-13	Oxygen	4.043	0.1184	0.019	1.0767
	Argon	0.580	0.3898	0.144	0.1105
Cal06	Oxygen	4.060	2.6204	0.125	23.8297
	Argon	0.573	3.4492	1.201	0.9779
N4-2	Oxygen	4.060	2.0036	0.092	18.2206
	Argon	0.573	2.9768	1.010	0.8440
N4-3	Oxygen	4.073	1.3879	0.072	12.6215
	Argon	0.580	2.0408	0.705	0.5786
N4-4	Oxygen	4.063	0.8874	0.050	8.0700
	Argon	0.576	1.1712	0.412	0.3321
N4-5	Oxygen	4.093	0.3690	0.028	3.3557
	Argon	0.580	0.6828	0.229	0.1936
N4-6	Oxygen	4.076	0.1380	0.019	1.2550
	Argon	0.580	0.4737	0.165	0.1343
N4-7	Oxygen	4.186	0.1547	0.016	1.4068
	Argon	0.586	0.2398	0.090	0.0680
N4-8	Oxygen	4.043	0.1441	0.020	1.3104
	Argon	0.583	0.3523	0.134	0.0999
N4-9	Oxygen	4.123	0.1996	0.022	1.8151
	Argon	0.580	0.3906	0.151	0.1107
N4-11	Oxygen	4.120	0.2392	0.025	2.1753
	Argon	0.580	0.4672	0.173	0.1325
N4-13	Oxygen	4.063	0.1964	0.020	1.7860
	Argon	0.580	0.4372	0.164	0.1240
Cal07	Oxygen	4.006	2.3550	0.117	20.9987
	Argon	0.573	3.3628	1.237	0.9313
N5-2	Oxygen	4.023	1.8612	0.098	16.9256
	Argon	0.573	2.6728	0.962	0.7578
N5-3	Oxygen	4.046	0.9008	0.054	8.0321
	Argon	0.576	1.6703	0.597	0.4626

N5-4	Oxygen	4.193	0.3734	0.025	3.3295
	Argon	0.583	0.5944	0.208	0.1646
N5-5	Oxygen	4.106	0.2684	0.021	2.3932
	Argon	0.580	0.3754	0.142	0.1040
N5-6	Oxygen	4.116	0.1690	0.019	1.5069
	Argon	0.583	0.3726	0.130	0.1032
N5-7	Oxygen	4.113	0.3298	0.025	2.9407
	Argon	0.576	0.5648	0.207	0.1564
N5-8	Oxygen	4.036	0.2598	0.023	2.3165
	Argon	0.586	0.3600	0.149	0.0997
N5-9	Oxygen	4.066	0.2182	0.021	1.9456
	Argon	0.583	0.3804	0.143	0.1054
N5-11	Oxygen	4.053	0.1484	0.017	1.3232
	Argon	0.583	0.3316	0.135	0.0918
N5-13	Oxygen	4.096	0.1628	0.019	1.4516
	Argon	0.583	0.3920	0.130	0.1086

31-May-13					
Sample ID	**Parameter**	**Retention (min)**	**Area**	**Height**	**External (%)**
Cal01	Oxygen	4.023	2.5112	0.122	21.0815
	Argon	0.576	3.3516	1.243	0.9200
N1-2	Oxygen	4.023	1.0752	0.053	9.0263
	Argon	0.576	1.1832	0.459	0.3248
N1-3	Oxygen	4.026	0.5085	0.032	4.2689
	Argon	0.580	0.4098	0.164	0.1125
N1-4	Oxygen	4.040	0.3076	0.026	2.5823
	Argon	0.580	0.4228	0.148	0.1164
N1-5	Oxygen	4.073	0.3652	0.024	3.0659
	Argon	0.576	0.3840	0.155	0.1054
N1-6	Oxygen	4.016	0.1983	0.017	1.6647
	Argon	0.580	0.2992	0.117	0.0821
N1-7	Oxygen	4.096	0.1260	0.015	1.0578
	Argon	0.586	0.2812	0.103	0.0772
N1-8	Oxygen	4.080	0.1622	0.018	1.3617
	Argon	0.580	0.4280	0.170	0.1175
N1-9	Oxygen	4.173	0.1695	0.016	1.4230
	Argon	0.586	0.2698	0.109	0.0741
N1-11	Oxygen	4.146	0.1547	0.018	1.2987
	Argon	0.586	0.2468	0.103	0.0677

N1-13	Oxygen	4.063	0.2302	0.018	1.9325
	Argon	0.583	0.3855	0.134	0.1058
N2-2	Oxygen	3.993	1.6668	0.080	13.9928
	Argon	0.573	2.2542	0.819	0.6188
N2-3	Oxygen	4.040	0.9234	0.053	7.7519
	Argon	0.576	1.3542	0.493	0.3717
N2-4	Oxygen	4.040	0.5674	0.030	5.0516
	Argon	0.573	0.6520	0.236	0.1790
N2-5	Oxygen	<DL	<DL	<DL	<DL
	Argon	0.576	0.4216	0.148	0.1157
N2-6	Oxygen	4.016	0.1752	0.022	1.5598
	Argon	0.586	0.3956	0.141	0.1086
N2-7	Oxygen	4.050	0.1752	0.020	1.5598
	Argon	0.580	0.5064	0.179	0.1390
N2-8	Oxygen	4.026	0.2388	0.025	2.1260
	Argon	0.580	0.4200	0.133	0.1153
N2-9	Oxygen	4.086	0.1170	0.017	1.0417
	Argon	0.583	0.3672	0.120	0.1008
N2-11	Oxygen	4.190	0.2074	0.018	1.8465
	Argon	0.583	0.4038	0.133	0.1108
N3-2	Oxygen	4.050	1.8108	0.092	16.1216
	Argon	0.573	2.6612	0.961	0.7305
N3-3	Oxygen	4.050	1.4320	0.067	12.7491
	Argon	0.576	1.7838	0.662	0.4897
N3-4	Oxygen	4.093	0.3214	0.026	2.8614
	Argon	0.583	0.4484	0.177	0.1231
N3-5	Oxygen	4.056	0.4098	0.034	3.6485
	Argon	0.576	0.7648	0.268	0.2099
N3-6	Oxygen	4.054	0.2221	0.021	1.9774
	Argon	0.583	0.3588	0.135	0.0985
N3-7	Oxygen	4.196	0.2192	0.016	1.9515
	Argon	0.583	0.2836	0.108	0.0779
N3-9	Oxygen	4.120	0.2200	0.020	1.9587
	Argon	0.580	0.3912	0.134	0.1074
N3-11	Oxygen	4.136	0.1717	0.016	1.5286
	Argon	0.580	0.4268	0.139	0.1172
N3-13	Oxygen	<DL	<DL	<DL	<DL
	Argon	0.583	0.3233	0.128	0.0887
Cal03	Oxygen	4.000	2.6268	0.114	22.5194

	Argon	0.570	3.2788	1.170	0.9154
Cal04	Oxygen	4.020	1.9772	0.098	18.2821
	Argon	0.570	2.8064	1.016	0.8297
Cal05	Oxygen	4.023	2.5024	0.110	22.1316
	Argon	0.570	3.1476	1.143	0.9512
N4-2	Oxygen	3.996	2.0396	0.094	17.4854
	Argon	0.573	2.8508	1.032	0.7959
N4-3	Oxygen	4.026	1.5468	0.066	13.2606
	Argon	0.576	1.9144	0.683	0.5345
N4-4	Oxygen	3.980	0.5053	0.032	4.3319
	Argon	0.573	0.9360	0.344	0.2613
N4-5	Oxygen	4.100	0.4956	0.030	4.5825
	Argon	0.576	0.6036	0.239	0.1785
N4-6	Oxygen	4.110	0.2257	0.023	1.9961
	Argon	0.583	0.3468	0.123	0.1048
N4-7	Oxygen	4.130	0.2407	0.021	2.1288
	Argon	0.586	0.3120	0.111	0.0943
N4-8	Oxygen	4.040	0.1796	0.019	1.5884
	Argon	0.583	0.3709	0.141	0.1121
N4-9	Oxygen	4.076	0.2148	0.021	1.8997
	Argon	0.583	0.2852	0.105	0.0862
N4-11	Oxygen	4.053	0.1559	0.019	1.3788
	Argon	0.586	0.3612	0.135	0.1091
N5-2	Oxygen	4.063	1.6180	0.084	14.3098
	Argon	0.573	2.5756	0.904	0.7783
N5-3	Oxygen	4.026	1.5056	0.066	13.3157
	Argon	0.576	1.5800	0.557	0.4774
N5-4	Oxygen	4.000	0.6068	0.034	5.3666
	Argon	0.580	0.6789	0.245	0.2052
N5-5	Oxygen	4.070	0.3520	0.024	3.1131
	Argon	0.583	0.4428	0.174	0.1338
N5-6	Oxygen	4.030	0.2050	0.017	1.8130
	Argon	0.586	0.2972	0.112	0.0898
N5-7	Oxygen	4.076	0.3309	0.024	2.9265
	Argon	0.580	0.3789	0.152	0.1145
N5-8	Oxygen	4.160	0.2468	0.021	2.1827
	Argon	0.590	0.2600	0.101	0.0786
N5-9	Oxygen	4.073	0.1712	0.015	1.5141
	Argon	0.580	0.2872	0.104	0.0868

N5-11	Oxygen	4.116	0.1180	0.017	1.0436
	Argon	0.580	0.3848	0.125	0.1163

3-Jun-13					
Sample ID	**Parameter**	**Retention (min)**	**Area**	**Height**	**External (%)**
Cal01	Oxygen	4.053	2.2774	0.110	21.1832
	Argon	0.576	2.7302	1.018	0.8771
Cal02	Oxygen	4.046	2.3884	0.120	20.9412
	Argon	0.576	3.0485	1.113	0.9528
Cal03	Oxygen	4.050	2.5750	0.127	22.3509
	Argon	0.580	3.2325	1.161	1.0008
N1-2	Oxygen	4.043	0.7943	0.043	6.8945
	Argon	0.583	0.7404	0.283	0.2292
N1-3	Oxygen	4.120	0.4322	0.025	3.7515
	Argon	0.586	0.4706	0.175	0.1452
N1-4	Oxygen	4.133	0.2936	0.023	2.5484
	Argon	0.580	0.3197	0.119	0.0990
N1-5	Oxygen	4.210	0.1760	0.020	1.5277
	Argon	0.590	0.4152	0.152	0.1286
N1-6	Oxygen	4.170	0.2200	0.019	1.9096
	Argon	0.583	0.2608	0.100	0.0807
N1-7	Oxygen	4.066	0.1898	0.017	1.6475
	Argon	0.590	0.2856	0.117	0.0884
N1-8	Oxygen	4.143	0.1602	0.017	1.3905
	Argon	0.583	0.2366	0.096	0.0733
N1-9	Oxygen	4.086	0.1468	0.014	1.2742
	Argon	0.590	0.2616	0.099	0.0810
N1-11	Oxygen	4.083	0.1874	0.021	1.6266
	Argon	0.580	0.2370	0.093	0.0734
N1-13	Oxygen	4.046	0.1916	0.023	1.6794
	Argon	0.580	0.4116	0.173	0.1176
Cal04	Oxygen	4.013	2.2072	0.112	19.3460
	Argon	0.573	3.4838	1.260	0.9954
N2-2	Oxygen	4.026	1.3604	0.071	11.9238
	Argon	0.570	1.9991	0.730	0.5712
N2-3	Oxygen	4.100	0.5341	0.037	4.6814
	Argon	0.576	0.7004	0.274	0.2001
N2-4	Oxygen	4.063	0.1596	0.016	1.3989
	Argon	0.586	0.2820	0.100	0.0806

N2-5	Oxygen	4.100	0.1779	0.018	1.5593
	Argon	0.583	0.2594	0.095	0.0741
N2-6	Oxygen	4.023	0.2672	0.022	2.3420
	Argon	0.576	0.3851	0.143	0.1100
N2-7	Oxygen	4.096	0.1843	0.018	1.6154
	Argon	0.583	0.3056	0.100	0.0873
N2-8	Oxygen	4.103	0.1416	0.020	1.2411
	Argon	0.586	0.3061	0.096	0.0875
N2-9	Oxygen	4.083	0.1904	0.018	1.6688
	Argon	0.583	0.2640	0.108	0.0754
N2-11	Oxygen	4.030	0.1912	0.020	1.6759
	Argon	0.586	0.2564	0.104	0.0733
Cal05	Oxygen	4.063	2.4638	0.124	21.3704
	Argon	0.570	3.4507	1.230	0.9859
N3-2	Oxygen	4.043	1.8596	0.092	16.1297
	Argon	0.576	2.5280	0.910	0.7223
N3-3	Oxygen	4.043	1.5180	0.063	13.4270
	Argon	0.576	1.4918	0.556	0.4262
N3-4	Oxygen	4.056	0.2254	0.023	1.9551
	Argon	0.583	0.7602	0.267	0.2172
N3-5	Oxygen	4.073	0.3869	0.028	3.3559
	Argon	0.583	0.4789	0.174	0.1368
N3-6	Oxygen	4.010	0.1720	0.016	1.4919
	Argon	0.590	0.2940	0.113	0.0840
N3-7	Oxygen	4.126	0.1988	0.023	1.7243
	Argon	0.583	0.2073	0.095	0.0592
N3-8	Oxygen	4.093	0.2140	0.021	1.8562
	Argon	0.580	0.3179	0.116	0.0908
N3-9	Oxygen	4.173	0.1566	0.020	1.3583
	Argon	0.586	0.2428	0.101	0.0694
N3-11	Oxygen	4.126	0.2165	0.020	1.8779
	Argon	0.583	0.2631	0.104	0.0752
N4-2	Oxygen	4.076	1.7746	0.086	15.3924
	Argon	0.576	2.4577	0.886	0.7022
N4-3	Oxygen	4.076	1.1562	0.060	10.0286
	Argon	0.573	1.5092	0.560	0.4312
N4-4	Oxygen	4.110	0.7372	0.038	6.3943
	Argon	0.583	0.7980	0.298	0.2280
N4-5	Oxygen	4.110	0.3490	0.059	3.0271

	Argon	0.583	0.4339	0.169	0.1240
N4-6	Oxygen	4.106	0.2394	0.022	2.0765
	Argon	0.586	0.2832	0.114	0.0809
N4-7	Oxygen	4.223	0.2086	0.019	1.8093
	Argon	0.586	0.2542	0.089	0.0726
N4-8	Oxygen	4.110	0.2088	0.018	1.8111
	Argon	0.586	0.3084	0.111	0.0910
N4-9	Oxygen	4.203	0.1960	0.018	1.7001
	Argon	0.580	0.2455	0.097	0.0701
N4-11	Oxygen	4.066	0.1964	0.019	1.7035
	Argon	0.590	0.2822	0.092	0.0806
Cal06	Oxygen	4.040	2.5784	0.121	22.3539
	Argon	0.576	3.4528	1.190	0.9473
N5-2	Oxygen	4.043	1.5287	0.079	13.2533
	Argon	0.573	2.4017	0.845	0.6589
N5-3	Oxygen	4.050	1.0064	0.055	8.7252
	Argon	0.576	1.5236	0.556	0.4180
N5-4	Oxygen	4.100	0.6396	0.040	5.5451
	Argon	0.580	0.8139	0.307	0.2233
N5-5	Oxygen	4.216	0.4333	0.028	3.7566
	Argon	0.580	0.5416	0.207	0.1486
N5-6	Oxygen	4.053	0.2568	0.020	2.2264
	Argon	0.580	0.3566	0.130	0.0978
N5-7	Oxygen	4.156	0.2064	0.024	1.7894
	Argon	0.580	0.3626	0.126	0.0995
N5-8	Oxygen	4.093	0.1960	0.024	1.6933
	Argon	0.586	0.2926	0.112	0.0803
N5-9	Oxygen	4.170	0.1568	0.017	1.3594
	Argon	0.583	0.3068	0.112	0.0842

5-Jun-13					
Sample ID	**Parameter**	**Retention (min)**	**Area**	**Height**	**External (%)**
Cal01	Oxygen	4.040	2.6366	0.117	21.5802
	Argon	0.576	3.1838	1.168	0.8777
Cal02	Oxygen	4.063	2.4736	0.114	20.2203
	Argon	0.573	3.1280	1.160	0.8938
Cal03	Oxygen	4.066	2.4780	0.117	20.5243
	Argon	0.576	3.2660	1.197	0.8414
N1-2	Oxygen	4.083	0.6366	0.042	5.2727

	Argon	0.586	0.6668	0.241	0.1942
N1-3	Oxygen	4.113	0.1956	0.018	1.6201
	Argon	0.583	0.2780	0.117	0.0810
N1-4	Oxygen	4.103	0.2368	0.020	1.9613
	Argon	0.583	0.4096	0.140	0.1193
N1-5	Oxygen	4.200	0.2084	0.022	1.7261
	Argon	0.583	0.2600	0.099	0.0757
N1-6	Oxygen	4.006	0.2016	0.018	1.6698
	Argon	0.586	0.2081	0.089	0.0606
N2-2	Oxygen	4.076	1.2054	0.065	9.9638
	Argon	0.576	1.8853	0.672	0.5492
N2-3	Oxygen	4.073	0.3866	0.031	3.2021
	Argon	0.583	0.5873	0.223	0.1711
N2-4	Oxygen	4.093	0.1528	0.019	1.2656
	Argon	0.590	0.3532	0.129	0.1029
N2-5	Oxygen	4.123	0.1896	0.015	1.5704
	Argon	0.586	0.2678	0.114	0.0780
N2-6	Oxygen	4.150	0.3234	0.024	2.6786
	Argon	0.583	0.3058	0.126	0.0891
N2-7	Oxygen	4.063	0.2098	0.024	1.7377
	Argon	0.583	0.3656	0.142	0.1065
N3-2	Oxygen	4.040	1.8824	0.086	15.5912
	Argon	0.576	2.3072	0.859	0.6721
N3-3	Oxygen	4.110	0.9148	0.056	7.5769
	Argon	0.576	1.3516	0.485	0.3937
N3-4	Oxygen	4.250	0.2360	0.019	1.9547
	Argon	0.576	0.4848	0.158	0.1412
N3-5	Oxygen	4.026	0.1516	0.018	1.2556
	Argon	0.590	0.2511	0.095	0.0731
N3-6	Oxygen	4.146	0.3016	0.021	2.4980
	Argon	0.576	0.2716	0.113	0.0791
N4-2	Oxygen	4.033	1.8606	0.090	15.4106
	Argon	0.573	2.6304	0.946	0.7662
N4-3	Oxygen	4.063	1.0714	0.058	8.8740
	Argon	0.573	1.5584	0.537	0.4540
N4-4	Oxygen	4.036	0.6778	0.035	5.6139
	Argon	0.576	0.9350	0.346	0.2724
N4-5	Oxygen	4.016	0.2120	0.018	1.7559
	Argon	0.580	0.6051	0.185	0.1763

N4-6	Oxygen	4.083	0.2754	0.028	2.2810
	Argon	0.593	0.2958	0.107	0.0862
N5-2	Oxygen	4.030	1.8032	0.095	14.9352
	Argon	0.560	2.5582	0.901	0.7452
N5-3	Oxygen	4.033	0.9500	0.054	7.8685
	Argon	0.570	1.5037	0.532	0.4380
N5-4	Oxygen	4.026	0.6121	0.032	5.0698
	Argon	0.576	0.8252	0.280	0.2404
N5-5	Oxygen	4.063	0.2140	0.022	1.7725
	Argon	0.580	0.3961	0.144	0.1154
N5-6	Oxygen	4.096	0.2597	0.025	2.1510
	Argon	0.583	0.3360	0.133	0.0979

45 cm Fluctuation Experiment

9-Jul-13					
Sample ID	**Parameter**	**Retention (min)**	**Area**	**Height**	**External (%)**
Cal01	Oxygen	3.786	2.0024	0.083	24.4732
	Argon	0.570	2.0819	0.773	0.9335
Cal02	Oxygen	3.793	1.5660	0.082	18.5606
	Argon	0.556	2.1634	0.801	0.9697
Cal03	Oxygen	3.776	1.8432	0.091	21.4068
	Argon	0.570	2.3964	0.917	1.0159
N1-2	Oxygen	3.836	1.6844	0.090	19.5625
	Argon	0.576	1.9536	0.746	0.8282
N1-3	Oxygen	3.846	1.6788	0.086	19.4975
	Argon	0.566	1.9456	0.746	0.8248
N1-4	Oxygen	3.846	1.6788	0.086	19.4975
	Argon	0.566	1.9456	0.746	0.8248
N1-5	Oxygen	3.806	1.5071	0.081	17.5034
	Argon	0.570	1.9062	0.746	0.8081
N1-6	Oxygen	3.823	1.6858	0.084	19.5788
	Argon	0.576	2.0644	0.796	0.8752
N1-7	Oxygen	3.850	0.8972	0.052	10.4200
	Argon	0.576	1.1126	0.412	0.4717
N1-8	Oxygen	3.826	0.7220	0.052	8.3853
	Argon	0.573	1.1404	0.438	0.4835
N1-9	Oxygen	3.876	0.4516	0.033	5.2449
	Argon	0.566	0.6060	0.227	0.2568

N1-10	Oxygen	3.843	0.2066	0.020	2.3994
	Argon	0.580	0.4280	0.184	0.1814
N1-11	Oxygen	3.866	0.2101	0.025	2.4401
	Argon	0.586	0.2932	0.126	0.1243
N1-12	Oxygen	0.830	0.1684	0.021	1.9558
	Argon	0.590	0.2916	0.129	0.1236
N2-2	Oxygen	3.766	1.6820	0.086	19.5346
	Argon	0.573	2.1124	0.753	0.8955
N2-3	Oxygen	3.793	1.6106	0.090	18.7054
	Argon	0.566	2.2428	0.871	0.9508
N2-4	Oxygen	3.803	1.5200	0.099	17.6532
	Argon	0.566	2.8032	1.019	1.1884
N2-5	Oxygen	3.793	1.3932	0.076	16.1805
	Argon	0.570	2.0484	0.764	0.8684
N2-6	Oxygen	3.810	1.6658	0.098	18.8525
	Argon	0.570	2.6506	0.999	1.0186
Cal04	Oxygen	3.806	2.1442	0.106	24.2668
	Argon	0.570	2.7004	0.989	1.0377
N2-7	Oxygen	3.816	1.5818	0.083	17.9018
	Argon	0.573	2.1210	0.777	0.8151
N2-8	Oxygen	3.640	1.7940	0.095	20.3034
	Argon	0.403	2.3804	0.923	0.9148
N2-9	Oxygen	3.833	1.3020	0.078	14.7352
	Argon	0.570	2.3912	0.845	0.9189
N2-10	Oxygen	3.900	0.9005	0.053	10.1913
	Argon	0.580	1.2078	0.426	0.4641
N2-11	Oxygen	3.923	0.3030	0.025	3.4292
	Argon	0.583	0.6070	0.212	0.2333
N2-12	Oxygen	3.933	0.3060	0.025	3.4631
	Argon	0.590	0.6133	0.200	0.2357
N3-2	Oxygen	3.814	1.7156	0.095	19.4161
	Argon	0.570	2.6534	0.984	1.0197
N3-4	Oxygen	3.843	1.5488	0.074	17.5284
	Argon	0.566	1.6312	0.588	0.6268
Cal05	Oxygen	3.833	2.3580	0.106	23.3555
	Argon	0.570	2.8356	1.050	0.9973
Cal06	Oxygen	3.836	1.9376	0.100	18.9102
	Argon	0.570	2.8842	1.074	0.9557
Cal07	Oxygen	3.813	2.2544	0.105	21.6319

	Argon	0.566	2.8486	1.066	0.9275
N3-5	Oxygen	3.870	1.7464	0.093	16.7574
	Argon	0.566	2.4084	0.930	0.7842
N3-6	Oxygen	3.823	1.6230	0.094	15.5734
	Argon	0.566	2.3726	0.926	0.7726
N3-7	Oxygen	3.826	1.8896	0.099	18.1315
	Argon	0.570	2.4636	0.953	0.8022
N3-8	Oxygen	3.816	0.9624	0.063	9.2346
	Argon	0.573	1.6851	0.623	0.5487
N3-9	Oxygen	3.790	1.9560	0.097	18.7686
	Argon	0.570	2.6184	0.987	0.8526
N3-10	Oxygen	3.823	1.1196	0.068	10.7430
	Argon	0.570	1.6296	0.615	0.5306
N3-11	Oxygen	3.873	0.2776	0.025	2.6637
	Argon	0.583	0.4540	0.165	0.1478
N3-12	Oxygen	3.790	0.1609	0.024	1.5439
	Argon	0.563	0.3768	0.168	0.1227
N4-2	Oxygen	3.840	1.6398	0.090	15.7346
	Argon	0.566	2.3311	0.870	0.7590
N4-4	Oxygen	3.836	2.0396	0.103	19.5708
	Argon	0.563	2.8049	1.059	0.9133
N4-5	Oxygen	3.796	1.9532	0.098	18.7418
	Argon	0.563	2.7575	1.028	0.8979
N4-6	Oxygen	3.773	1.6926	0.089	16.2412
	Argon	0.566	2.6916	1.003	0.8764
N4-7	Oxygen	3.803	1.5044	0.070	14.4353
	Argon	0.566	1.9244	0.697	0.6266
N4-8	Oxygen	3.806	1.6162	0.084	15.5081
	Argon	0.570	2.1196	0.784	0.6902
N4-9	Oxygen	3.816	1.9324	0.102	18.5422
	Argon	0.563	2.6832	1.003	0.8737
N4-10	Oxygen	3.780	1.5442	0.085	14.8172
	Argon	0.570	2.1420	0.789	0.6975
N4-11	Oxygen	3.883	0.3904	0.028	3.7461
	Argon	0.580	0.4418	0.180	0.1439
N4-12	Oxygen	4.026	0.1344	0.019	1.2896
	Argon	0.603	0.1933	0.077	0.0629
N5-2	Oxygen	3.893	1.8174	0.097	17.4387
	Argon	0.570	2.5654	0.960	0.8353

N5-4	Oxygen	3.830	1.7922	0.091	17.1969
	Argon	0.573	2.5001	0.937	0.8141
N5-6	Oxygen	3.853	2.1248	0.099	20.3883
	Argon	0.573	2.7955	1.038	0.9103
N5-8	Oxygen	3.853	2.0668	0.104	19.8318
	Argon	0.576	2.5579	0.994	0.8329
N5-9	Oxygen	3.853	1.2652	0.077	12.1401
	Argon	0.583	1.9090	0.710	0.6216
N5-10	Oxygen	3.900	1.4692	0.087	14.0976
	Argon	0.580	2.2530	0.829	0.7336
N5-11	Oxygen	3.876	0.3467	0.031	3.3267
	Argon	0.590	0.6742	0.252	0.2195
N5-12	Oxygen	3.983	0.1356	0.018	1.3011
	Argon	0.606	0.1908	0.068	0.0621

13-Jul-13					
Sample ID	**Parameter**	**Retention (min)**	**Area**	**Height**	**External (%)**
Cal01	Oxygen	3.826	2.8260	0.113	25.3084
	Argon	0.570	2.8760	1.104	0.9321
Cal02	Oxygen	3.833	2.1784	0.109	18.8616
	Argon	0.576	2.8920	1.098	0.9364
Cal03	Oxygen	3.843	2.2060	0.107	19.2288
	Argon	0.573	2.9552	1.105	0.9452
N1-2	Oxygen	3.843	1.7212	0.096	15.0030
	Argon	0.573	2.5890	0.969	0.8281
N1-3	Oxygen	3.850	1.5984	0.089	13.9326
	Argon	0.570	2.3876	0.891	0.7636
N1-4	Oxygen	3.843	1.7738	0.093	15.4615
	Argon	0.573	2.2844	0.863	0.7306
N1-5	Oxygen	3.833	1.4800	0.076	12.9005
	Argon	0.573	1.9332	0.768	0.6183
N1-6	Oxygen	3.863	1.3598	0.073	11.8528
	Argon	0.573	1.8768	0.702	0.6003
N1-7	Oxygen	3.840	0.8432	0.055	7.3498
	Argon	0.576	1.1980	0.487	0.3832
N1-8	Oxygen	3.843	0.8524	0.054	7.4300
	Argon	0.573	1.2006	0.477	0.3840
N1-9	Oxygen	3.860	0.5134	0.039	4.4751
	Argon	0.576	0.8335	0.326	0.2666

N1-10	Oxygen	3.850	0.4952	0.034	4.3164
	Argon	0.576	0.5745	0.244	0.1837
N1-11	Oxygen	3.876	0.1208	0.021	1.0530
	Argon	0.593	0.2510	0.097	0.0803
N1-12	Oxygen	3.953	0.1110	0.018	0.9675
	Argon	0.593	0.2284	0.101	0.0731
N2-2	Oxygen	3.833	1.8172	0.091	15.8398
	Argon	0.553	2.3666	0.921	0.7569
N2-3	Oxygen	3.830	2.0044	0.104	17.4715
	Argon	0.570	2.7898	1.072	0.8923
N2-4	Oxygen	3.820	2.0184	0.102	17.5935
	Argon	0.570	2.7490	1.065	0.8792
N2-5	Oxygen	3.870	1.7072	0.089	14.8809
	Argon	0.570	2.3810	0.899	0.7615
N2-6	Oxygen	3.860	2.0220	0.105	17.6249
	Argon	0.576	2.8368	1.075	0.9073
N2-7	Oxygen	3.846	1.4764	0.083	12.8692
	Argon	0.573	2.1183	0.819	0.6775
N2-8	Oxygen	3.850	2.1620	0.102	18.8452
	Argon	0.576	2.7428	1.048	0.8772
N2-9	Oxygen	3.850	1.5770	0.082	13.7460
	Argon	0.576	2.1480	0.825	0.6870
N2-10	Oxygen	3.836	0.7332	0.044	6.3910
	Argon	0.580	0.8784	0.362	0.2809
N2-11	Oxygen	3.970	0.1038	0.017	0.9048
	Argon	0.603	0.1979	0.086	0.0633
N2-12	Oxygen	3.866	0.1348	0.026	1.1750
	Argon	0.590	0.2882	0.125	0.0922
N3-2	Oxygen	3.843	1.8016	0.099	15.7038
	Argon	0.573	2.7582	1.001	0.8822
N3-3	Oxygen	3.830	2.0260	0.108	17.6598
	Argon	0.566	2.7637	1.035	0.8839
N3-4	Oxygen	3.836	2.0158	0.097	17.5709
	Argon	0.570	2.4660	0.924	0.7887
N3-5	Oxygen	3.820	1.8588	0.095	16.2024
	Argon	0.570	2.6668	0.984	0.8529
N3-6	Oxygen	3.840	1.8548	0.096	16.1675
	Argon	0.570	2.8300	1.035	0.9051
N3-7	Oxygen	3.866	1.7806	0.098	15.5207

	Argon	0.570	2.6255	0.986	0.8397
N3-8	Oxygen	3.836	1.4916	0.081	13.0016
	Argon	0.573	2.0492	0.795	0.6554
N3-9	Oxygen	3.830	1.9352	0.103	16.8683
	Argon	0.570	2.7578	1.035	0.8820
N3-10	Oxygen	3.826	1.2248	0.064	10.6761
	Argon	0.570	1.6623	0.630	0.5317
N3-11	Oxygen	3.900	0.1686	0.020	1.4696
	Argon	0.576	0.2952	0.141	0.0944
N4-2	Oxygen	3.813	1.8152	0.091	15.8223
	Argon	0.566	2.6996	1.019	0.8634
N4-3	Oxygen	3.813	1.7020	0.083	14.8356
	Argon	0.563	2.4692	0.901	0.7897
N4-4	Oxygen	3.823	2.0064	0.104	17.4889
	Argon	0.560	2.9111	1.062	0.9311
N4-5	Oxygen	3.836	2.0652	0.105	18.0015
	Argon	0.566	2.8885	1.082	0.9238
N4-6	Oxygen	3.886	2.1606	0.095	18.8330
	Argon	0.570	2.7072	1.003	0.8659
N4-7	Oxygen	3.823	1.7840	0.079	15.2401
	Argon	0.570	2.0430	0.773	0.6534
N4-8	Oxygen	3.830	1.9974	0.097	17.4105
	Argon	0.566	2.7725	1.075	0.8867
N4-9	Oxygen	3.883	1.9646	0.100	17.1246
	Argon	0.570	2.7250	1.037	0.8716
N4-10	Oxygen	3.873	1.5278	0.078	13.3172
	Argon	0.570	1.9655	0.760	0.6286
N4-11	Oxygen	3.853	0.6916	0.040	6.0284
	Argon	0.576	0.7727	0.290	0.2471
N4-12	Oxygen	3.936	0.2209	0.026	1.9255
	Argon	0.583	0.4831	0.204	0.1545
N4-13	Oxygen	3.950	0.2464	0.024	2.1478
	Argon	0.583	0.3718	0.165	0.1189
N5-2	Oxygen	3.870	1.6522	0.076	14.4015
	Argon	0.573	1.8940	0.719	0.6058
N5-3	Oxygen	3.903	2.1536	0.109	18.7720
	Argon	0.576	2.7225	1.008	0.8708
N5-4	Oxygen	3.873	2.2584	0.112	19.6855
	Argon	0.573	2.8698	1.078	0.9179

N5-5	Oxygen	0.387	1.8642	0.098	16.2494
	Argon	0.573	2.8056	1.057	0.8973
N5-6	Oxygen	3.863	2.2860	0.112	19.9261
	Argon	0.570	2.8792	1.077	0.9209
N5-7	Oxygen	3.880	1.6850	0.089	14.6874
	Argon	0.573	2.3673	0.937	0.7571
N5-8	Oxygen	3.880	1.7432	0.082	15.1947
	Argon	0.573	2.2988	0.868	0.7352
N5-9	Oxygen	3.890	1.5976	0.080	13.9256
	Argon	0.576	1.9460	0.731	0.6224
N5-10	Oxygen	3.850	1.3500	0.069	11.7674
	Argon	0.576	2.0164	0.754	0.6449
N5-11	Oxygen	3.876	0.7052	0.045	6.1469
	Argon	0.576	0.8161	0.330	0.2610

23-Jul-13					
Sample ID	**Parameter**	**Retention (min)**	**Area**	**Height**	**External (%)**
N1-2	Oxygen	3.823	1.4640	0.068	15.9345
	Argon	0.570	1.6532	0.640	0.6283
N1-3	Oxygen	3.796	0.9212	0.047	10.0266
	Argon	0.573	1.0684	0.407	0.4061
N1-4	Oxygen	3.820	0.6704	0.036	7.2968
	Argon	0.573	0.6484	0.280	0.2464
Cal01	Oxygen	3.823	1.9392	0.096	22.8708
	Argon	0.566	2.4816	0.961	0.9758
Cal03	Oxygen	3.816	1.9380	0.098	24.7608
	Argon	0.566	2.6014	1.011	1.0679
Cal02	Oxygen	3.810	1.8972	0.097	20.6496
	Argon	0.570	2.2580	0.905	0.8582
N1-5	Oxygen	3.960	0.4072	0.030	4.4321
	Argon	0.576	0.5074	0.222	0.1928
N1-6	Oxygen	3.813	0.2966	0.021	3.2283
	Argon	0.583	0.3566	0.151	0.1355
N1-7	Oxygen	3.956	0.1296	0.015	1.4106
	Argon	0.583	0.2928	0.123	0.1113
N1-8	Oxygen	3.883	0.1063	0.090	1.1570
	Argon	0.593	0.1924	0.074	0.0731
N2-2	Oxygen	3.806	1.4336	0.083	15.6037
	Argon	0.566	2.2312	0.858	0.8480

N2-3	Oxygen	3.833	1.7312	0.086	18.8428
	Argon	0.566	2.4707	0.958	0.9390
N2-4	Oxygen	3.800	2.1518	0.102	23.4207
	Argon	0.563	2.8128	1.067	1.0690
N2-5	Oxygen	3.800	1.6554	0.084	18.0178
	Argon	0.570	2.1936	0.864	0.8337
N2-6	Oxygen	3.846	2.0596	0.102	22.4172
	Argon	0.566	2.7868	1.057	1.0591
N2-7	Oxygen	3.810	1.6102	0.073	17.4279
	Argon	0.570	1.9188	0.736	0.7293
N2-8	Oxygen	3.850	1.2188	0.059	13.2657
	Argon	0.570	1.5047	0.596	0.5719
N2-9	Oxygen	3.833	1.0296	0.052	11.2064
	Argon	0.570	1.3244	0.499	0.5033
N2-10	Oxygen	3.870	0.6334	0.036	6.8941
	Argon	0.573	0.5646	0.225	0.2146
N2-11	Oxygen	3.876	0.1846	0.024	2.0092
	Argon	0.580	0.2262	0.102	0.0860
N3-2	Oxygen	3.826	1.8260	0.099	19.8746
	Argon	0.566	2.5983	0.977	0.9875
N3-4	Oxygen	3.846	1.6010	0.086	17.4257
	Argon	0.563	2.2634	0.865	0.8602
N3-6	Oxygen	3.816	1.7668	0.098	19.2303
	Argon	0.530	2.5688	0.973	0.9300
N3-7	Oxygen	3.823	2.0408	0.087	22.2126
	Argon	0.563	2.3839	0.918	0.9060
N3-8	Oxygen	3.876	0.8724	0.057	9.4954
	Argon	0.576	1.4457	0.565	0.5494
N3-9	Oxygen	3.866	1.7348	0.091	18.8820
	Argon	0.566	2.2312	0.840	0.8480
N3-10	Oxygen	3.883	1.1864	0.062	12.9131
	Argon	0.570	1.5496	0.578	0.5889
N3-11	Oxygen	3.960	0.1790	0.021	1.9483
	Argon	0.580	0.3056	0.125	0.1161
N3-12	Oxygen	3.946	0.1273	0.017	1.3856
	Argon	0.593	0.1625	0.079	0.0618
N4-4	Oxygen	3.820	2.0096	0.097	21.8730
	Argon	0.566	2.7092	1.031	1.0297
N4-6	Oxygen	3.853	1.9782	0.100	21.5312

	Argon	0.566	2.9052	1.091	1.1041
N4-8	Oxygen	3.860	2.1112	0.102	22.9788
	Argon	0.570	2.8892	1.071	1.0981
N4-9	Oxygen	3.833	1.9988	0.098	21.7554
	Argon	0.566	2.7452	1.015	1.0433
N4-10	Oxygen	3.850	1.8872	0.093	20.5408
	Argon	0.566	2.5541	0.945	0.9707
N4-11	Oxygen	4.040	0.2020	0.021	2.1986
	Argon	0.586	0.2324	0.098	0.0883
N5-2	Oxygen	3.853	1.3744	0.065	14.9593
	Argon	0.573	1.6228	0.610	0.6168
N5-4	Oxygen	3.853	1.9544	0.102	21.2722
	Argon	0.570	3.0420	1.117	1.1561
N5-6	Oxygen	3.860	2.0644	0.106	22.4694
	Argon	0.566	2.9935	1.091	1.1377
N5-8	Oxygen	3.880	1.9732	0.101	21.4768
	Argon	0.566	2.8670	1.045	1.0896
N5-10	Oxygen	3.863	1.3574	0.073	14.7743
	Argon	0.573	1.8826	0.683	0.7155
N5-11	Oxygen	3.866	0.6175	0.038	6.7210
	Argon	0.560	0.8029	0.315	0.3051
N5-12	Oxygen	3.960	0.1084	0.015	1.1799
	Argon	0.590	0.1109	0.048	0.0421

29-Jul-13					
Sample ID	**Parameter**	**Retention (min)**	**Area**	**Height**	**External (%)**
Cal02	Oxygen	3.913	1.7200	0.086	19.4554
	Argon	0.576	2.3836	0.896	0.9336
Cal03	Oxygen	3.880	2.0060	0.093	22.4209
	Argon	0.570	2.6308	1.019	1.0093
N1-2	Oxygen	3.923	0.7584	0.045	8.4766
	Argon	0.580	0.8940	0.363	0.3430
N1-3	Oxygen	3.850	0.6470	0.024	3.8784
	Argon	0.530	0.5570	0.221	0.2137
N1-4	Oxygen	3.960	0.1136	0.016	1.2694
	Argon	0.593	0.2624	0.125	0.1007
N1-5	Oxygen	3.936	0.1543	0.020	1.7246
	Argon	0.590	0.2404	0.116	0.0922
N2-2	Oxygen	3.870	1.7830	0.081	19.9284

	Argon	0.573	2.3862	0.880	0.9154
N2-4	Oxygen	0.860	2.0820	0.102	23.2703
	Argon	0.573	2.8627	1.066	1.0983
N2-5	Oxygen	3.876	1.2638	0.066	14.1254
	Argon	0.573	1.7820	0.654	0.6837
N2-6	Oxygen	3.886	1.7648	0.086	19.7250
	Argon	0.543	2.4408	0.890	0.9364
N2-7	Oxygen	3.873	1.3112	0.072	14.6552
	Argon	0.573	1.7254	0.632	0.6619
N2-8	Oxygen	3.916	0.9450	0.057	10.5622
	Argon	0.576	1.6013	0.600	0.6143
N2-9	Oxygen	3.943	0.7140	0.043	7.9803
	Argon	0.586	0.7176	0.287	0.2753
N2-10	Oxygen	3.933	0.1252	0.018	1.3993
	Argon	0.590	0.3343	0.150	0.1283
N3-2	Oxygen	3.856	2.0766	0.094	23.2100
	Argon	0.573	2.6200	0.968	1.0051
N3-4	Oxygen	3.883	1.8352	0.089	20.5119
	Argon	0.570	2.3668	0.888	0.9080
N3-6	Oxygen	3.903	2.0842	0.106	23.2949
	Argon	0.570	2.9648	1.099	1.1374
N3-8	Oxygen	3.903	1.6204	0.080	18.1111
	Argon	0.573	2.2368	0.808	0.8581
N3-9	Oxygen	3.866	1.8072	0.083	20.1989
	Argon	0.573	2.3936	0.884	0.9183
N3-10	Oxygen	3.906	0.7550	0.037	8.4386
	Argon	0.580	0.8768	0.335	0.3364
N3-11	Oxygen	3.920	0.3949	0.032	4.4138
	Argon	0.580	0.4868	0.181	0.1868
N3-12	Oxygen	3.970	0.1644	0.020	1.8375
	Argon	0.586	0.2208	0.119	0.0847
N4-2	Oxygen	3.866	1.8572	0.097	20.7578
	Argon	0.570	2.5618	0.986	0.9828
N4-4	Oxygen	3.850	1.8674	0.098	20.8718
	Argon	0.570	2.7400	1.056	1.0512
N4-6	Oxygen	3.850	2.3860	0.115	26.6681
	Argon	0.570	3.0352	1.153	1.1644
N4-8	Oxygen	3.840	2.0750	0.098	23.1921
	Argon	0.566	2.6692	1.032	1.0240

N4-10	Oxygen	3.890	0.9476	0.050	10.5912
	Argon	0.573	1.1668	0.461	0.4476
N4-11	Oxygen	3.853	0.6808	0.034	7.6092
	Argon	0.580	0.7214	0.272	0.2768
N4-12	Oxygen	3.976	0.2022	0.023	2.2600
	Argon	0.586	0.3757	0.163	0.1441
N5-2	Oxygen	3.853	1.9516	0.095	21.8129
	Argon	0.573	2.7551	1.041	1.0570
N5-5	Oxygen	3.850	2.1268	0.105	23.7711
	Argon	0.566	2.9134	1.124	1.1177
N5-9	Oxygen	3.883	1.5260	0.078	17.0560
	Argon	0.573	1.8826	0.728	0.7222
N5-10	Oxygen	3.836	1.5012	0.075	16.7788
	Argon	0.553	1.9142	0.740	0.7344
N5-11	Oxygen	3.946	0.4470	0.034	4.9961
	Argon	0.576	0.6692	0.282	0.2567
N5-13	Oxygen	3.896	0.1200	0.019	1.3412
	Argon	0.583	0.2228	0.116	0.0855

6-Aug-13					
Sample ID	**Parameter**	**Retention (min)**	**Area**	**Height**	**External (%)**
Cal01	Oxygen	3.836	2.0700	0.111	22.4464
	Argon	0.566	2.9518	1.138	1.0338
Cal02	Oxygen	3.850	2.2928	0.117	22.6263
	Argon	0.566	2.7560	1.096	0.9221
Cal03	Oxygen	3.846	2.2420	0.115	21.3344
	Argon	0.566	2.9444	1.152	0.9852
N1-2	Oxygen	3.850	0.3860	0.032	3.6731
	Argon	0.573	0.4820	0.212	0.1613
N1-3	Oxygen	3.843	0.1077	0.016	1.0249
	Argon	0.576	0.2585	0.129	0.0865
N1-4	Oxygen	3.826	0.1662	0.024	1.5815
	Argon	0.583	0.2333	0.110	0.0781
N2-2	Oxygen	3.793	1.7242	0.082	16.4072
	Argon	0.566	2.0512	0.798	0.6863
N2-3	Oxygen	3.820	1.4310	0.079	13.6171
	Argon	0.563	2.1808	0.840	0.7297

N2-4	Oxygen	3.823	1.5098	0.084	14.3670
	Argon	0.570	2.0900	0.805	0.6993
N2-6	Oxygen	3.893	1.0558	0.058	10.0468
	Argon	0.566	1.4100	0.538	0.4718
N2-7	Oxygen	3.850	0.7712	0.038	7.3386
	Argon	0.573	0.6630	0.291	0.2218
N2-9	Oxygen	3.900	0.1004	0.018	0.9554
	Argon	0.580	0.2531	0.105	0.0847
N2-11	Oxygen	3.946	0.1676	0.022	1.5948
	Argon	0.583	0.1709	0.080	0.0572
N3-2	Oxygen	3.900	1.8740	0.091	17.8326
	Argon	0.570	2.3376	0.877	0.7821
N3-4	Oxygen	3.866	1.8400	0.086	17.5091
	Argon	0.566	2.2960	0.875	0.7682
N3-6	Oxygen	3.853	1.5136	0.070	14.4031
	Argon	0.570	1.5648	0.610	0.5236
N3-8	Oxygen	3.853	1.2252	0.060	11.6588
	Argon	0.566	1.5772	0.615	0.5277
N3-9	Oxygen	3.850	1.4544	0.068	13.8398
	Argon	0.566	1.7128	0.643	0.5731
N3-10	Oxygen	3.840	0.3844	0.030	3.6579
	Argon	0.573	0.8366	0.334	0.2799
N3-12	Oxygen	3.910	0.1692	0.023	1.6101
	Argon	0.576	0.4257	0.148	0.1424
N4-2	Oxygen	3.830	1.4826	0.077	14.1081
	Argon	0.566	2.1699	0.802	0.7260
N4-4	Oxygen	3.830	1.8504	0.098	17.6080
	Argon	0.563	2.6760	1.003	0.8954
N4-7	Oxygen	3.833	1.4864	0.076	14.1443
	Argon	0.566	2.9940	0.751	0.8028
N4-9	Oxygen	3.850	1.8974	0.092	18.0553
	Argon	0.563	2.5308	0.984	0.8468
N4-11	Oxygen	3.840	0.2162	0.020	2.0573
	Argon	0.573	0.4130	0.180	0.1382
N5-2	Oxygen	3.803	1.9066	0.100	18.1428
	Argon	0.560	2.6843	1.010	0.8981
N5-5	Oxygen	3.856	1.9566	0.099	18.6186
	Argon	0.566	2.5408	0.853	0.8501
N5-8	Oxygen	3.843	2.0012	0.103	19.0430

	Argon	0.563	2.7711	1.078	0.9272
N5-11	Oxygen	3.853	0.8484	0.045	8.0732
	Argon	0.566	0.8523	0.331	0.2852
N5-13	Oxygen	3.846	0.1756	0.021	1.6710
	Argon	0.580	0.1677	0.071	0.0561

13-Aug-13 **Sample ID**	**Parameter**	**Retention (min)**	**Area**	**Height**	**External (%)**
Cal02	Oxygen	3.876	2.1762	0.110	20.3802
	Argon	0.566	2.9613	1.172	0.8530
Cal03	Oxygen	3.853	1.8596	0.100	17.4156
	Argon	0.566	3.0008	1.166	0.9603
N1-2	Oxygen	3.876	0.4538	0.030	4.2499
	Argon	0.576	0.5840	0.260	0.1869
N1-3	Oxygen	3.843	0.1120	0.014	1.0489
	Argon	0.576	0.2424	0.120	0.0776
N2-2	Oxygen	3.840	1.3868	0.072	12.9877
	Argon	0.573	1.8417	0.742	0.5894
N2-4	Oxygen	3.890	0.9116	0.047	8.5373
	Argon	0.573	0.9369	0.403	0.2998
N2-6	Oxygen	3.866	0.1603	0.015	1.5012
	Argon	0.580	0.3702	0.154	0.1185
N2-8	Oxygen	3.836	0.2760	0.021	2.5848
	Argon	0.576	0.4360	0.187	0.1395
N2-10	Oxygen	3.916	0.1623	0.025	1.5200
	Argon	0.583	0.2688	0.123	0.0860
N3-2	Oxygen	3.840	2.1940	0.100	20.5473
	Argon	0.566	2.6002	0.989	0.8321
N3-5	Oxygen	3.860	2.0030	0.091	18.7585
	Argon	0.566	2.3324	0.901	0.7464
N3-8	Oxygen	3.893	1.2276	0.058	11.4967
	Argon	0.553	1.5337	0.582	0.4908
N3-10	Oxygen	3.920	0.1506	0.020	1.4104
	Argon	0.586	0.2857	0.145	0.0914
N3-12	Oxygen	3.906	0.1046	0.018	0.9796
	Argon	0.586	0.1852	0.092	0.0593
N4-2	Oxygen	3.903	1.4500	0.075	13.5796
	Argon	0.570	1.9460	0.724	0.6228
N4-5	Oxygen	3.896	1.9630	0.104	18.3839

	Argon	0.570	2.9583	1.097	0.9467
N4-8	Oxygen	3.903	1.9598	0.096	18.3540
	Argon	0.570	2.5756	0.985	0.8243
N4-10	Oxygen	3.880	1.1616	0.063	10.8786
	Argon	0.570	1.4450	0.536	0.4495
N4-11	Oxygen	3.966	0.1338	0.019	1.2531
	Argon	0.586	0.2816	0.123	0.0901
N5-2	Oxygen	3.883	2.0500	0.102	19.1987
	Argon	0.570	2.8683	1.104	0.9179
N5-5	Oxygen	3.926	2.3116	0.106	21.6486
	Argon	0.570	2.8907	1.111	0.9251
N5-8	Oxygen	3.870	1.9228	0.097	18.0074
	Argon	0.570	2.8146	1.050	0.9007
N5-10	Oxygen	3.863	1.3346	0.073	12.4988
	Argon	0.570	1.9886	0.745	0.6364
N5-11	Oxygen	3.940	0.8124	0.037	7.6083
	Argon	0.576	0.8556	0.317	0.2738
N5-13	Oxygen	3.963	0.1250	0.015	1.1707
	Argon	0.586	0.2152	0.093	0.0689

26-Aug-13					
Sample ID	**Parameter**	**Retention (min)**	**Area**	**Height**	**External (%)**
Cal01	Oxygen	3.860	2.3730	0.113	21.9612
	Argon	0.560	2.9208	1.159	0.9174
Cal02	Oxygen	3.836	2.2876	0.109	21.0297
	Argon	0.560	3.0394	1.176	0.9464
Cal03	Oxygen	3.846	2.2716	0.117	20.5952
	Argon	0.563	3.0147	1.189	0.9371
N1-2	Oxygen	3.860	0.4080	0.030	3.6991
	Argon	0.576	0.4532	0.203	0.1409
N1-3	Oxygen	3.886	0.1308	0.013	1.1859
	Argon	0.576	0.1880	0.093	0.0584
N2-2	Oxygen	3.853	0.7524	0.044	6.8215
	Argon	0.566	0.9864	0.404	0.3066
N2-4	Oxygen	3.786	0.2162	0.028	1.9602
	Argon	0.573	0.3895	0.186	0.1211
N2-6	Oxygen	3.840	0.1184	0.014	1.0735
	Argon	0.580	0.2394	0.106	0.0744
N2-8	Oxygen	3.876	0.3470	0.028	3.1460

	Argon	0.570	0.5096	0.229	0.1584
N3-2	Oxygen	3.840	1.9604	0.097	17.7737
	Argon	0.563	2.4354	0.938	0.7571
N3-4	Oxygen	3.873	1.2548	0.063	11.3765
	Argon	0.566	1.4936	0.606	0.4643
N3-6	Oxygen	3.830	1.2300	0.066	11.1517
	Argon	0.566	1.6612	0.651	0.5164
N3-7	Oxygen	3.833	0.5720	0.036	5.1860
	Argon	0.570	0.7168	0.323	0.2228
N3-8	Oxygen	3.876	0.2636	0.023	2.3899
	Argon	0.573	0.4054	0.192	0.1260
N3-10	Oxygen	3.876	0.1878	0.016	1.7207
	Argon	0.580	0.2532	0.109	0.0787
N4-2	Oxygen	3.880	1.1064	0.057	10.0310
	Argon	0.563	1.5328	0.589	0.4765
N4-4	Oxygen	3.883	1.4464	0.078	13.1136
	Argon	0.566	2.1074	0.806	0.6551
N4-6	Oxygen	3.870	1.2128	0.068	10.9957
	Argon	0.570	1.6663	0.652	0.5180
N4-8	Oxygen	3.836	1.3492	0.068	12.2324
	Argon	0.566	1.9280	0.749	0.5993
N4-10	Oxygen	3.896	0.7336	0.044	6.6511
	Argon	0.573	0.9212	0.357	0.2864
N4-12	Oxygen	3.970	0.1876	0.021	1.7009
	Argon	0.583	0.2035	0.091	0.0633
N5-2	Oxygen	3.833	1.2527	0.070	11.3575
	Argon	0.566	1.7830	0.666	0.5543
N5-5	Oxygen	3.860	1.6708	0.085	15.1481
	Argon	0.560	2.3876	0.895	0.7422
N5-8	Oxygen	3.866	1.9792	0.092	17.9442
	Argon	0.566	2.4800	0.922	0.7709
N5-10	Oxygen	3.833	1.2088	0.062	10.9594
	Argon	0.563	1.3360	0.542	0.4153
N5-11	Oxygen	3.946	0.3346	0.029	3.0336
	Argon	0.570	0.5254	0.228	0.1633
N5-12	Oxygen	3.833	0.1200	0.018	1.0880
	Argon	0.573	0.2012	0.103	0.0625

8-Sep-13

Sample ID	Parameter	Retention (min)	Area	Height	External (%)
Cal01	Oxygen	3.926	2.3468	0.113	21.3577
	Argon	0.570	3.4214	1.302	1.0074
Cal02	Oxygen	3.886	2.2710	0.102	20.7177
	Argon	0.570	2.7371	1.110	0.8325
Cal03	Oxygen	3.886	2.0726	0.109	19.4701
	Argon	0.570	2.9300	1.169	0.8995
N1-2	Oxygen	4.003	0.2384	0.024	2.2395
	Argon	0.583	0.4097	0.184	0.1258
N1-3	Oxygen	3.963	0.1952	0.017	1.8337
	Argon	0.586	0.2286	0.111	0.0702
N1-9	Oxygen	3.906	0.1384	0.020	1.3001
	Argon	0.583	0.2702	0.121	0.0829
N2-2	Oxygen	3.913	0.5180	0.034	4.8661
	Argon	0.576	0.7884	0.300	0.2420
N2-3	Oxygen	3.890	0.2104	0.021	1.9765
	Argon	0.580	0.4223	0.162	0.1296
N2-4	Oxygen	3.980	0.1370	0.022	1.2870
	Argon	0.576	0.2687	0.122	0.0825
N2-10	Oxygen	3.940	0.1113	0.022	1.0456
	Argon	0.583	0.2532	0.111	0.0777
N3-2	Oxygen	3.930	1.0662	0.049	10.0159
	Argon	0.570	1.3352	0.531	0.4099
N3-4	Oxygen	3.886	0.5298	0.035	4.9770
	Argon	0.573	0.8780	0.338	0.2695
N3-5	Oxygen	3.983	0.2580	0.025	2.4237
	Argon	0.570	0.3340	0.167	0.1025
N3-6	Oxygen	3.953	0.1304	0.023	1.2250
	Argon	0.580	0.2642	0.113	0.0811
N4-2	Oxygen	3.853	1.6452	0.081	15.4551
	Argon	0.566	2.1976	0.824	0.6746
N4-4	Oxygen	3.876	1.6374	0.083	15.3818
	Argon	0.563	2.3792	0.936	0.7304
N4-6	Oxygen	3.883	1.6820	0.082	15.8008
	Argon	0.563	2.3382	0.900	0.7178
N4-8	Oxygen	3.826	1.0168	0.056	9.5519
	Argon	0.563	1.6532	0.623	0.5075
N4-9	Oxygen	3.850	0.6351	0.035	5.9662
	Argon	0.570	0.7470	0.283	0.2293

N4-10	Oxygen	3.883	0.1135	0.016	1.0662
	Argon	0.580	0.1921	0.086	0.0590
N5-2	Oxygen	3.866	1.8218	0.094	17.1141
	Argon	0.563	2.4992	0.950	0.7672
N5-4	Oxygen	3.856	1.9580	0.097	18.3936
	Argon	0.560	2.7620	1.029	0.8479
N5-8	Oxygen	3.863	1.8904	0.096	17.7585
	Argon	0.563	2.8872	1.096	0.8863
N5-9	Oxygen	3.856	1.3256	0.065	12.4528
	Argon	0.566	1.7644	0.645	0.5416
N5-10	Oxygen	3.873	0.9454	0.045	8.8811
	Argon	0.573	1.2491	0.465	0.3835
N5-11	Oxygen	3.926	0.3304	0.023	3.1038
	Argon	0.573	0.5084	0.183	0.1561
N5-12	Oxygen	3.986	0.1100	0.018	1.0333
	Argon	0.583	0.1840	0.082	0.0565

20-Sep-13					
Sample ID	**Parameter**	**Retention (min)**	**Area**	**Height**	**External (%)**
Cal01	Oxygen	3.796	2.2204	0.110	21.2602
	Argon	0.560	2.8412	1.142	0.9317
Cal02	Oxygen	3.816	2.0414	0.118	20.2548
	Argon	0.560	2.7664	1.137	0.9040
Cal03	Oxygen	3.840	2.0074	0.110	20.1246
	Argon	0.556	2.8390	1.152	0.9378
N1-2	Oxygen	3.853	0.3624	0.029	3.6331
	Argon	0.570	0.5196	0.224	0.1716
N1-3	Oxygen	3.833	0.1504	0.020	1.5078
	Argon	0.573	0.2000	0.100	0.0661
N1-10	Oxygen	3.830	0.1906	0.021	1.9108
	Argon	0.566	0.3832	0.182	0.1266
N2-2	Oxygen	3.796	0.3913	0.034	3.9229
	Argon	0.566	0.7032	0.303	0.2323
N2-3	Oxygen	3.883	0.2072	0.019	2.0772
	Argon	0.563	0.4472	0.207	0.1477
N2-4	Oxygen	3.906	0.1702	0.021	1.7063
	Argon	0.576	0.2656	0.128	0.0877

N3-2	Oxygen	3.860	1.4036	0.075	14.0714
	Argon	0.566	2.0020	0.758	0.6613
N3-3	Oxygen	3.883	0.3296	0.029	3.3043
	Argon	0.576	0.5192	0.229	0.1715
N3-4	Oxygen	3.926	0.1736	0.026	1.7404
	Argon	0.573	0.2730	0.124	0.0902
N3-6	Oxygen	3.890	0.1672	0.017	1.6762
	Argon	0.576	0.2587	0.122	0.0855
N4-2	Oxygen	3.880	1.5728	0.083	15.7676
	Argon	0.566	2.2729	0.877	0.7508
N4-4	Oxygen	3.866	1.7804	0.078	17.8489
	Argon	0.570	2.1470	0.837	0.7092
N4-6	Oxygen	3.890	1.1428	0.062	11.4568
	Argon	0.570	1.4074	0.578	0.4649
N4-8	Oxygen	0.032	4.2808	0.032	4.2808
	Argon	0.573	0.6580	0.252	0.2173
N4-9	Oxygen	3.910	0.1926	0.022	1.9309
	Argon	0.576	0.3075	0.149	0.1016
N5-2	Oxygen	3.870	2.1472	0.100	21.5261
	Argon	0.563	2.8170	1.076	0.9308
N5-5	Oxygen	3.893	2.1428	0.102	21.4820
	Argon	0.563	2.8328	1.080	0.9357
N5-8	Oxygen	3.893	1.8868	0.103	18.9156
	Argon	0.560	2.5324	0.992	0.8365
N5-10	Oxygen	3.900	0.3604	0.030	3.6131
	Argon	0.573	0.5618	0.257	0.1856
N5-12	Oxygen	3.910	0.1892	0.024	1.8968
	Argon	0.580	0.2081	0.094	0.0687

4-Oct-13					
Sample ID	**Parameter**	**Retention (min)**	**Area**	**Height**	**External (%)**
Cal01	Oxygen	3.843	2.2532	0.111	21.8277
	Argon	0.563	2.7460	1.126	0.8900
Cal02	Oxygen	3.870	2.2272	0.114	22.3039
	Argon	0.563	3.0237	1.193	0.9776
N1-2	Oxygen	3.780	0.2664	0.020	2.5807
	Argon	0.566	0.4118	0.198	0.1335
N1-3	Oxygen	3.833	0.1574	0.018	1.5248
	Argon	0.580	0.2168	0.104	0.0703

N2-2	Oxygen	3.860	0.2976	0.024	2.8830
	Argon	0.566	0.6288	0.251	0.2038
N2-3	Oxygen	3.936	0.1404	0.016	1.3601
	Argon	0.573	0.2992	0.143	0.0970
N2-4	Oxygen	3.833	0.1762	0.019	1.7069
	Argon	0.570	0.2566	0.124	0.0832
N3-2	Oxygen	3.853	0.3122	0.026	3.0244
	Argon	0.566	0.6212	0.296	0.2013
N3-3	Oxygen	3.866	0.1854	0.020	1.7960
	Argon	0.570	0.2724	0.128	0.0883
N4-2	Oxygen	3.866	0.2552	0.029	2.4722
	Argon	0.563	0.8612	0.333	0.2791
N4-4	Oxygen	3.843	1.0996	0.062	10.6523
	Argon	0.543	1.5250	0.596	0.4942
N4-6	Oxygen	3.830	0.1204	0.022	1.1664
	Argon	0.570	0.3000	0.142	0.0972
N4-8	Oxygen	3.963	0.1012	0.016	0.9804
	Argon	0.573	0.1842	0.078	0.0597
N5-2	Oxygen	3.860	1.7944	0.085	17.3831
	Argon	0.566	2.3225	0.922	0.7527
N5-4	Oxygen	3.823	1.7148	0.090	16.6120
	Argon	0.553	2.4024	0.918	0.7786
N5-7	Oxygen	3.816	1.4028	0.070	13.5895
	Argon	0.563	1.8540	0.724	0.6009
N5-9	Oxygen	3.860	0.4836	0.035	4.6848
	Argon	0.566	0.6844	0.286	0.2218
N5-11	Oxygen	4.016	0.1072	0.017	1.0385
	Argon	0.573	0.2443	0.110	0.0792

20-Oct-13					
Sample ID	**Parameter**	**Retention (min)**	**Area**	**Height**	**External (%)**
Cal01	Oxygen	3.853	2.3252	0.110	21.4733
	Argon	0.563	3.2002	1.220	0.9954
Cal02	Oxygen	3.860	2.2746	0.112	20.8607
	Argon	0.563	3.1186	1.209	0.9599
Cal03	Oxygen	3.856	2.2932	0.109	20.9093
	Argon	0.560	3.0498	1.214	0.9082
N1-2	Oxygen	3.900	0.2359	0.020	2.1509
	Argon	0.570	0.4149	0.185	0.1236

N1-3	Oxygen	3.976	0.1188	0.018	1.0832
	Argon	0.580	0.2613	0.117	0.0778
N2-2	Oxygen	3.916	0.4028	0.034	3.6727
	Argon	0.573	0.6016	0.248	0.1792
N2-3	Oxygen	3.903	0.2286	0.023	2.0844
	Argon	0.570	0.3104	0.143	0.0924
N3-3	Oxygen	3.836	0.1552	0.025	1.4151
	Argon	0.576	0.2762	0.132	0.0823
N4-2	Oxygen	3.920	0.6637	0.045	6.0516
	Argon	0.570	1.0690	0.421	0.3184
N4-4	Oxygen	3.886	0.1556	0.018	1.4188
	Argon	0.576	0.2504	0.125	0.0746
N5-2	Oxygen	3.876	1.6008	0.081	14.5960
	Argon	0.566	2.1540	0.819	0.6415
N5-4	Oxygen	3.846	1.5240	0.069	13.8957
	Argon	0.566	1.6576	0.645	0.4936
N5-6	Oxygen	3.910	0.8240	0.044	7.5132
	Argon	0.563	0.8852	0.367	0.2636
N5-8	Oxygen	3.916	0.1570	0.023	1.4315
	Argon	0.570	0.2431	0.127	0.0724

1-Nov-13					
Sample ID	**Parameter**	**Retention (min)**	**Area**	**Height**	**External (%)**
N1-2	Oxygen	3.816	0.2668	0.025	2.4327
	Argon	0.563	0.3520	0.170	0.1048
N1-3	Oxygen	3.873	0.1448	0.019	1.3203
	Argon	0.576	0.1938	0.091	0.0577
N2-2	Oxygen	3.923	0.3276	0.027	2.9870
	Argon	0.563	0.4424	0.205	0.1317
N3-3	Oxygen	3.836	0.1520	0.021	1.3859
	Argon	0.563	0.3021	0.150	0.0900
N4-2	Oxygen	3.830	0.5452	0.045	4.9711
	Argon	0.556	0.8806	0.365	0.2622
N4-3	Oxygen	3.866	0.1468	0.018	1.3385
	Argon	0.566	0.3380	0.169	0.0994
N5-2	Oxygen	3.866	1.0882	0.063	9.2210
	Argon	0.556	1.5208	0.630	0.4529
N5-5	Oxygen	3.880	0.3651	0.028	3.3290
	Argon	0.563	0.4644	0.216	0.1383

N5-7	Oxygen	3.836	0.1529	0.021	1.3941
	Argon	0.563	0.3612	0.166	0.1076

16-Nov-13					
Sample ID	**Parameter**	**Retention (min)**	**Area**	**Height**	**External (%)**
N5-2	Oxygen	3.766	0.5612	0.040	5.9376
	Argon	0.560	1.1292	0.493	0.3363
N5-4	Oxygen	3.880	0.3876	0.033	3.5341
	Argon	0.560	0.5244	0.248	0.1562
N5-5	Oxygen	3.816	0.1420	0.018	1.2947
	Argon	0.566	0.2624	0.137	0.0781
N4-2	Oxygen	3.830	0.4586	0.035	4.1906
	Argon	0.560	0.6200	0.313	0.1846
N4-3	Oxygen	3.876	0.1732	0.018	1.5792
	Argon	0.560	0.3232	0.164	0.0963
N3-3	Oxygen	3.816	0.1972	0.022	1.7981
	Argon	0.563	0.3460	0.167	0.1030
N2-2	Oxygen	3.876	0.2632	0.028	2.3998
	Argon	0.560	0.3976	0.181	0.1184
N2-3	Oxygen	3.896	0.1235	0.017	1.1261
	Argon	0.566	0.1448	0.080	0.0431
N1-2	Oxygen	3.840	0.2259	0.024	2.0597
	Argon	0.563	0.2442	0.115	0.0727

6-Dec-13					
Sample ID	**Parameter**	**Retention (min)**	**Area**	**Height**	**External (%)**
N5-2	Oxygen	3.903	0.6328	0.044	5.7698
	Argon	0.566	1.0637	0.424	0.3168
N5-3	Oxygen	3.936	0.3392	0.031	3.0928
	Argon	0.570	0.5564	0.248	0.1657
N5-4	Oxygen	3.870	0.2292	0.022	2.0898
	Argon	0.573	0.3256	0.164	0.0970
N4-2	Oxygen	3.870	0.5340	0.036	4.8690
	Argon	0.566	0.5855	0.279	0.1744
N4-3	Oxygen	3.946	0.2070	0.024	1.8874
	Argon	0.566	0.3662	0.174	1.0910
N3-3	Oxygen	3.926	0.2965	0.028	2.7035
	Argon	0.570	0.3740	0.174	0.1114
N2-2	Oxygen	3.993	0.1604	0.017	1.4625

	Argon	0.563	0.3352	0.172	0.0998
N2-3	Oxygen	3.836	0.1256	0.016	1.1452
	Argon	0.413	0.1640	0.090	0.0488
N1-2	Oxygen	3.860	0.3016	0.028	2.7500
	Argon	0.566	0.4712	0.235	0.1403